2015

Holecene Paleoenvironmental Reconstruction from the Shark River Estuary, Everglades, Florida

Qiang Yao
Louisiana State University and Agricultural and Mechanical College

HOLOCENE PALEOENVIRONMENTAL RECONSTRUCTION FROM THE SHARK RIVER ESTUARY, EVERGLADES, FLORIDA

A Dissertation

Submitted to the Graduate Faculty of the
Louisiana State University and
Agricultural and Mechanical College
in partial fulfillment of the
requirements for the degree of
Doctor of Philosophy

in

The Department of Oceanography and Coastal Sciences

by
Qiang Yao
B.S., Mahidol University International College, 2008
May 2015

ACKNOWLEDGEMENTS

This study is supported by grants from the National Science Foundation (NSF DDRI Grant No. BCS-1303114) and the Inter-American Institute for Global Change Research (IAI #CRN2050).

I am deeply grateful to my major professor Dr. Kam-biu Liu for his support and encouragement during the development of my dissertation. He spent a countless number of hours mentoring me into a palynologist and geographer. I will always remember his passion and enthusiasm for science. I would also like to thank my committee members, Dr. John R. White, Dr. William J. Platt, and Dr. Victor H. Rivera-Monroy for their valuable guidance and support. I would like to express my sincere appreciation to Dr. Terrence McCloskey and Dr. Thomas Bianchette for their friendship, support, dedication, and valuable advice during these past years of my career.

I also thank Dr. Terrence McCloskey, Dr. Thomas Bianchette, Dr. Edward Castañeda-Moya, and Florida International University, center of the FCE-LTER program for their valuable assistance during field trips and laboratory work.

Special thanks to my parents Yao Minghu and Tang Guiying, and my dog Seven for their endless love and support in all my endeavors over the years. Finally, I dedicate this dissertation to my grandpa, Tang Jiguang, who passed away at October 10th. I don't know whether or not you are at a special place, or if such place even exits. But if I have the opportunity to make a wish, I am willing to give up all my possessions to spend one more day with you and ask you if I have made you proud.

TABLE OF CONTENTS

ABSTRACT

This dissertation examines the paleoecological records from the Shark River Estuary in the southwestern part of the Everglades National Park (ENP), Florida, with primary goal of reconstructing the Holocene history of the coastal mangrove ecosystem in the Florida Coastal Everglades. Roughly 15 meters of sediments were collected from 4 study sites and subjected to loss-on ignition, palynological, and X-ray fluorescence analyses.

According to the literature, the earliest communities of *Rhizophora mangle* (red mangrove) occurred prior to 8,000 cal yr BP in the south-central area of the Belize Barrier Reef Platform. Between 7,000 and 5,000 cal yr BP, *Rhizophora* was established in the Caribbean coast of South America and Central America. With warmer winter sea-surface temperature and a decreased rate of sea-level rise between 5,000 and 3,000 cal yr BP, *Rhizophora* eventually colonized the coastlines of the Yucatan, South Florida, and Bermuda.

Statistical analysis of 25 modern pollen spectra from the Everglades National Park shows that different wetland sub-environments in the Everglades can be identified based on their palynological signature. Accordingly, palynological data from sediment cores can be used to accurately reconstruct past wetland responses to a variety of environmental and climatic changes in the Everglades.

Multi-proxy analyses of sediment cores from four study sites along the Shark River Estuary reveal that the mid-Holocene sea-level rise is the dominant cause of vegetation change. The Shark River Estuary underwent three major transformations

during the last six millennia: (1) Short-hydroperiod marl prairies were progressively replaced by long hydroperiod prairies and sloughs from ~5,700 to 3,800 cal yr BP. (2) Long hydroperiod prairies and sloughs were replaced by brackish marsh from 3,800 to 2,000 cal yr BP. (3) A significant expansion of mangroves occurred over the last 2,000 years. In addition to Hurricane Wilma in 2005, the southwestern Everglades were directly impacted by at least six major hurricanes at ~3,000, 1,700, 950, 580, 350, and 120 cal yr BP. At ~1,100 cal yr BP, as the shoreline became stabilized, a mixed mangrove forest was formed at the mouth of the Shark River.

CHAPTER 1. INTRODUCTION

The Everglades of southern Florida contains the largest freshwater marshes and mangrove swamps in North America (Lodge, 2010). However, the structure and composition of this valuable natural resource have been impacted by rapid sea-level rise and human activities (Snedaker, 1993; Rudnick et al, 1999; Simard et al, 2006; Alongi, 2008). Tidal gauges from South Florida record that the rate of sea-level rise (SLR) has increased to 3.8 mm/yr since AD 1930, a rate that is 6 to 10 times that of the past 3200 years (0.4 mm/yr) (Wanless et al, 1994). Such pace has the potential to trigger permanent inundation, salinization, and erosion in the Everglades' coastal wetlands (Snedaker, 1993). Additionally, human alteration of the hydrological system during the last 100 years has also caused freshwater reduction and salinization in the coastal Everglades (Rudnick et al, 1999; Simard et al, 2006). As a direct result of SLR and human activity, more inland dispersion of salt tolerant species (e.g. mangrove) has been observed along the southern Florida coasts. It has been documented that the mangrove zones have migrated 3.5 km and 1.5 km inland in the Florida Bay and Key West areas, respectively, since 1940 (Ross et al, 2000).

Currently, an 8 billion USD restoration project has been launched to restore the hydrological systems in South Florida and reverse the structural and compositional changes to its coastal wetlands (CERP, 2000; Simard et al, 2006). However, the restoration project is challenged by accelerating climate changes. The Intergovernmental Panel on Climate Change (IPCC) predicts that the rate of SLR, which is the biggest threat to coastal wetlands, will increase as a consequence of global

warming during the 21st century (Farnsworth and Ellison, 1997; Valiela et al., 2001; Alongi, 2002; Duke et al., 2007; IPCC, 2014). The restoration process is further complicated by projected more frequent major hurricanes (category 3-5) in the next 100 years (Elsner et al, 2008; Bender et al, 2010). Increased hurricane disturbances have the potential to cause massive mangrove mortality, soil erosion, peat collapse, as well as allochthonous nutrient and sediment input to coastal wetlands in southern Florida (Smith et al., 1994, 2009; Chen and Twilley 1999a, b; Castañeda-Moya et al, 2010).

To aid the success of the Everglades restoration project, we need to predict how coastal wetlands will respond to future global climate changes, especially on timescales of decades to centuries. Therefore a long-term perspective, which can only be acquired from a paleoecological study, is necessary to reveal the response of mangrove ecosystems to past climate changes and sea-level fluctuations. However, no palynological records older than 5,000 cal yr BP are available in the literature from the coastal Everglades. We aim to fill this gap by presenting a 5,700 years multi-proxy record from 4 coring sites on a 20 km transect along the Shark River Estuary (SRE) in the southwestern part of the Everglades National Park (ENP). This study will integrate palynology and paleotempestology to reveal the history of coastal wetland development since the mid-Holocene and record the long-term response of coastal mangrove communities to sea-level rise and recurrent hurricanes in the ENP. Such a long-term study is vital for the restoration of Everglades' mangrove ecosystems and helping to expand our knowledge of the relationships between modern pollen rain and vegetation in the mangrove ecosystems. This study will also fill an important data gap

in the paleotempestology data network between the Gulf of Mexico coast and the Atlantic coast of the U.S. by recording the paleohurricane activities for South Florida.

Chapter 2 reviews the pollen and associated paleoecological records of mangrove-dominant environments from 24 study sites in the western North Atlantic (WNA). Study areas include the Caribbean basin, Bermuda, and South Florida. A variety of proxy data including pollen, marine microfossils, microscopic charcoal, mangrove peat stratigraphy, and chemical and isotopic records are examined, with a particular focus on the establishment and expansion of *Rhizophora sp.*

Chapter 3 examines 18 surface pollen samples from a 20 km transect along the SRE and 7 samples from 3 major wetland sub-environments (wet prairie, pine savanna, and cypress forest) in the ENP. The objective is to establish the spatial and statistical relationships between surface pollen assemblages and local vegetation, and reveal the chemical characteristics of the surface soil in different wetland environments by using X-ray fluorescence (XRF) analysis.

Chapter 4 presents core SRM, which is retrieved from the mouth of the SRE and contains an estimated 5,700 years of palynological history. The objectives of this chapter are to document the formation of freshwater wetlands, to demonstrate how they have changed over time, to explore their transition to mangrove swamp, and to identify the timing of these important transitions during the mid to late Holocene.

Chapter 5 evaluates the distinctive carbonate-rich clastic layer left by Hurricane Wilma (2005). The primary goal is to identify the sedimentary signature of Hurricane

Wilma by multi-proxy analyses (loss-on-ignition, XRF, pollen), and use this storm as a modern analog to identify other paleohurricane events in the sedimentary record.

Chapter 6 presents palynological, XRF, and loss-on-ignition data of all 4 cores retrieved from a 20 km transect along the Shark River Estuary. The objective is to document evolution of the Shark River Estuary from the mid-Holocene and the millennial-scale vegetation dynamics driven by climatic changes and allogenic forcing in the Everglades.

Finally, **Chapter 7** summarizes the main discoveries and hypotheses generated from this dissertation and identify questions that need to be answered in future studies.

References

Alongi, D.M., 2002, Present state and future of the world's mangrove forests, Environmental Conservation, 29:331-349

Alongi, D.M., 2008, Mangrove forests: resilience, protection from tsunamis, and response to global climate change. Estuarine, Coastal and Shelf Science 76: 1-14

Bender, M.A., Knutson, T.R., Tuleya, R.E., Sirutis,J.J., Vecchi, G.A., Garner, S.T., and Held, I.M., 2010, Modeled Impact of Anthropogenic Warming on the Frequency of Intense Atlantic Hurricanes, Science, 327: 454-458

Castañeda-Moya, E., Twilley, R.R., Rivera-Monroy, V,H., Zhang, K.Q., Davis III, S.E., and Ross, M.S., 2010, Sediment and Nutrient Deposition Associated with Hurricane Wilma in Mangroves of the Florida Coastal Everglades, Estuaries and Coasts, 33: 45-58

CERP, 2000, Comprehensive Everglades Restoration Plan, U.S. Army Corps of Engineer and South Florida Water Management District, Florida, URL: http://www.evergladesplan.org/ (Accessed 24 December 2014)

Chen, R., and Twilley, R.R., 1999a, A simulation model of organic matter and nutrient accumulation in mangrove wetland soils, Biogeochemistry, 44: 93-118

Chen, R., and Twilley, R.R., 1999b, Patterns of mangrove forest structure and soil nutrient dynamics along the Shark River Estuary, Florida, Estuaries, 22: 955-970

Duke, N.C., Meynecke, J.O., Dittmann, S., Ellison, A.M., Anger, K., Berger, U., Cannicci, S., Diele, K., Ewel, K.C., Field, C.D., Koedam, N., Lee, S.Y., Marchand, C., Nordhaus, I., and Dahdouh-Guebas, F., 2007, A world without mangroves? Science, 317: 41-42

Elsner, J.B., Kossin, J.P., and Jagger, T.H., 2008. The increasing intensity of the strongest tropical cyclones, Nature 455: 92–95

Farnsworth, E.J., and Ellison, A.M., 1997, The global conservation status of mangroves, Ambio, 26: 328-334

Intergovernmental Panel on Climate Change (IPCC) (2014), Climate Change 2013: The Scientific Basis. Contribution of Working Group I to the Fifth Assessment Report of the Intergovernmental Panel on Climate Change, edited by S. Solomon et al., Cambridge Univ. Press, New York.

Lodge, T.E., 2010, The Everglades Handbook: Understanding the Ecosystem, second edition, Boca Raton, Florida: CRC Press.

Ross, M.S., Meeder, J.F., Sah, J.P., Ruiz, P.L., and Telesnicki, G.J., 2000, The southeast saline Everglades revisited: 50 years of coastal vegetation change, Journal of Vegetation Science, 11:101–112

Rudnick, D., Chen, Z., Childers, D., Boyer, J., and Fontaine, T., 1999, Phosphorus and nitrogen inputs to Florida Bay: The importance of the Everglades watershed, Estuaries 22:398–416.

Simard, M., Zhang, K.Q., Rivera-Monroy, V.H., Ross, M.S., Ruiz, P.L., Castañeda-Moya, E., Twilley, R.R., and Rodriguez, E., 2006, Mapping height and biomass of mangrove forests in Everglades National Park with SRTM elevation data, Photogrammetric Engineering and Remote Sensing, 72: 299-311

Smith III, T.J., Anderson, G.H., Balentine, K., Tiling, G., Ward, G.A., Whelan, K.R.T., 2009, Cumulative impacts of hurricanes on Florida mangrove ecosystems: Sediment deposition, storm surges and vegetation, Wetlands, 29: 24-34

Smith III, T.J., Robblee, M.B., Wanless, H.R., and Doyle, T.W., 1994, Mangroves, Hurricanes, and Lightning Strikes, BioScience, 44: 256-263

Snedaker, S.C. 1993, Impact on mangroves. In: Climatic change in the Intra-Americas Sea. (Ed. G.A. Maul), Edward Arnold, London, pp. 282-305.

Valiela, I., Bowen, J.L., and York, J.K., 2001, Mangrove forests: one of the world's threatened major tropical environments, BioScience, 51: 807-815

Wanless, H.R., Parkinson, R.W., and Tedesco, L.P., 1994, Sea level control on stability of Everglades wetlands, In Everglades. The ecosystem and its restoration, S.M. Davis, and J.C. Ogden, (Eds). St. Lucie Press, Delray Beach, FL: 199-223

CHAPTER 2. MID-HOLOCENE MANGROVE DEVELOPMENT ACROSS THE WESTERN NORTH ATLANTIC: A REVIEW OF POLLEN AND ASSOCIATED PALEOECOLOGICAL RECORDS

Introduction

Mangroves are salt-tolerant trees capable of forming unique intertidal forests along the tropical/subtropical coasts. Mangrove forests are extremely productive, second only to coral reefs (Duarte and Cebrian 1996). Mangrove swamps also provide essential ecological services to coastal ecosystems and society by providing habitats for other biota (Cannicci et al., 2008; Bouillon et al., 2004; Kristensen et al., 2008; Nagelkerken et al., 2008) and offering shoreline protection against storm surges, tsunamis, waves, and erosion (Badolaand Hussain, 2005; Barbier et al., 2008; Dahdouh-Guebas et al., 2005; Kaplan et al., 2009; Olwig et al., 2007). Because of their unique morphological and ecophysiological features, the distribution and development history of mangroves provide important insights into past climate and sea-level changes (Alongi, 2002; Ellison, 2008).

Due to the stabilization of sea level and the development of modern shorelines (Scholl et al., 1969; Gleason and Stone, 1994, Digerfeldt and Hendry 1987; Torrescano and Islebe, 2006), the mid-Holocene is the most important period for mangrove development along the western North Atlantic (WNA), one of the world's largest and most productive mangrove habitats (Giri et al., 2011; McKee et al., 2007). However, few studies have documented the long-term development of mangroves and the timing and factors controlling the establishment and expansion of mangroves in this region during the early to mid-Holocene. Such studies are very important due to

the sensitivity of mangroves to extreme temperature fluctuations, and their use as sea-level indicators (Ellison, 2008; Alongi, 2008).

Palynological data provide detailed records of long-term coastal vegetation changes (Chappell and Grindrod, 1985; Liu et al., 2008; Willard and Bernhardt, 2011). Anaerobic conditions in mangrove sediment allow the long-term preservation of fossil pollen, hence, the combination of fossil pollen analysis and radiocarbon dating provides accurate records of mangrove and sea-level history.

This chapter reviews the paleoecological records of mangrove-dominant habitats from 24 study sites in the WNA (Fig. 1, Table 1), with particular emphasis on the developmental history of *Rhizophora*. Study areas include the Caribbean basin, Bermuda, and South Florida. A variety of proxy data including pollen, marine microfossils, microscopic charcoal, mangrove peat stratigraphy, and chemical and isotopic records are examined. These published palynological and associated records provide abundant geographic information in regards to mangroves in the WNA. The purpose of this review is to (1) summarize the history of sea-level rise (SLR) and climate changes in the WNA; (2) document the spatial and chronological patterns of the establishment and expansion of *Rhizophora*; (3) identify the factors controlling the development of *Rhizophora* in this region; and (4) identify the response of *Rhizophora* to regional climatic changes from the pollen records. It should be noted that the paucity of accurate chronologies has limited our ability to document the timing of mangrove development at some specific sites.

Regional climate and sea-level history during the Holocene

Climate

Due to the lack of suitable sites for palynological and paleolimnological studies, the number of long-term Caribbean environmental records for the Holocene is limited (Higuera-Gundy et al., 1999). In general, the climate in the Caribbean basin is humid during the early to mid-Holocene, followed by a drier climate to the present. Oxygen isotopic and pollen records from Lake Miragoane in southern Haiti show increased humidity from 8,000 to 3,200 cal yr BP (Hodell et al., 1991), supported by a pollen study from the same site showing a shift from a shrubby community between 10,000 to 7,000 ^{14}C yr BP to a moist forest between 7,000 to 3,200 ^{14}C yr BP (Higuera-Gundy et al., 1999). A study from the Mexican-Belizean border area also suggests a more humid climate than present at 5,000 cal yr BP (Torrescano and Islebe, 2006). After 3,200 cal yr BP, precipitation levels generally decreased with widespread evidence of drier conditions across the Caribbean basin (Hodell et al., 1991; Gleason and Stone, 1994; Kjellmark, 1996). A pollen record documenting a shift from *Rhizophora*-dominant to *Avicennia*-dominant stands along the Caribbean coast of Colombia suggests drier conditions between ~2,850 - 2,450 cal yr BP (Urrego et al., 2013), while a study from Quintana Roo, Mexico reveals drier climate since 1,500 cal yr BP (Islebe and Sanchez, 2002). A pollen record from the northern Yucatan showing the replacement of *Rhizophora* by *Conocarpus* indicates reduced precipitation from 3,500 to 1,000 cal yr BP (Aragón-Moreno et al., 2012). The severe droughts associated with the collapse of the ancient Maya civilization ~1,000 cal yr BP are another indication of increasing aridity during the late Holocene, and these

episodes of drought mark the transition to present climate conditions in the Caribbean basin (Islebe and Sanchez, 2002; Torrescano and Islebe, 2006).

The paleoenvironmental records from southern Florida show a different precipitation history, with several studies revealing a stepwise increase in precipitation over the past 5,000 years. High-resolution pollen analyses record a shift from a drier *Quercus*-dominant system to a wetter *Pinus*-dominant system in many sites in Florida during the middle Holocene (Grimm et al., 1993; Watts and Stuiver, 1980; Donders et al., 2005). Similar precipitation changes have been documented for southern Alabama (Delcourt, 1980) and southern Georgia (Watts, 1971). Donders et al. (2005) suggest that the intensification of El Niño-Southern Oscillation (ENSO) after 3500 cal yr BP increases the water availability in south Florida and marks the onset of modern-day precipitation patterns. This conclusion is supported by our pollen records from the Shark River Estuary showing that short-hydroperiod prairies were replaced by long-hydroperiod prairies between 3,500 to 1,100 cal yr BP (**Chapter 4, 6**). However, the increased precipitation after the mid-Holocene is not reflected in the X-ray fluorescence (XRF) record from Charlotte Harbor, FL (van Soelen et al., 2012), which shows a maximum in precipitation and runoff around 5,000 cal yr BP followed by a decrease in precipitation.

Sea-level

Sea-level curves are generally very similar across the WNA from mid-to-late Holocene (Toscano and Macintyre, 2003). Sea-level curves from Florida and Bermuda (Wanless et al., 1994), Jamacia (Digerfeldt and Hendry, 1987), eastern

Venezuela (Rull et al., 1999), and Trinidad (Ramcharan, 2004) all show a rapid rate of sea-level rise (>5 mm/yr) between 8,000 and 5,500 cal yr BP, a moderate rate (2.3 mm/yr) from 55,00 to 4,000 cal yr BP, and a slow rate after ~3,000–2,500 cal yr BP (0.4 mm/yr), at which time sea-level began to stabilizes across the WNA (Scholl et al., 1969; Wanless et al., 1994; Ross et al., 2009; Rull et al., 1999; Behling et al., 2001). This mid-to-late Holocene sea-level history can also be observed in pollen histories from across the entire Caribbean (Ramcharan, 2004 and 2005; Ramcharan and McAndrews, 2006; Peros et al., 2007; Urrego et al., 2013) and South Florida (Yao et al., 2015), primarily associated with the establishment and expansion of mangrove species (*Rhizophora* in particular), because *Rhizophora* generally grow between mean sea-level and mean high water, and their sedimentary records are commonly utilized as a sea-level indicator (Ellison, 2008).

Mangrove ecology

Mangroves in the WNA occur across a wide range of sedimentary environments, from alluvial habitats with abundant mineral input to oceanic mangroves rooted in their own peat (McKee et al., 2007). In the WNA, mangroves typically occupy the inter-tidal zone in the tropical and subtropical regions below the ~28 °N latitude (Smithsonian Marine Station), with their distribution limited by the 20 °C isotherm for winter sea surface temperature (SST) (Alongi, 2008). These mangrove forests typically consist of three true tree mangrove species: *Rhizophora mangle* (red mangrove), *Avicennia germinans* (black mangrove), and *Laguncularia racemosa* (white mangrove), as well as *Conocarpus erectus* (buttonwood), a mangrove associate

(Urrego et al., 2010). Dense mangrove forests occupy >1 million ha from Bermuda through the Caribbean coast of South America (FAO, 2003; Simard et al., 2006).

The wind-pollinated *Rhizophora* is the most prolific pollen producer among the mangrove species in the region (Behling et al., 2001). Being insect-pollinated, *Avicennia*, *Laguncularia*, and *Conocarpus* are usually underrepresented in pollen records (Urrego et al., 2010). *Rhizophora* has unique aerial roots which allow them to colonize sites with unstable substrate and direct tidal influence (Hogarth, 2007). *Avicennia* typically colonize highly saline environments, with *Laguncularia* and *Conocarpus* generally occurring in slightly fresher environments (Hogarth, 2007). Propagules of *Rhizophora* and *Avicennia* can float in seawater for more than 100 days and produce roots after 40 days (Ellison, 1996). These results indicate that ocean currents (especially the Loop Current and Gulf Stream) can function as a viable distribution system for *Rhizophora* and *Avicennia*.

Interpretation of the mangrove pollen records

The analysis of mangrove pollen has been an essential element in coastal environmental reconstructions throughout the tropics. By common usage, due to its prolific production of pollen, *Rhizophora* percentages of >50% in total pollen assemblages are accepted as indicating *Rhizophora* dominant pure mangrove stands, while percentages of < 50% indicate sites adjacent to *Rhizophora* stands (Chappell and Grindrod, 1985; Woodroffe et al., 1985; Behling et al., 2001). Due to the poor representation of *Avicennia* and *Laguncularia*, percentages of 2 to 5% of these taxa in total pollen sum have been interpreted to represent *Avicennia* and *Laguncularia*

dominant mangrove forests (Behling et al., 2001; Urrego et al., 2009, 2010). In addition, some studies have reported large mortality of *Rhizophora* caused by winds and storm surges generated by hurricanes because *Rhizophora* cannot resprout.

Due to their tolerance of high salinity, high percentage of *Avicennia* pollen typically reflects saline environments (Urrego et al., 2010). A sudden increase of *Avicennia* in pollen percentages has also been suggested as resulting from droughts and plagues (González et al., 2010). Unlike *Rhizophora*, *Avicennia* and *Laguncularia* have been shown to recover rapidly after massive defoliation due to their resprouting capability (Smith et al., 1994; Baldwin et al, 1995, 2001; Thaxton et al, 2007). They have been reported as pioneer colonizers in gap openings created by hurricanes (Benfield et al., 2005; Hogarth, 2007). Therefore, increased percentages of *Avicennia* and *Laguncularia* pollens often indicate changes caused by hurricanes and other disturbances (Medina et al., 1990; Urrego et al., 2013). Replacement of *Rhizophora* by *Conocarpus* has likewise been suggested as resulting from disturbances such as hurricanes and droughts (Islebe and Sanchez, 2002; Aragón-Moreno et al., 2012).

Proxy records from the western North Atlantic

Early palynological records identify *Rhizophora* as the first mangroves to occur in the WNA, with an earliest appearance in the upper Eocene, and reaching high percentages in the Miocene (Germeraad et al., 1968). *Rhizophora* occurrences are recorded for the Oligocene in Puerto Rico (Graham, 1995) and for the Oligo-Miocene in Mexico (Langenheim et al., 1967). *Avicennia* made its first appearance in the

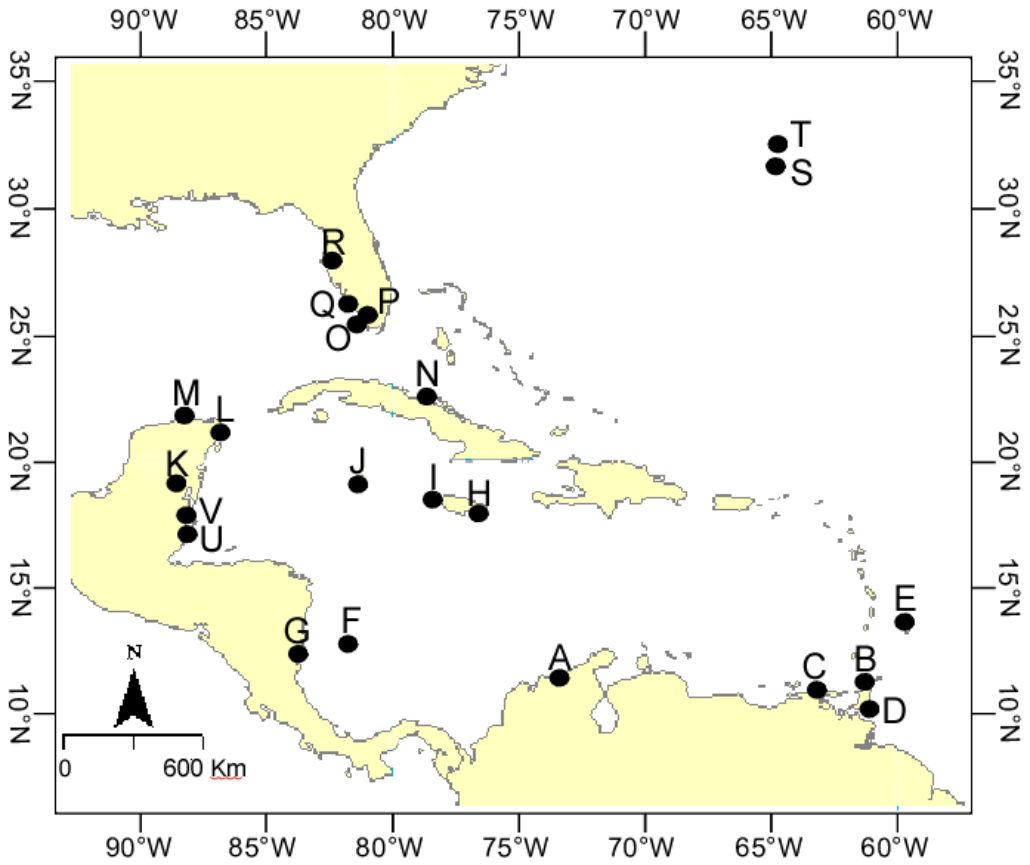

Figure 1. A map including all the study sites reviewed in this paper. See Table 1 for more details of each site.

region during the late Miocene (Graham, 1995). During the early Holocene, mangroves were rapidly established and drowned in coastal areas of the Caribbean due to the rapid sea-level rise (Purdy et al., 1975; Ebanks, 1975; Halley et al., 1977; Macintyre et al., 1995). During the mid-Holocene when the rate of SLR slowed appreciably, mangroves recolonized the Caribbean coasts, as modern shorelines were formed (Scholl et al., 1969, Gleason and Stone, 1994, Digerfeldt and Hendry 1987; Torrescano and Islebe, 2006).

Table 1. Letters in the first column correspond with the study sites in Figure 1. The ages for the establishment of mangroves are presented as calibrated years before present (cal yr BP). Asterisk (*) indicates that the pollen threshold of establishment of Rhizophora is 5%.

Site	Location	Latitude	Current Elevation	*Establishment of Mangroves (cal yr BP)	Reference
A	Navio Quebrado, Colombia	11° 23' 38"	1 m	> 6,000	Urrego et al., 2013
B	Maracas Swamp, Trinidad	10° 45' 00"	1 m	> 6,700	Ramcharan, 2004; Ramcharan and McAndrews, 2006
C	Playa Medina bay, Venezuela	10° 42' 53"	>5m	7,804	Rull et al., 1999
D	Nariva Swamp, Trinidad	10° 24' 33"	< 5 m	> 6,000	Ramcharan, 2004
E	The Graeme Hall swamp, Barbados	13° 04' 21"	5 m	> 1,300	Ramcharan, 2005
F	San Andres, Colombia	12° 33' 04"	1 m	≈ 3,000	González et al., 2010
G	Bluefields Bay, Nicaragua	12° 06' 43"	0 m	5,000	McCloskey and Liu, 2012
H	Black River, Jamaica	18° 01' 38"	< 0.5 m	6,480	Digerfeldt and Hendry, 1987
I	Negrill, Jamaica	18° 17' 47"	< 0.5 m	7,500	Digerfeldt and Hendry, 1987
J	Grand Cayman, Cayman Islands	19° 21' 34"	3-4 m below MSL	4,000	Ellison, 2008
K	El Palmar, Mexico	18° 26' 49"	10 m	5,000	Torrescano and Islebe, 2006
L	Quintana Roo, Mexico	20° 50' 54"	5 m	> 2,500	Islebe and Sanchez, 2002
M	Northern Yucatan, Mexico	21° 34' 44"	2 m	> 3,800	Aragón-Moreno et al., 2012
N	Laguna de la Leche, Cuba	22° 11' 60"	2.5 m below msl	4,000	Peros et al., 2007
O	Shark River Mouth, Everglades	25° 21' 07"	0 m	3,700	Yao et al., sumbitted
P	Ten Thousands Islands, Everglades	25° 51' 31"	Below msl	3,500	Parkinson, 1989
Q	Tarpon Bay, Everglades	24° 24' 36"	0 m	2,300	Willard and Bernhardt, 2011
R	Tampa Bay, Florida	27° 50' 24"	4 m below msl	7,500	van Soelen et al., 2010
S	Hungry Bay, Bermuda	32° 17' 26"	< 0.5 m	2,100	Ellison, 1996
T	Mangrove lake, Bermuda	32° 19' 59"	Below msl	3,000	Ellison, 1993
U-1	Tcc2, Twin Cays, Belize	16° 49' 58"	0 m	8,240	Wooller et al., 2004
U-2	Tcc1, Twin Cays, Belize	16° 49' 48"	0 m	8,000	Wooller et al., 2007
U-3	Twin Cays, Belize	16° 49' 48"	0 m	8,101	Macintyre et al., 2004
V	Spanish Lookout Cay, Belize	17° 25' 05"	0 m	8,000	Monacci et al., 2009

The Caribbean Coast of South America

Several pollen records exist for the Caribbean Coast of South America. A study from Playa Medina, Venezuela, uses pollen analysis, anatomical analysis of wood, and radiocarbon dating to document the occurrence of mangroves in the Caribbean in the Holocene (Rull et al., 1999). Very significant levels of *Rhizophora* and *Avicennia* (33% and 18% respectively) were found in a peat layer 920 cm below the present sea level and dated at ~ 7,800 cal yr BP. This is the earliest occurrence of mangroves on the Caribbean coast of South America. However, this mangrove peat layer is buried by sand and clay. Therefore the evidence does not support the continuous establishment of the mangroves at the site throughout the Holocene.

The earliest continuous *Rhizophora* pollen record is found in a 980 cm long sediment core from Maracas Swamp, Trinidad, which dated back to 6,700 cal yr BP (Ramcharan and McAndrews, 2006). *Rhizophora* is the dominant taxa in pollen record from 6,700 cal yr BP, thereby indicating continuous presence of an *in situ Rhizophora* stand at the site. Another core from Trinidad reveals the displacement of terrestrial flora by *Rhizophora* in the Nariva swamps at 6,000 cal yr BP with a significant *Rhizophora* expansion at 4,700 cal yr BP followed by a substantial decline at 4,000 cal yr BP (Ramcharan, 2004). Both pollen records from Trinidad show replacement of *Rhizophora* by freshwater marsh species from ~1,500 cal yr BP. *Rhizophora* was gradually replaced by Cyperaceae and *Polypodium* at Maracas Swamp, and replaced by Cyperaceae and Gramineae at Nariva swamps.

Urrego et al. (2013) present palynological data from Nav ́o Quebrado elucidating the development of mangrove forests along the Caribbean coast of Colombia (Fig. 2). Their

high-resolution pollen record indicates that accelerated sea-level rise favored the colonization of *Rhizophora* at the coastal lagoons at ~ 6,280 cal yr BP. Between 6,280 and 3,840 cal yr BP, a salt marsh environment fringed by sparse mangrove forests were developed at the study site, as evidenced by high percentages of Poaceae and Cyperaceae and low proportions of mangrove pollen. The period between 3840 and 2,000 cal yr BP is characterized by marine still-stand and the expansion of the mangrove species (*Laguncularia* and *Rhizophora*). During this period, *Rhizophora* became the dominant vegetation at the Nav ó Quebrado, except for the period between 2,850 and 2,450 cal yr BP, when *Rhizophora* was replaced by *Avicennia*, Cyperaceae, and forest taxa. After 2,000 cal yr BP, mangroves declined in spite of stable sea-level (Toscano and Macintyre, 2003), probably due to the extreme seasonality and regional drought associated with the Medieval Warm Period (MWP) (Haug et al., 2001; Hodell et al., 2001). Toscano and Macintyre (2003) suggest that although the establishment of mangroves was influenced by many factors (high air temperatures, tidal and fresh water input, salinity, geomorphological setting, soil type, and nutrient and light availability), stabilization of the SL around 3,000–2,500 cal yr BP plays the most important role in the expansion of the mangroves in the Caribbean coast of Colombia.

The occurrence of large tropical storms can sometimes be inferred from palynological studies conducted in mangrove-dominant areas. Ramcharan (2005) suggests that a strong storm at ~600-700 cal yr BP caused the abrupt and permanent replacement of a *Rhizophora*-dominant coastal forest in Barbados by weedy flora. Gonzalez et al. (2010) identifies a catastrophic storm at ~350 cal yr BP as removing ~2000 years of deposition at the base of the core from San Andres Island. This event coincides with the pollen-barren interval

in a layer of organic matter mixed with gravels. Their pollen diagram also suggests that mangrove forests already existed before 2,500 cal yr BP. However, it is worth noting that the possible reworking at the bottom of the core caused by the storm makes it difficult to interpret the basal radiocarbon date.

The Caribbean coast of Central America

Pollen records from Twin Cays along the inner shelf of Belize indicate that mangroves are established there during the early-Holocene, much earlier than other locations in the WNA (Wooller et al., 2004, 2007; Macintyre et al., 2004; Monacci et al., 2009). Pollen and isotopic analyses by Wooller et al. (2004) indicate that tall *Rhizophora* stands mixed with *Avicennia* and *Laguncularia* were already established at Twin Cays, Belize from over 9,000 cal yr BP (Fig. 2). They suggest that a marked increase of *Myrsine* at ~6,300 cal yr BP was resulted from a disturbance event (possibly hurricane or fire), while attributing the second increase in *Myrsine* and *Avicennia* from 2,500 to 1,000 cal yr BP to a drop in sea-level. A low peat accumulation rate suggests that scrub *Rhizophora* is the dominant taxa at the site from 4040 cal yr BP to the present, possibly due to phosphorus limitation associated with a decrease in the rate of sea-level rise after 5,000 cal yr BP. Another study from Twin Cays, Belize presents a similar mangrove history. *Rhizophora* has been the dominant taxa at the site since 8,100 cal yr BP, apart for the period from 6,300 to 3,500 cal yr BP, which is a marked by an increase in *Myrsine* and *Avicennia* (Wooller et al., 2007). These results agree with an earlier study by Macintyre et al. (2004), whose sedimentary record, based on 19 vibracores collected along two transects across Twin Cays, shows that mangrove communities were established at ~8000 years ago. Although this record indicates that mangroves were drowned

and covered by lagoonal sand at several locations, in most areas mangrove communities kept pace with sea level. The authors state that radiocarbon dates of peat and sediment from this study are in agreement with the most commonly used sea-level curve for WNA (Toscano and Macintyre, 2003).

Monacci et al. (2009) presents a pollen and isotopic study from Spanish Lookout Cay, Belize. Their radiocarbon chronology shows that *Rhizophora* has been the dominant taxa at the site since 8,000 cal yr BP, although *Avicennia* and *Laguncularia* were also present. Their pollen record also indicates a decrease of *Rhizophora* and an increase of non-halophytic plants (*Myrsine*, Amaranthaceae) between 3,600 and 600 cal yr BP, similar to Wooller et al.'s (2004, 2007) record from Twin Cays. All of these studies attribute this change to a less-saline environment resulting from increased freshwater input. In general, studies from Twin Cays and Spanish Lookout Cay, Belize, show similar Holocene sea-level and vegetation history, and document that mangroves became established on Belizean cays inside the barrier reef much earlier than in other locations within the Caribbean basin.

McCloskey and Liu (2012) present a proxy record from Bluefields Bay that reveals the history of paleoecological changes and hurricane strikes for the southern Caribbean coast of Nicaragua. Their pollen record suggests that a thick *Rhizophora*-dominant fringing mangrove forest developed at ~5,000 cal yr BP and expanded at 3,000 cal yr BP when the site became a shallow marine lagoon. From ~2,200 to 1,000 cal yr BP, mangroves were replaced by less halophytic species such as *Morella* and palms, probably representing the development of a backbarrier swamp surrounded by bushes and tropical forests. The results indicate that the deposition of *in situ* peat has kept pace with SLR since 3,000 cal yr BP. Their record is

consistent with the timing of the sea-level stabilization in the Caribbean basin (Rull et al., 1999; Behling et al., 2001).

Several pollen studies investigating Holocene sea-level and climate changes have been produced from the Yucatan peninsula of Mexico (Islebe and Sanchez, 2002; Torrescano and Islebe, 2006; Aragón-Moreno et al., 2012). A pollen study from El Palmar (Fig. 2), Mexico reconstructs the environmental history of the mangrove and tropical forests for the last 5000 years (Torrescano and Islebe, 2006). *Conocarpus* and *Rhizophora* became the dominant species at 4,600 cal yr BP due to the seasonal flooding of the Rio Hondo River, which deposited saline sediments due to higher sea level. By ~3,800 cal yr BP, the pollen assemblage resembles the present vegetation with *Conocarpus* as the dominant mangrove species. Islebe and Sanchez (2002) present a pollen record from Quintana Roo, on the Caribbean coast of Mexico, which shows that *Rhizophora* has been the dominant taxa at the coastline from at least 2,500 cal yr BP until ~500 cal yr BP when *Conocarpus* began to be the dominant taxa. During the period between 1,400 and 1,000 cal yr BP, *Rhizophora* disappeared and was replaced by *Conocarpus* and secondary forest communities (Apocynaceae, Moraceae, Ulmaceae, *Hedyosmum*, and Poaceae). Because *Rhizophora* pollen is > 70% of the total pollen sum at the very bottom of the core, it is reasonable to assume that *Rhizophora* became established earlier than 2,500 cal yr BP.

A fossil pollen record from the northern Yucatan Peninsula documents climate and vegetation changes over the past 3800 years (Aragón-Moreno et al., 2012). *Rhizophora* is the dominant mangrove species between 3,800 and 3,450 cal yr BP, suggesting high precipitation and salinity in flooded areas (Hogarth, 2010). *Conocarpus* gradually replaces *Rhizophora*

after 3,460 cal yr BP. The pollen record shows a couple of fluctuations between *Conocarpus* and *Rhizophora* from 1,720 cal yr BP, interpreted as resulting from humidity changes. The authors state that the replacement of *Rhizophora* by *Conocarpus,* which commonly occurs in inland habitats, suggests a drier climate; and this shift in vegetation composition at the late Holocene suggests a trend toward a dryer climate, marking the transition to present conditions in the Yucatan (Aragón-Moreno et al., 2012).

The Greater Antilles

Two mangrove macrofossil records from Jamaica suggest the initiation of mangrove forests at ~7,500 and ~6,500 cal yr BP (Digerfeldt and Hendry, 1987). However, as the study is based on the identification of peat types and the microscopic analysis of rootlets, the composition of the mangrove forest cannot be determined at either site. Both study sites are *Rhizophora* and *Conocarpus*-codominant at the present time. A study from the Cayman Island using similar methods finds 3 m of mangrove peat, deposited at least 3000 years ago, under a seagrass bed presently 4 m below the mean sea-level (MSL) (Ellison, 2008).The author interprets this peat layer as a landward mangrove zone that became submerged under the rapid SLR. It is worth noting that neither studies show solid evidence to support continuous occurrence of mangroves at the study sites.

Peros et al. (2007) applied loss-on-ignition, pollen, calcareous microfossil, and plant macrofossil analyses on cores taken from Laguna de la Leche to determine the ecological and hydrological changes in the coastal area of northern Cuba. This multi-proxy record shows that a shallow lake is formed in the basin ~6,200 cal yr BP due to SLR-driven elevation increase of the aquifer. Pollen analysis suggests that mangrove became established at ~5,000

cal yr BP and a large-scale expansion of *Rhizophora* started from 1,700 cal yr BP (Fig. 3). Evidence of this late-Holocene mangrove expansion has been found in multiple coring sites from Laguna de la Leche. Their study concludes that SLR is the dominant cause of the development of mangroves during the mid-Holocene on the northern coast of central Cuba and the southeastern United States.

South Florida and Bermuda

The earliest evidence of mangroves in Florida occurs in a pollen record from Tampa Bay, FL (van Soelen et al., 2010). *Rhizophora* pollen is found at 7,500 cal yr BP, but the percentages are consistently low (≤5 %) throughout the record. Because *Rhizophora* is a very prolific pollen producer (Behling et al., 2001), such low percentage possibly indicates a non-local, water-transported origin. The oldest definitive evidence of mangrove peat is dated at 2,900 to 3,600 cal yr BP from southwest Florida (Scholl et al., 1969; Parkinson, 1989). These sedimentary records suggest that the coastal mangrove forests began keeping pace with rising sea level only during the last 3000 years, during which time sea level has risen only slightly > 1 m. The authors conclude that that shoreline stabilization and establishment of mangroves started about 3,500 cal yr BP (Scholl et al., 1969; Parkinson, 1989).

Chapter 4 and **6** show multi-proxy record from the Shark River Estuary, FL, which uses XRF, loss-on-ignition, and pollen analyses to investigate the development of coastal wetlands in southwest Florida over the past 5700 years. My record indicates that mangroves appeared at the mouth of the Shark River Estuary since ~3,800 cal yr BP, and became fully established at 1,150 cal yr BP. These data suggest that the timing of shoreline stabilization and formation of mangrove forest in southwest Florida may have been significantly younger than has been

previously proposed for this area. It is worth noting that during the period between ~ 2,000 to 1,300 cal yr BP, abundance of *Pinus* and *Morella* increases in the pollen assemblage. Pollen record from a more recent study shows that *Rhizophora* first appeared at Tarpon Bay, FL (20 km inland from the mouth of the Shark River Estuary), from ~2,200 cal yr BP (Willard and Bernhardt, 2011). *Rhizophora* disappeared and replaced *by Morella* from 1,600 to 1,200 cal yr BP, and became the dominant species from 1,200 cal yr BP.

At 32 °N, Bermuda hosts the most northernmost mangrove communities location in the world, owing to its subtropical climate associated with the warm Gulf Stream that passes to the west and north (Ellison, 1993). Pollen records show that mangroves appears as early as 3,000 cal yr BP in Mangrove Lake, and at ~ 2,100 cal yr BP at Hungry Bay, the largest mangrove area in Bermuda (Ellison, 1993, 1996). Only *Rhizophora* is found in the records with no records of *Avicennia* and *Laguncularia* ever being present in Bermuda (Watts and Hansen, 1986; Ellison, 1996). These studies are consistent with records from Florida, where expansive mangroves were not present until after 3,500 cal yr BP (Scholl et al., 1969; Yao et al., 2015).

Methods

This chapter concentrates on the last nine millennia (calibrated), for which a reasonable amount of high-quality data are available. The data used consist of 16 pollen diagrams and 8 macrofossil records ranging from 10 °42' 36"N to 32 °19' 48"N (Table 1). Ages referred in this paper are reported as calibrated years before present (cal yr BP). The *Rhizophora* percentage curves from each pollen diagram and the *Rhizophora* macrofossil records have been digitized and complied (Fig. 2). All the *Rhizophora* profiles in Figure 2 are presented

with age as the Y-axis. *Rhizophora* profiles originally presented in this format are used unchanged. For profiles originally presented with depth as the Y-axis, a comprehensive core chronology is calculated on the assumption of constant sedimentation rates between the dated samples. For profiles for which only ^{14}C dates are given, dates are calibrated using CALIB 7.0 and the associated dataset by Stuiver et al., (2010), and a chronology is developed based on the assumption of a constant sedimentation rate between dates. Based on the compiled pollen record, maps are made to show th**e** migration of *Rhizophora* during Holocene (Fig. 3).

Synthesis

Factors controlling the expansion of *Rhizophora*

Among the 24 reviewed records (Fig.2, Table 1), 16 are pollen records showing continuous presence of *Rhizophora* pollen of >5%. Five studies contain mangrove peat with identified *Rhizophora* macrofossils at some point in the stratigraphy. Three studies have macrofossil records supporting the continuous presence of *Rhizophora*. We define the establishment of *Rhizophora* as when continuous presence of this mangrove species started to occur in pollen or macrofossil records. The threshold of 5% pollen is used to mark the beginning of *Rhizophora* establishment at each site (Fig. 3).

Among all the mangrove records reviewed in this paper, the earliest establishment of *Rhizophora* occurred in Belize from more than 8,000 cal yr BP (Fig. 2). During the early Holocene, mangrove communities rapidly colonized the WNA and then were flooded due to the rising sea-level (Purdy et al., 1975; Ebanks, 1975; Halley et al., 1977; Macintyre et al., 1995). However, *Rhizophora* communities managed to keep pace with the rapid early Holocene sea-level rise and formed thick accumulations of peat on the underlying Pleistocene

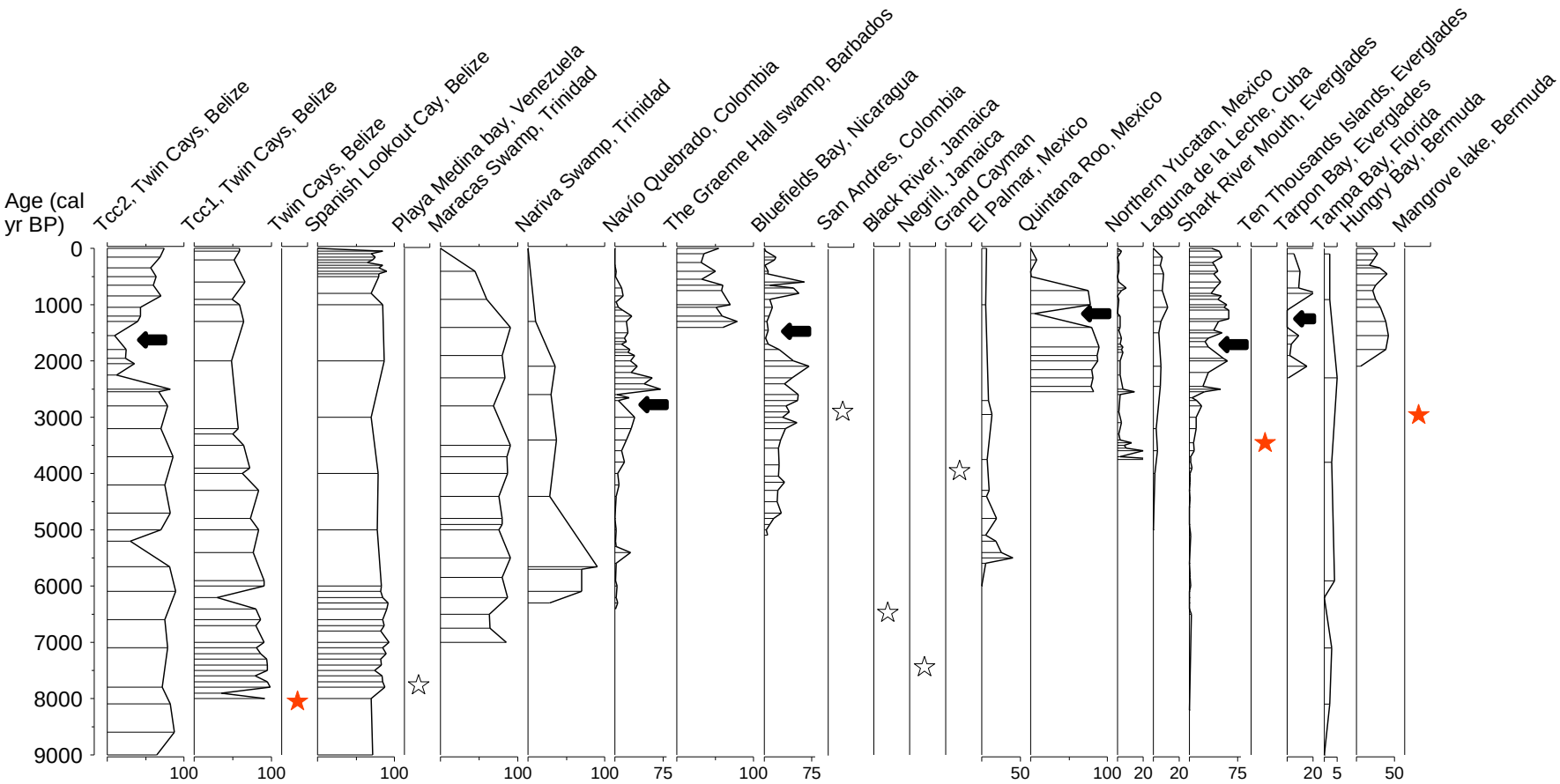

Figure 2. Pollen (%) and macrofossil records of *Rhizophora* compiled from 24 studies summarized in Table 1. Red stars represent macrofossil evidence showing establishment of *Rhizophora* from the marked time to present. White stars represent occurrence of *Rhizophora* only at the marked time during the Holocene. The arrows point to the temporary recession of *Rhizophora* during the late Holocene.

limestone in the south-central area of the Belize Barrier Reef Platform, particularly at Twin Cays (Macintyre et al., 1995). A combination of factors contributed to this anomaly. The most important factor is that hydrological conditions on Twin Cays resulted in very slow decomposition as the flooded, anaerobic conditions prevented the microbial community from decomposing refractory root tissues underground (Middleton and McKee, 2001). As a result, mangroves at Twin Cays have very high rates of below ground accumulation, which contributed substantially to surface elevation of the Belize Barrier Reef Platform and permitted mangrove peat to keep up with the rapid sea-level rise (3 mm/yr) during the early Holocene (Toscano and Macintyre, 2003; McKee et al., 2007). Additionally, the geological setting in the south-central area of the Belize Barrier Reef Platform might be in favor of mangroves to survive strong storm surges that played an important role on regulating the growth of the mangroves. Intense storms can cause massive mangrove mortality, due to mechanical damage, environmental stresses, the erosion of the supporting substrate, and peat collapse (Smith et al., 1994, 2009; Sherman and Fahey, 2001; Woodroffe and Grime, 1999; Cahoon et al., 2003, 2006; Piou et al., 2006). The damage can be especially severe to *Rhizophora* forests, which are incapable of resprouting after defoliation by storms (Baldwin et al, 1995, 2001; Thaxton et al, 2007). At Twin Cays, an extensive offshore barrier reef shelters the low-lying coastline and attenuates the storm surge (Macintyre et al., 2004; McIvor et al., 2013). Therefore, these site-specific conditions may have increased the survivability of *Rhizophora* in the south-central area of the Belize Barrier Reef Platform during the early Holocene.

Figure 2 shows that the earliest records of continuous *Rhizophora* communities on the Caribbean Coast of South America are from Maracas Swamp, Trinidad (>6,700 cal yr BP), Nariva Swamp, Trinidad (>6,000 cal yr BP), and Navío Quebrado, Colombia (>6000 cal yr BP) (Ramcharan, 2004; Ramcharan and McAndrews, 2006; Urrego et al., 2013). By 5,000 cal yr BP, *Rhizophora* has settled at sites from below 11 °N to at least 18 °N at El Palmar, Mexico, just a couple hundred kilometers north of Twin Cays, Belize (Fig. 3) (Torrescano and Islebe, 2006; McCloskey and Liu, 2012). A relatively rapid migration of *Rhizophora* occurs from 5,000 to 3,000 cal yr BP (Fig. 2, 3). Pollen records (Fig. 2, 3) suggest that *Rhizophora* communities established in both Cuba and the Cayman Islands around 4,000 cal yr BP (Peros et al, 2007; Ellison, 2008); in northern Yucatan, Mexico (Aragón-Moreno et al., 2012), Ten Thousands Islands (Parkinson, 1989), and Shark River Estuary, Everglades (**Chapter 4, 6**) around 3,500 cal yr BP; and Bermuda (32 °20' N), the most northerly mangroves in the world, around 3000 cal yr BP (Ellison, 1993). During the next 1500 years, *Rhizophora* rapidly colonized the coastlines of the Yucatan Peninsula and South Florida (Islebe and Sanchez, 2002; Willard and Bernhardt, 2011).

Although many site-specific factors such as local sediment supply, salinity, and nutrient and light availability have been shown to influence the growth rate of mangroves (Krauss etal., 2008), the rate of SLR is generally considered the most important control over the establishment and expansion of mangroves in the WNA during the Holocene (Urrego et al., 2013; Peros et al., 2007). If the rate of mangrove peat accumulation can match the rate of SLR, then mangroves can continuously

colonize the coastal area and develop a pure-stand mangrove community (McKee et al., 2007). Since sea-level records across the WNA region show similar histories (Toscano and Macintyre, 2003; Rull, 1999; Ramcharan, 2004; Milneet al., 2005; Carvalho do Amaral et al., 2006), one would expect the colonization of *Rhizophora* to be synchronized at a regional scale. However, our complied mangrove record suggests a slow, progressive south-to-north migration of *Rhizophora* from the southern edges of the Caribbean Basin toward the Gulf Coast, spanning thousands of years (Fig. 3). Although the oldest *in situ* mangrove forest formed before 8,000 cal yr BP, it took 4000 years for mangroves to reach the northern edge of the Caribbean Basin and Florida (Fig. 2). It is likely that the rate of sea-level rise is not the only major factor controlling the establishment and expansion of *Rhizophora*.

Studies have shown that the global distribution of mangroves is related to winter seawater temperature (Alongi, 2002, 2008). Mangroves prevail in locations with mild winters. Severe freezes can defoliate mangroves and suppress their reproduction, especially the more cold-intolerant *Rhizophora* (Stevens et al., 2006). Thus, the latitudinal limits of mangroves are determined primarily by winter temperatures (Kangas and Lugo, 1990). Across the WNA, increases in average temperature, especially the winter sea surface temperature (SST), is a hallmark of the Holocene (Lorenz et al., 2006; Leduc et al., 2010). Therefore, we hypothesize that a northern migration in threshold winter SST is another major factor controlling the expansion of *Rhizophora* during the Holocene in this region.

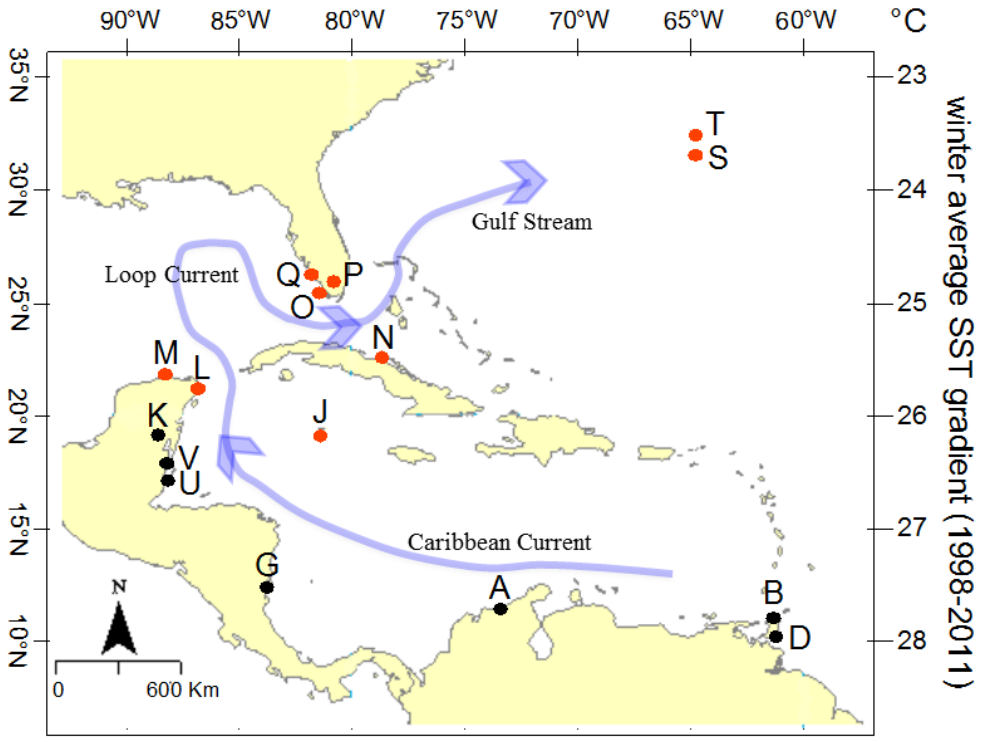

Figure 3. Map showing the expansion of *Rhizophora*. Black dots represent sites where *Rhizophora* established prior to 5,000 yr BP. Red dots represent sites where *Rhizophora* established after and around 3,500 yr BP. The site labels are tied to Table 1. The blue curves represent the course and direction of the Gulf Stream, Caribbean Current, and Loop Current. The winter (December–February) average sea-surface temperature (SST) gradient of the corresponding latitude is showing at the right side. (METED, http://www.meted.ucar.edu/oceans/gulfmexico_carib/print_2.php)

Although the Holocene has been marked by relatively minor climate changes (Mayewski et al., 2004), paleotemperature reconstructions clearly show a significant long-term increase of boreal winter insolation during the Holocene epoch (Laskar, 2004; Lorenz et al., 2006; Leduc et al., 2010). As a result of the shift in perihelion from September to January, and a decrease in axial tilt from 24.2 °to 23.4 °during the last 7000 years (Milankovitch, 1941; Lorenz et al., 2006), boreal winter insolation has increased by ~ 25 W/m^2 in the tropics (Laskar et al., 2004) (Fig. 4). The effects of boreal winter insolation increase have been observed in alkenone-based record, which preferentially captures the boreal winter SST (Huybers and Wunsch, 2003; Rimbu et

al., 2003). Alkenone-derived SST record from Carioca Basin indicates a significant warming of up to 2 °C in the WNA during the Holocene (Herbert and Schuffert, 2000, Leduc et al., 2010) (Fig. 4). Clearly winter SST are highly variable both spatially and temporally across the region. A 13 year winter SST record (1998 to 2011) shows an 3 ° C diffidence between the Caribbean Coast of South America and South Florida (Fig. 3) (METED). Therefore, it is likely that the much warmer winter SST allowed *Rhizophora* to establish on the Caribbean coast of South America (7,000-6,000 cal yr BP) much earlier than at higher latitudes. The temporal pattern of *Rhizophora* establishment shows a migration from the warmest part of the region (Caribbean coast of South America) to the coolest part of the region (South Florida) (Fig. 3). Between 5,000 and 3,000 cal yr BP, as the increase of boreal winter insolation results in higher winter SST across the WNA (Fig. 4) (Lorenz et al., 2006), *Rhizophora* would have been able to establish at higher latitudes, and eventually colonized the coastlines of the Yucatan, South Florida, and Bermuda (Fig. 3). The Gulf Stream joins the Caribbean Current which transports significant amounts of water into the Gulf of Mexico, via the Yucatan Current, and flows to Bermuda through the Straits of Florida (Fig. 3). Given the characteristics of the course of these currents and the ability of *Rhizophora* propagules to remain viable during long periods of salt water immersion (Ellison, 1996), current-driven transportation from south to north across the Caribbean Basin to South Florida seems reasonable during this period. Therefore, we conclude that winter SST is a major factor controlling the survival and expansion of *Rhizophora* along WNA during the Holocene.

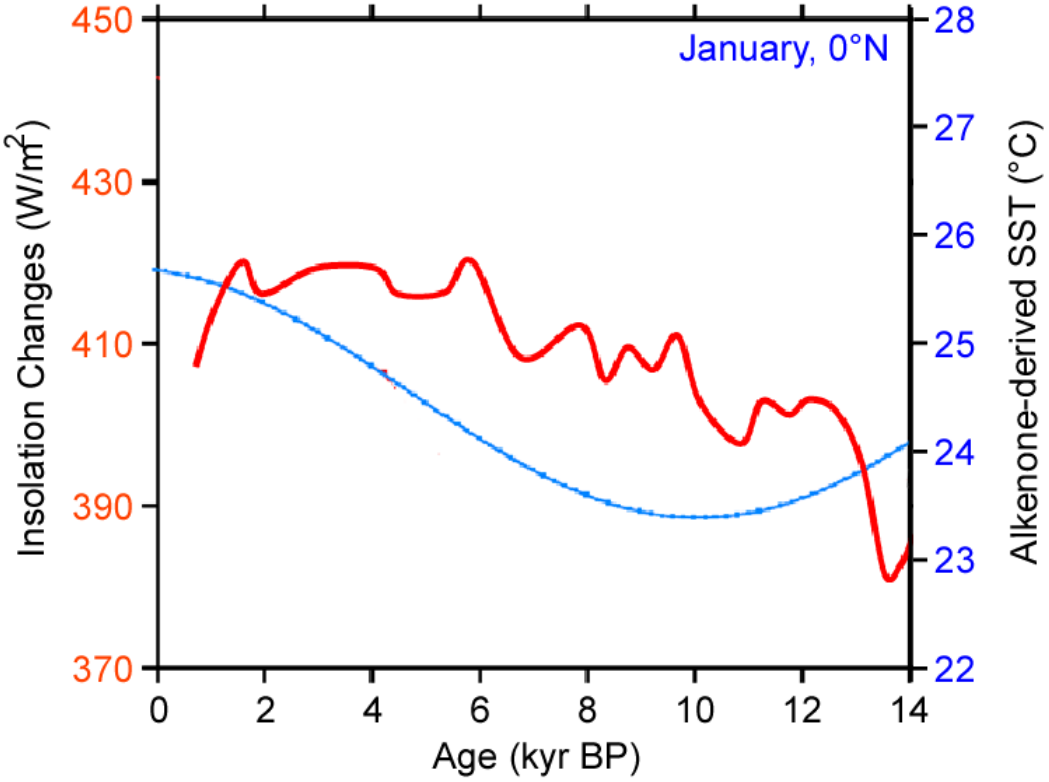

Figure 4. Red curve represents Alkenone-derived Holocene winter SST records of the Western North Atlantic from Cariaco Basin (Herbert and Schuffert, 2000). Blue curve represents record of Holocene boreal winter insolation changes (Laskar et al., 2004). This figure is compiled from Leduc et al., (2010).

Decline of *Rhizophora* between 3,000 and 1,000 cal yr BP

Among the 16 continuous pollen record reviewed in the Chapter, 6 of them show a clear temporary decline of *Rhizophora* between 3,000 to 1,000 cal yr BP (Fig. 2). Pollen record of core Tcc2 from Twin Cays shows that *Rhizophora* was replaced by *Myrsine* and *Avicennia* from 2,500 to 1,000 cal yr BP (Wooller et al., 2004). Pollen record from Nav ó Quebrado, Colombia shows that *Rhizophora* was replaced by *Avicennia*, Cyperaceae, and forest taxa between 2,850 and 2,450 cal yr BP (Urrego et al., 2013). Pollen record from Bluefields Bay shows that *Rhizophora* was replaced by less halophytic species such as *Morella*, *Ilex*, and palms from ~2,200 to 1,000 cal yr

BP (McCloskey and Liu, 2012). Pollen record from Quintana Roo, Mexico shows that *Rhizophora* disappeared and was replaced by *Conocarpus* and upland taxa between 1,400 and 1,000 cal yr BP (Islebe and Sanchez, 2002). The pollen record from the mouth of the Shark River Estuary shows that during the period between ~ 2,000 to 1,300 cal yr BP, abundance of *Pinus* and *Morella* increases, and *Rhizophora* decreases (**Chapter 4 and 6**). Finally, the pollen record from Tarpon Bay (20 km inland from the mouth of the Shark River Estuary) shows that *Rhizophora* disappeared and was replaced *by Morella* from 1,600 to 1,200 cal yr BP (Willard and Bernhardt, 2011).

The events listed above show some similarities. First, *Rhizophora* was replaced by mainly freshwater communities (e.g., *Myrsine*, marsh species, *Myrica*, upland taxa, *Cornocarpus*, *Pinus*....etc). Second, they increased and became the dominant pollen type again after these temporary declines. More importantly, the timelines of these events are in line with each other. Based on these observations, it is likely that a common factor/driver is behind the temporary declines of *Rhizophora* across the WNA from ~3,000 to 1,000 cal yr BP. One possible explanation is that hurricanes are the causative agents for these temporary *Rhizophora* recessions, because hurricane induced replacement of *Rhizophora* by herbaceous and other mangrove species has been reported from studies across the WNA (Smith et al., 1994; Baldwin et al, 1995, 2001; Thaxton et al, 2007), and the recovery of *Rhizophora* takes decades to centuries (Gonz áez et al., 2010; Urrego et al., 2010). The most useful proxy for the detection of paleohurricane events is proven to be overwash clastic sediment layers preserved in sediment cores retrieved from coastal lakes and marshes (Liu and Fearn, 1993, 2000;

Donnelly et al., 2001). In the Bluefields Bay record, McCloskey and Liu (2012) discovered a distinct clay layer embedded in the peat section when Rhizophora was diminished. In the Nav ó Quebrado record, the period of *Rhizophora* recession also consists of clastic materials that are coarser than other deposits in the core (Urrego et al., 2013). These patterns are strong evidence in support of the hypothesis of hurricane induced *Rhizophora* recession. Although clastic materials are absent during the other 4 temporary *Rhizophora* recessions (Islebe and Sanchez, 2002; Wooller et al., 2004; Willard and Bernhardt, 2011, **Chapter 4**), this hypothesis can still be valid because paleohurricane events have been detected in peat cores from mangrove ecosystems where allochthonous sediment source is scarce (**Chapter 5**). More importantly, some studies show elevated north Atlantic hurricane activities during the late Holocene (Liu and Fearn, 1993, 2000; van Soelen et al., 2012; Lane et al., 2011; **Chapter 5**). Based on these data, it is possible that during 3,000 to 1,000 cal yr BP, frequent hurricane strikes changed the composition of the coastal vegetation once was *Rhizophora*-dominant. Although tsunamis are another high-energy source causing massive destruction of coastal vegetation and deposition of clastic sediments, they are unlikely responsible for these *Rhizophora* recessions. Tsunami deposits are normally much coarser, containing pebbles, rocks, and even boulders due to the powerful waves (Goff et al., 2004; Kortekaas and Dawson, 2007), but such sediment types are not mentioned in all the mangrove records summarized in this chapter.

An alternative hypothesis is that they were caused by a regional dry climate between 3,000 and 1,000 cal yr BP. Urrego et al. (2013) stated that low precipitation

and minimum alluvial water input was responsible for the decrease of *Rhizophora* at Nav ó Quebrado, Colombia, between 2,850 and 2,450 cal yr BP. Their hypothesis is supported by Islebe and Sanchez (2002) that the decline of *Rhizophora* at Quintana Roo, Mexico, was cause by drought during late Holocene. Their hypothesis is supported by evidence of widespread precipitation decrease across the WNA during the late Holocene (Hodell *et al.*, 1991; Gleason and Stone, 1994; Kjellmark, 1996; Haug et al., 2001).

A third hypothesis is that the sea-level at the WNA temporarily dropped during the late Holocene. This hypothesis is supported by Wooller et al. (2004). They think that a temporarily decreased sea-level is responsible for elevated topography at Twin Cays that allowed the replacement of *Rhizophora* by *Myrsine*, a shrub that grows in terrestrial environments, between 2,500 and 1,000 cal yr BP. During all the temporary recessions that we observed (Fig. 2), *Rhizophora* was replaced by mainly non-tidal vegetation communities. It implies a markedly different ecosystem at the time, because *Rhizophora* typically is the dominant taxa at sites with unstable substrate and direct tidal influence (Hogarth, 2007). Based on these data, it is possible that the sea-level was lower than present during the late Holocene, and the lower sea-level resulted in shoreline transgression toward offshore to enable marsh, upland, and other mangrove species to occupied coastal areas once was *Rhizophora*-dominant.

Conclusion

This chapter presented a critical review of 24 paleoecological studies addressing the development and expansion of *Rhizophora* in the WNA. By documenting the

regional history of mangrove development, factors controlling these processes during the Holocene were formulated. Previous studies have indicated that the establishment of mangroves in the region is controlled by the rate of the Holocene sea-level rise (Urrego et al., 2013; Peros et al., 2007). However, this hypothesis does not explain the lag of 4,000 years in the occurrence of *Rhizophora* between the South Caribbean Basin and Florida (Fig. 2, 3). It is likely that winter SST has acted as an important control over the distribution pattern of *Rhizophora*, as evidenced by the progressive migration of *Rhizophora* from the southern part of the Caribbean Basin toward the Gulf Coast, which spanned four thousand years. This gradual expansion were likely driven by an increase in the boreal winter insolation of ~25 W/m^2 in the tropics, which increased the winter SST of WNA by ~2 ℃. With warmer winter SST and stable SLR after 3,500 cal yr BP, *Rhizophora* was able to establish at higher latitudes and eventually colonized the coastlines of Yucatan, South Florida, and Bermuda.

We also observe that *Rhizophora* communities across the WNA shown a widespread, though spatially and temporally variable, decline from 3,000 to 1,000 cal yr BP (Fig. 2). These *Rhizophora* recessions are possibly caused by a period of elevated hurricane activities, dry climate, or a temporary drop in the regional sea-level. Further studies using isotopes, geochemistry, or other proxy evidence are needed to test these hypotheses.

References

Alongi, D.M., 2002. Present state and future of the world's mangrove forests. Environmental Conservation 29, 331-349.

Alongi, D.M., 2008. Mangrove forests: resilience, protection from tsunamis, and responses to global climate change. Estuarine, Coastal and Shelf Science 76, 1-13.

Aragón-Moreno, A.A., and Islebe, G.A., 2012. A 3800-yr, high-resolution record of vegetation and climate change on the north coast of the Yucatan Peninsula. Review of Palaeobotany and Palynology 178, 35–42.

Badola, R., and Hussain, S.A., 2005. Valuing ecosystem functions: an empirical study on the storm protection function of Bhitarkanika mangrove ecosystem, India. Environmental Conservation 32, 85–92.

Baldwin, A.H., Platt, W.J., and Gathen, K.L., et al., 1995. Hurricane damage and regeneration in fringe mangrove forests of southeast Florida, USA. Journal of Coastal Research 21, 169-183.

Baldwin, A.H., Egnotovich, M.S., and Ford, M.A., et al., 2001. Regeneration in fringe mangrove forests damaged by Hurricane Andrew. Plant Ecology 57, 151-164.

Barbier, E.B., Koch, E.W., and Silliman, B.R., et al., 2008. Coastal ecosystem–based management with nonlinear ecological functions and values. Science 319, 321-323.

Behling, H., Cohen, M.C.L., and Lara, R.J., 2001. Studies on Holocene mangrove ecosystem dynamics of the Braganc, a Peninsula in north-eastern Para´, Brazil. Palaeogeography, Palaeoclimatology, Palaeoecology 167, 225–242.

Benfield SL, Guzman HM, and Mair JM., 2005. Temporal mangrove dynamics in relation to coastal development in Pacific Panama. Journal of Environmental Management 76, 263–276.

Cahoon DR, Hensel PF, and Spencer T, et al., 2006. Coastal wetland vulnerability to relative sea-level rise, wetland elevation trends and process controls. Ecological Studies 190, 271–292.

Cahoon DR, Hensel P, and Rybczyk J, et al., 2003. Mass tree mortality leads to mangrove peat collapse at Bay Islands, Honduras after Hurricane Mitch. Journal of Ecology 91, 1093–1105.

Cannicci S, Burrows D, and Fratini S, et al., 2008. Faunistic impact on vegetation structure and ecosystem function in mangrove forests, a review. Aquatic Botany 89, 186-200.

Carvalho do Amaral PG, Ledru MP, and Branco FR., 2006. Late Holocene development of a mangrove ecosystem in southeastern Brazil. Palaeogeography, Palaeoclimatology, Palaeoecology 241, 608–620.

Chappell, JMA, and Grindrod J., 1985. Pollen analysis, a key to past mangrove communities and successional changes in North Australian coastal environments. In: Bardsley KN, Davie JDS, and Woodroffe CD (Eds) Coasts and Tidal Wetlands of the Australian Monsoon Region. Australian National University, Canberra, 225–236.

Dahdouh-Guebas F, Jayatissa LP, and Di Nitto D, et al., 2005. How effective were mangroves as a defence against the recent tsunami? Current Biology 15, 443-447.

Davis MB and Botkin DB, 1985. Sensitivity of the fossil pollen record to sudden climatic change. Quaternary Research 23, 327- 340.

Delcourt PA, 1980. Goshen Springs: Late Quaternary Vegetation Record for Southern Alabama. Ecology 61, 371–386.

Digerfeldt G and Hendry MD, 1987. An 8000 year Holocene sea-level record from Jamaica: implications for interpretation of Caribbean reef and coastal history. Coral Reefs 5, 165-169.

Donders TH, Wagner F, and Dilcher DL, et al., 2005. Mid- to late-Holocene El Niño-Southern Oscillation dynamics reflected in the subtropical terrestrial realm. PNAS 102, 10,904–10,908.

Donnelly, J.P., Bryant, S.S., Butler, J., Dowling, J., Fan, L., Hausmann, N., Newby, P., Shuman, B., Stern, J., Westover, K., and Webb, T., III, 2001. 700 yr sedimentary record of intense hurricane landfalls in southern New England. Bulletin of the Geological Society of America 113, 714-27.

Duarte CM and Cebrian J, 1996. The fate of autotrophic production in the sea. Limnology and Oceanography Methods 41, 1758-1766.

Ebanks WJ, 1975. Holocene carbonate sedimentation and diagenesis, Ambergris Cay, Belize. In: Wantland KF and Pusey WC (Eds). Belize Shelf- Carbonate Sediments, Clastic Sediments, and Ecology. American Association of Petroleum Geologists, Studies in Geology 2, 1-39.

Ellison JC, 1993. Mangrove retreat with rising sea-level, Bermuda. Estuary Coast Shelf. Science 37, 75–87.

Ellison JC, 1996. Pollen evidence of Late Holocene mangrove development in Bermuda. Global Ecology Biogeography 5, 315–326.

Ellison JC, and Stoddart DR 1990. Mangrove ecosystem collapse during predicted sea- level rise: Holocene analogues and implications. Journal of Coastal Research 7, 151-165.

Ellison JC, 2008. Long-term retrospection on mangrove development using sediment cores and pollen analysis: A review. Aquatic Botany 89, 93–104.

Food and Agriculture Organization of the United Nations, 2003. State of the world's forests.

Germeraad JH, Hopping CA, and Muller J, 1968. Palynology of tertiary sediments from Tropical Areas. Review of Palaeobotany and Palynology 6, 189–348.

Gleason PJ and Stone PA, 1994. Age, origin and landscape evolution of the Everglades peatland. In: Davis SM and Ogden JC (Eds). Everglades, the Ecosystem and its Restoration. St. Lucie Press, Delray Beach, FL, 149-198.

Giri, C, Ochieng E, and Tieszen L, 2011. Status and distribution of mangrove forests of the world using earth observation satellite data. Global Ecology and Biogeography, 20, 154–159.

Goff, J., McFadgen, B.G., Chague-Goff, C., 2004. Sedimentary differences between the 2002 Easter storm and the 15th-century Okoropunga tsunami, southeastern North Island, New Zealand. Marine Geology 204, 235–250.

Gonzalez C, Urrego LE, and Martinez JI, 2010. Mangrove dynamics in the southwestern Caribbean since the 'Little Ice Age': A history of human and natural disturbances. Holocene 20, 849–861.

Graham A, 1995. Diversification of Gulf Caribbean mangrove communities through Cenozoic time. Biotropica 27, 17–20.

Grimm EC, Jacobson GL, and Watts WA, et al., 1993. A 50,000-Year Record of Climate Oscillations from Florida and Its Temporal Correlation with the Heinrich Events. Science 261, 198–200.

Haug GH, Hughen KA, and Sigman DM, et al., 2001. Southward migration of the Intertropical Convergence Zone through the Holocene. Science 293, 1304–1308.

Halley RB, Shim EA, and Hudson JH, et al., 1977. Recent and relict topography of Boo Bee patch reef, Belize. Proceedings, 3rd International Coral Reef Symposium, Miami, Florida 2,29-35.

Herbert TD and Schuffert JD, 2000. Alkenone unsaturation estimates of sea-surface temperatures at ODP Site 1002 over a full glacial cycle. Proceedings of the Ocean Drilling Program 165, 239 –247.

Higuera-Gundy A, Brenner M, and Hodell DA, et al., 1999. A 10,300 ^{14}C yr record of climate and vegetation change from Haiti. Quaternary Research 52, 159-170.

Hodell DA, Curtis JH, and Jones GA, et al., 1991. Reconstruction of Caribbean climate change over the past 10,500 years. Nature, 352, 790–793.

Hodell DA, Brenner M, and Curtis JH, eet al., 2001. Solar forcing of drought frequency in the Maya Lowlands. Science 292, 1367–1370.

Hogarth PJ, 2007. The biology of mangroves and seagrasses, second edition, Oxford University Press

Huybers P and Wunsch C, 2003. Rectification and precession-period signals in the climate system. Geophysical Research Letters 30, 3.1–3.4.

Islebe G and Sánchez O, 2002. History of late Holocene vegetation at Quintana Roo, Caribbean coast of Mexico. Plant Ecology 160, 187–192.

Kangas PC and Lugo AE, 1990. The distribution of mangroves and saltmarshes in Florida. Tropical Ecology 31, 32-39.

Kaplan M, Renaud FG, and Lüchters G, 2009. Vulnerability assessment and protective effects of coastal vegetation during the 2004 Tsunami in Sri Lanka. Natural Hazards and Earth System Sciences 9, 1479-1494.

Kjellmark E, 1996. Late Holocene Climate Change and Human Disturbance on Andros Island, Bahamas. Journal of Paleolimnology 15, 133-145.

Kjerfve B, 1981. Tides of the Caribbean Sea. Journal of Geophysical Research 86, 148-227.

Kortekaas, S., Dawson, A.G., 2007. Distinguishing tsunami and storm deposits: an example from Martinhal SW Portugal. Sedimentary Geology 200, 208–211.

Krauss KW, Lovelock CE, and McKee KL, et al., 2008. Environmental drivers in mangrove establishment and early development, a review. Aquatic Botany 89, 105–127.

Kristensen E, Bouillon S, and Dittmar T, et al., 2008. Organic carbon dynamics in mangrove ecosystems: a review. Aquatic Botany 89, 201-219.

Kutzbach JE, 1981. Monsoon climate of the early Holocene: climate experiment with the earth's orbital parameters for 9000 years ago. Science 214, 59-61.

Lane, P., Donnelly, J.P., and Woodruff, J.D., 2011. A decadally resolved paleohurricane record archived in the late Holocene sediments of a Florida sinkhole. Marine Geology 287, 14–30.

Langenheim JH, Hackner BL, and Bartlett A, 1967. Mangrove pollen at the depositional site of Oligo-Miocene amber from Chiapas, Mexico. Botanical Museum leaflets 21, 289–324.

Laskar J, Robutel P, and Joutel F, et al., 2004. A long-term numerical solution for the insolation quantities of the Earth. Astronomy and Astrophysics 428, 261–285.

Leduc G, Schneider RR, and Kim JH, et al., 2010. Holocene and Eemian Sea surface temperature trends as revealed by alkenone and Mg/Ca paleothermometry. Quaternary Science Reviews 29, 989-1004.

Liu, K.B., and Fearn, M.L., 1993. Lake sediment record of late Holocene hurricane activities from coastal Alabama. Geology 21, 793-796.

Liu, K.B., and Fearn, M.L., 2000. Reconstruction of prehistoric landfall frequencies of catastrophic hurricanes in northwestern Florida from lake sediment records. Quaternary Research 54, 238-245.

Liu KB, Lu HY, and Shen CM,, 2008. A 1,200-year proxy record of hurricanes and fires from the Gulf of Mexico coast: Testing the hypothesis of hurricane-fire interactions. Quaternary Research 69, 29-41.

Lorenz SJ, Kim JH, and Rimbu N, et al., 2006. Orbitally driven insolation forcing on Holocene climate trends: Evidence from alkenone data and climate modeling, Paleoceanography 21,1002.

Mancintyre IG, Toscano MA, and Lighty RG, et al., 2004. Holocene history of the mangrove islands of Twin Cays, Belize, Central American. Atoll Research Bulletin 510, 1-16.

Macintyre IG, Littler MM, and Littler DS, 1995. Holocene history of Tobacco Range, Belize, Central America. Atoll Research Bulletin 430, 1-18.

Mayewski PA, Rohling EE, and Stager JC, et al., 2004., Holocene climate variability, Quaternary Research 62, 243 – 255.

Medina E, Cuevas E, and Popp M, et al., 1990. Soil salinity, sun exposure, and growth of Acrostichum aureum, the mangrove fern. Botanical Gazette 151, 41–49.

METED, Forecasters' Overview of the Gulf of Mexico and Caribbean Sea http://www.meted.ucar.edu/oceans/gulfmexico_carib/print_2.php (Accessed 24 February 2015)

McKee KL, Cahoon DR, and Feller IC, 2007. Caribbean mangroves adjust to rising sea level through biotic controls on change in soil elevation. Global Ecology and Biogeography 16, 545–556.

McCloskey TA and Liu KB, 2012. A sedimentary-based history of hurricane strikes on the southern Caribbean coast of Nicaragua. Quaternary Research 78, 454–464.

McIvor AL, Spencer T, and Möller I, et al., 2013. The response of mangrove soil surface elevation to sea level rise. Natural Coastal Protection Series: Report 3. Cambridge Coastal Research Unit Working Paper 42. Nature Conservancy and Wetlands International.

Middleton BA and McKee KL, 2001. Degradation of mangrove tissues and implications for peat formation in Belizean island forests. Journal of Ecology 89, 818-828.

Milne GA, Long AJ, and Bassett SE, 2005. Modelling Holocene relative sea-level observations from the Caribbean and South America. Quaternary Science Reviews 24, 1183-1202

Milankovitch M, 1941. Canon of Insolation and the Ice-Age Problem. Special Publications of the Royal Serbian Academy, Israel Program for Scientific Translations 132, 484.

Monacci NM, Meier-Grünhagen U, and Finney BP, et al., 2009. Mangrove ecosystem changes during the Holocene at Spanish Lookout Cay, Belize. Palaeogeography, Palaeoclimatology, Palaeoecology 280, 37–46.

Nagelkerken I, Blaber S, and Bouillon S, et al., 2008. The habitat function of mangroves for terrestrial and marina fauna: a review. Aquatic Botany 89, 155-185.

Olwig MF, Sørensen MK, and Rasmussen MS, et al., 2007. Using remote sensing to assess the protective role of coastal woody vegetation against tsunami waves. International Journal of Remote Sensing 28, 3153-3169.

Parkinson RW, 1989. Decelerating Holocene Sea-Level Rise and Its Influence on Southwest Florida Coastal Evolution: A Transgressive/Regressive Stratigraphy. Journal of Sedimentary Petrology 59, 960-972.

Peros MC, Reinhardt EG, and Schwarcz HP, et al., 2007. High-resolution paleosalinity reconstruction from Laguna de la Leche, north coastal Cuba, using Sr, O, and C isotopes. Palaeogeography, Palaeoclimatology, Palaeoecology 245, 535-550.

Piou C, Feller I, and Berger U, et al., 2006. Zonation patterns of Belizean offshore mangrove forests 41 years after a catastrophic hurricane. Biotropica 38, 365-374.

Purdy EG, Pusey WC, and Wantland KF, 1975. Continental shelf of Belize - regional shelf attributes. In: Wantland K.F and Pusey WC (Eds). Belize Shelf- Carbonate Sediments, Clastic Sediments, and Ecology. American Association of Petroleum Geologists, Studies in Geology 2, 1-39.

Ramcharan EK, 2004. Mid-to-late Holocene sea level influence on coastal wetland development in Trinidad. Quaternary International 120, 145–151.

Ramcharan EK, 2005. Late Holocene ecological development of the Graeme Hall Swamp, Barbados, West Indies. Caribbean Journal of Science 41, 147-150.

Ramcharan EK and McAnderws JH, 2006. Holocene development of coastal wetland at Maracas Bay, Trinidad,West Indies. Journal of Coastal Research 22, 581–586.

Rimbu N, Lohmann G, and Kim JH, et al., 2003. Arctic/North Atlantic Oscillation signature in Holocene sea surface temperature trends as obtained from alkenone data. Geophysical Research Letters 30, 1280.

Ross MS, O'Brien JJ, and Ford RG, et al., 2009. Disturbance and the rising tide: the challenge of biodiversity management on low-island ecosystems. Frontiers in Ecology and the Environment 7, 471-478.

Rull V, Vegas-Vilarruibia T, and De Pernia NE, 1999. Palynological record of an Early-Mid Holocene mangrove in Eastern Venezuela: Implications for sea-level rise and disturbance history. Journal of Coastal Research 15, 496-504.

Scholl DW, Craighead FC, and Stuiver M, 1969. Florida submergence curve revisited: Its relation to coastal sedimentation rates. Science 163, 562-564.

Sherman RE and Fahey TJ, 2001. Hurricane impacts on a mangrove forest in the Dominican Republic: damage patterns and early recovery. Biotropica 33, 393–408.

Simard M, Zhang KQ, and Rivera-Monroy VH, et al., 2006. Mapping height and biomass of mangrove forests in Everglades National Park with SRTM elevation data. Photogrammetric Engineering and Remote Sensing 72, 299-311.

Smithsonian Marine Station at Fort Pierce. http://www.sms.si.edu/irLspec/Rhizop_mangle.htm (Accessed 24 December 2014)

Smith TJ, Robblee MB, and Wanless HR, et al., 1994. Mangroves, Hurricanes, and Lightning Strikes. BioScience 44, 256-263.

Smith TJ, Anderson GH, and Balentine K, 2009. Cumulative impacts of hurricanes on Florida mangrove ecosystems: Sediment deposition, storm surges and vegetation. Wetlands 29, 24-34.

Stevens PW, Fox SL, and Montague CL, 2006. The interplay between mangroves and saltmarshes at the transition between temperate and subtropical climate in Florida. Wetlands Ecology and Management 14, 435-444

Street EA and Grove AT, 1979. Global maps of lake-level fluctuations since 30000 yr B.P. Quaternary Research 12, 83-118.

Stuiver M, Reimer PJ, and Reimer RW, 2010. CALIB 7.0: http://calib.qub.ac.uk/calib/calib.html (Accessed 24 December 2014)

Toscano MA and Macintyre IG, 2003. Corrected western Atlantic sea-level curve for the last 11,000 years based on calibrated 14C dates from Acropora palmata framework and intertidal mangrove peat. Coral Reefs 22, 257–270.

Thaxton JM, DeWalt SJ, and Platt WJ, 2007. Spatial patterns of regeneration after Hurricane Andrew in two south Florida fringe mangrove forests. Florida Scientist 70, 148-156.

Torrescano N and Islebe GA, 2006. Tropical forest and mangrove history from southeastern Mexico: a 5000 yr pollen record and implications for sea level rise. Vegetation History and Archaeobotany 15, 191-195.

Urrego LE, Correa-Metrio A, and González C, et al., 2013. Contrasting responses of two Caribbean mangroves to sea-level rise in the Guajira Peninsula (Colombian Caribbean). Palaeogeography, Palaeoclimatology, Palaeoecology 370, 92–102.

Urrego LE, Bernal G, and Polanía J, 2009. Comparison of pollen distribution patterns in surface sediments of a Colombian Caribbean mangrove with geomorphology and vegetation. Review of Palaeobotany and Palynology 156, 358–375.

Urrego LE, González C, and Urán G, et al., 2010. Modern pollen rain in mangroves from San Andres Island, Colombian Caribbean. Review of Paleobotany and Palynology 162, 168-182.

van Soelen EE, Lammertsma EI, and Cremer H, 2010. Late Holocene sea-level rise in Tampa Bay: Integrated reconstruction using biomarkers, pollen, organic-walled dinoflagellate cysts, and diatoms. Estuarine, Coastal and Shelf Science 86, 216–224.

van Soelen, Brooks EE, and Larson GR, et al., 2012. Mid- to late-Holocene coastal environmental changes in southwest Florida, USA. The Holocene, 1-10.

Wanless HR, Parkinson RW, and Tedesco LP, 1994. Sea Level Control on Stability of Everglades Wetlands. In: Davis SM and Ogden JC (Eds). Everglades, the ecosystem and its restoration, St. Lucie Press, 199-222.

Watts WA and Stuiver M, 1980. Late Wisconsin climate of northem Florida and origin of species-rich deciduous forest. Science 210, 325-327.

Watts WA, 1971. Postglacial and Interglacial Vegetation History of Southern Georgia and Central Florida. Ecology 52, 676–690.

Watts WA and Hansen BCS, 1986. Holocene climate and vegetation of Bermuda. Pollen and Spores 28, 355-364.

Webb T, Richard PJH, and Mott RJ, 1983. A mapped history of Holocene vegetation in southern Quebec. Syllogeus 49, 273-336.

Webb T, 1986. Is vegetation in equilibrium with climate? How to interpret late-Quaternary pollen data. Vegetatio 67, 75-91.

Willard DA and Bernhardt CE, 2011. Impacts of past climate and sea level change on Everglades wetlands, placing a century of anthropogenic change into a late-Holocene context. Climatic Change 107, 59-80.

Woodroffe CD, Thom BG, and Chappell J, 1985. Development of widespread mangrove swamps in mid- Holocene times in northern Australia. Nature 317, 711–713.

Woodroffe CD and Grime D, 1999. Storm impact and evolution of a mangrove-fringed chernier plain, Shoal Bay, Darwin, Australia. Marine Geology 159, 303-321.

Wooller MJ, Behling H, and Smallwood BJ, 2004. Mangrove ecosystem dynamics and elemental cycling at Twin Cays, Belize, during the Holocene. Journal of Quaternary Science 19, 703–711.

Wooller MJ, Morgan R, and Fowell S,et al., 2007. A multi-proxy peat record of Holocene mangrove palaeoecology from Twin Cays, Belize. The Holocene 17, 1129-1139.

CHAPTER 3. A SURVEY OF MODERN POLLEN AND VEGETATION ALONG THE SHARK RIVER ESTUARY IN THE FLORIDA EVERGLADES

Introduction

The Everglades, situated at the southern tip of the Florida peninsula, contain the largest freshwater marshes and contiguous mangrove swamp in North America (Lodge, 2010). In order to restore the hydrological and environmental conditions of the Everglades back to its historical levels, numerous studies are being conducted along the Shark River Estuary, the largest freshwater drainage in the Everglades National Park (ENP). To understand the long-term ecological processes and development of these natural wetlands is an essential step for determining the path of the restoration of Everglades. Fossil pollen analysis has been proven to be a very useful method for the reconstruction of long term vegetation development and paleoecological changes (Chappell and Grindrod, 1985; Liu et al., 2008; Willard and Bernhardt, 2011).

To produce accurate paleoenvironmental reconstruction with fossil pollen record, it is very important to understand how the current vegetation is represented in the modern pollen rain of the study areas. In the Everglades National Park, few such studies have been conducted. Willard et al. (2001) documented the modern pollen rain from eight wetland sub-environments in the Florida Everglades and the results show that they have distinctive surface pollen assemblages. Their study also suggests that pollen record is useful for reconstructing past hydrologic and edaphic changes in the Everglades. Other fossil pollen records from the region suggest that the vegetation shifts of inland wetland communities are closely associated with the position of the

Inter-tropical Convergence Zone (ITCZ) and the state of the North Atlantic Oscillation (NAO) (Donders et al., 2005; Willard et al., 2011; Willard and Cronin, 2007; Bernhardt and Willard, 2009).

However, no comprehensive studies exist to document relationship between modern pollen and vegetation along the Shark River Estuary, where many projects are being conducted in the freshwater marsh and mangrove swamps (FCE LTER). In this study, we collected 18 modern pollen samples from a 20 km transect along the SRS and 7 samples from 3 major wetland sub-environments along the main park road in the ENP (Table. 1, Fig.1). Our goal is to establish the spatial and statistical relationships between surface pollen assemblages and local vegetation, and reveal the chemical characteristics of the surface soil at different wetland environments by using X-ray fluorescence (XRF) analysis. This study is a systematic analysis to compare the modern pollen rain of the Shark River Estuary with the interior part of ENP. These data will help to expand our knowledge of the modern relationships between pollen and vegetation in the region, especially in the mangrove ecosystems, and fill a gap in the pollen data network for the Shark River Estuary.

Study area

The study area (~600,000 ha), encompassing 25 surface soil samples, lies roughly between 25 °24'06" and 25 °21'10" N latitude, and between 80 °36'02" and 81 °06'53.6" W longitude (Table. 1). The sampled wetland sub-environments include wet prairies, pine savannas, cypress forests, and mangrove forests along the Shark River Estuary (Fig. 1).

The Everglades is situated in a tropical/subtropical environment. Tides are semi-diurnal with 1.1 m mean tidal amplitude in the southwestern region and >0.5 m in the southeastern region and Florida Bay (Wanless et al. 1994). The coastal area of the ENP, from Naples to Florida Bay, is covered by approximately 15,000 ha of dense mangrove forests (Simard et al, 2006). The interior part of the ENP contains 1,050,000 ha of sawgrass marshes, sloughs, wet prairies, and pine savanna (Bernhardt and Willard, 2009). However, these densely vegetated wetlands are phosphate-limited (Castañeda-Moya et al., 2010), where the limited nutrient is supplied by the Gulf of Mexico, rather than the upper watershed (Chen and Twilley, 1999 a, b). Currently, the relative sea-level at southern Florida is rising at a rate of 3.8 mm/yr and inland replacement of freshwater marshes by mangrove swamps has been observed in the ENP (Wanless, 1994; Ross et al. 2000). The study area is frequently impacted by hurricanes. The historical hurricane record shows that the ENP is impacted by 46 major hurricanes (category 3-5) in the last 135 years (NOAA).

The Everglades has distinct wet and dry seasons (Lodge, 2010). The wet season (June-November) is hot and humid, with an average temperature around 32°C and humidity over 90%. The average annual precipitation is 125 to 152 cm, and about 70–75% of rain falls during the wet season. The Atlantic hurricane season is from June through November, therefore afternoon thunderstorms and tropical storms are common during the wet season. The dry season (December-May) is mild and pleasant, though rare cold fronts may create near freezing conditions. Average temperatures in the dry season are between 25°C and 12°C.

Table 1. Surface sample sites in the Everglades National Park, south Florida. Sample ID is keyed to site numbers in Figure 1. Latitudes and longitudes for sites are determined using global positioning systems. Nutrient and canopy height data in the Shark River transect are from Castañeda-Moya (2010) and Simard et al., (2006).

Sample NO.	Site ID	GPS	Salinity (ppt)	N:P (soil)	Canopy Height	Vegetation type	Site description
1	EM	25°24'06", -80°36'02"	\	\	\	Wet prairie	*Cladium/Eleocharis* marsh close to pine savanna, marl forming
2	LPK	25°25'02", -80°39'58"	\	\	\	Pine savanna	Tall, sparse pineland imbedded in marl prairies, frequent fire
3	RRP	25°24'35", -80°47'05"	\	\	\	Tall cypress	Tall cypress surrounded by dense *Cladium* marsh
4	MHE	25°20'27", -80°48'51"	\	\	\	Scrub cypress	Scrub cypress surrounded by dense *Cladium* marsh
5	PP	25°17'17", -80°47'53"	\	\	\	Mixed Mangroves	Scrub *Rhizophora*, *Laguncularia*, *Avicennia*, and hardwood forest
6	NMP	25°14'36", -80°48'19"	\	\	\	Wet prairie	*Eleocharis* marsh, associate with *Cladium*, marl forming
7	CB	25°10'51", -80°53'57"	\	\	\	Inland mangroves	Conocarpus forest near brackish marsh
8	SRS4-1	25°24'35", -80°57'51"	4.6 ± 1.1	105	<5m	Mangroves	Dwarf *Rhizophora* >60%, *Laguncularia* >*Conocarpus*, no *Avicennia*
9	SRS4-2	25°24'32", -80°57'43"	4.6 ± 1.1	105	<5m	Brackish marsh	*Cladium* marsh behind the mangrove fringe, about 200 m from the estuary
10	SRS5-1	25°22'37", -81°01'57"	20.8 ± 3.1	46	8-10m	Mangroves	Tall *Rhizophora* >80%, few *Laguncularia* and *Avicennia*, No *Conocarpus*
11	SRS5-2	25°22'35", -81°01'53"	20.8 ± 3.1	46	8-10m	Mangroves	Tall *Rhizophora* >80%, few *Laguncularia* and *Avicennia*, No *Conocarpus*
12	SRS5-3	25°22'33", -81°01'52"	20.8 ± 3.1	46	8-10m	Ecotone	Ecotone between tall *Rhizophora* forest and *Cladium* marsh
13	SRS5-4	25°22'33", -81°01'51"	20.8 ± 3.1	46	8-10m	Brackish marsh	*Cladium* marsh behind the mangrove fringe, about 200 m from the river

Table 1 cont.

14	**SRS6-1**	**25 °21'53", -81 °04'40"**	**27 ± 2.6**	**28**	**>10m**	**Mangroves**	***Laguncularia* >40%, *Rhizophora* >25%, *Avicennia* >25%, No *Conocarpus***
15	SRS6-2	25 °21'52", -81 °04'40"	27 ± 2.6	28	>10m	Mangroves	*Laguncularia* >40%, *Rhizophora* >25%, *Avicennia* >25%, No *Conocarpus*
16	SRS6-3	25 °21'51", -81 °04'40"	27 ± 2.6	28	>10m	Mangroves	*Laguncularia* >40%, *Rhizophora* >25%, *Avicennia* >25%, No *Conocarpus*
17	SRS6-4	25 °21'50", -81 °04'40"	27 ± 2.6	28	>10m	Mangroves	*Laguncularia* >40%, *Rhizophora* >25%, *Avicennia* >25%, No *Conocarpus*
18	SRS6-5	25 °21'49", -81 °04'40"	27 ± 2.6	28	>10m	Mangroves	*Laguncularia* >40%, *Rhizophora* >25%, *Avicennia* >25%, No *Conocarpus*
19	SRS6-6	25 °21'48", -81 °04'40"	27 ± 2.6	28	>10m	Mangroves	*Laguncularia* >40%, *Rhizophora* >25%, *Avicennia* >25%, No *Conocarpus*
20	SRS6-7	25 °21'48", -81 °04'39"	27 ± 2.6	28	>10m	Mangroves	*Laguncularia* >40%, *Rhizophora* >25%, *Avicennia* >25%, No *Conocarpus*
21	SRM-1	25 °21'11", -81 °06'54"	>30	~16	>15m	Mangroves	Hurricane damaged mangrove forest, *Avicennia* fringe, *Laguncularia* and *Rhizophora* co-dominant, no *Conocarpus*
22	SRM-2	25 °21'11", -81 °06'53"	>30	~16	>15m	Mangroves	Hurricane damaged mangrove forest, *Avicennia* fringe, *Laguncularia* and *Rhizophora* co-dominant, no *Conocarpus*
23	SRM-3	25 °21'10", -81 °06'52"	>30	~16	>15m	Mangroves	Hurricane damaged mangrove forest, *Avicennia* fringe, *Laguncularia* and *Rhizophora* co-dominant, no *Conocarpus*
24	SRM-4	25 °21'10", -81 °06'51"	>30	~16	>15m	Mangroves	Hurricane damaged mangrove forest, *Avicennia* fringe, *Laguncularia* and *Rhizophora* co-dominant, no *Conocarpus*
25	SRM-5	25 °21'10", -81 °06'50"	>30	~16	>15m	Mangroves	Hurricane damaged mangrove forest, *Avicennia* fringe, *Laguncularia* and *Rhizophora* co-dominant, no *Conocarpus*

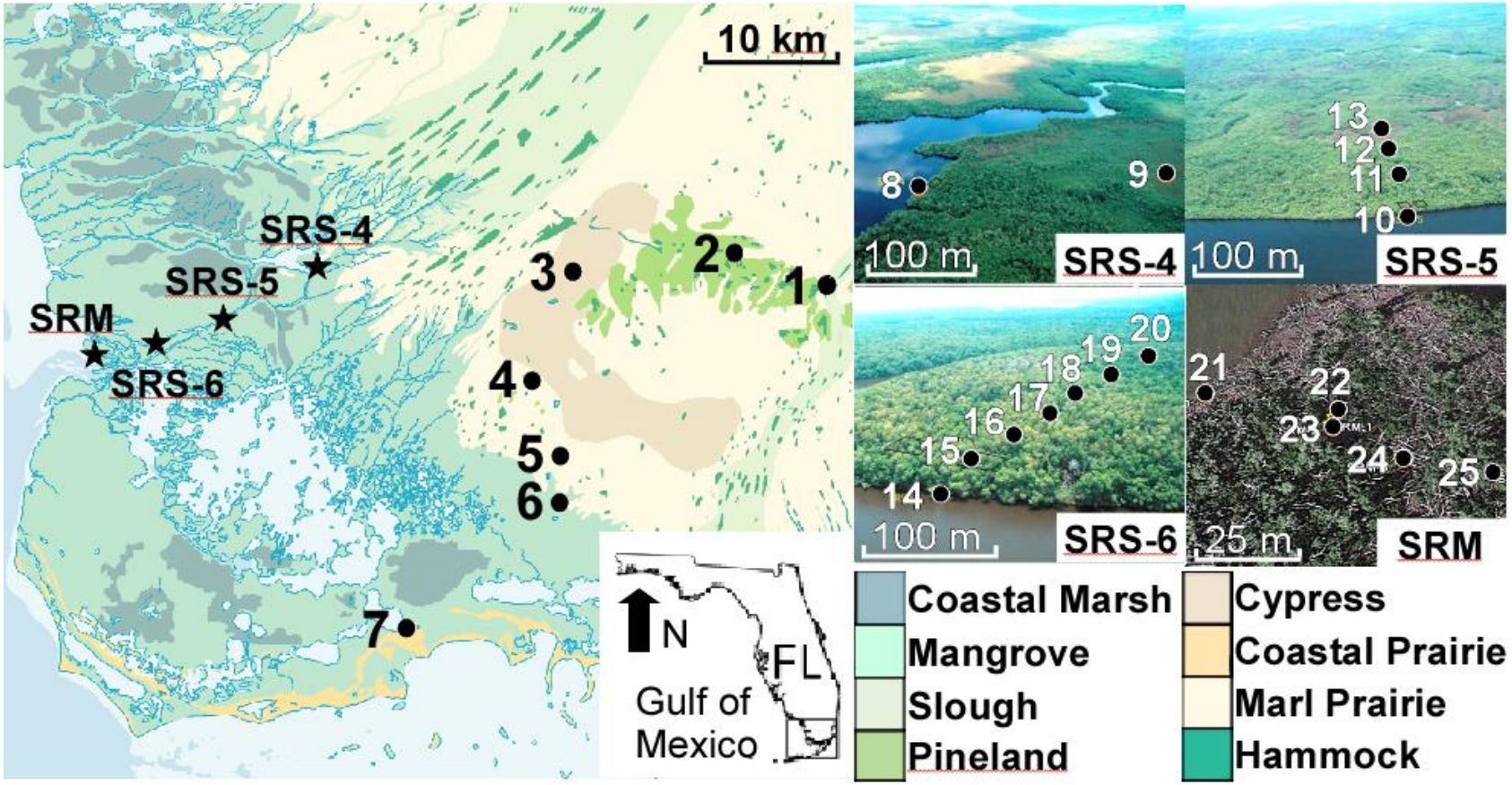

Figure 1. Location of surface sample sites in the Everglades National Park, south Florida. Circles indicate locations of the samples. Stars indicate the Shark River transect where multiple samples are taken at each site. Sample numbers are tied to Site IDs described in Table 1. Google Earth imagine of site SRM shows massive mortality of mangroves caused by Hurricane Wilma (2005)

Wet prairies

Wet prairies are the driest marsh type in the Everglades (Willard et al., 2001). Marl forming periphyton is a common component of wet prairies (Willard et al., 2001). Such wetlands are found from the northern Everglades to the Shark River Slough, Whitewater Bay, Cape Sable, and Florida Bay (Gleason and Stone, 1994, Lodge, 2010). The vegetation typically contains sawgrass (*Cladium jamaicense*) surrounded by willow thickets (*Salix*), with *Sagittaria* and *Typha* in more open areas (Slocum et al., 2003). Wet prairies typically have hydroperiods less than 12 months and thus dry seasonally, tending to burn more than once a decade, and even every 1-2 years if adjacent to pine savannas (Platt, 1999; Schmitz et al., 2002; Slocum et al., 2003).

Cypress forests

Cypress forests in the ENP lie in the vicinity of the wet prairie mosaic (Willard et al., 2001) and typically grow in deep depressions, therefore have a long hydroperiod resulting thick peat accumulation (up to 2 m) (Duever et al., 1984). They are bald cypress-dominant (*Taxodium distichum*), with other hardwoods (e.g. *Acer*, *Fraxinus*, *Annona*) forming the subcanopy, and *Utricularia*, *Eleocharis*, ferns, and Asteraceae present in the understory.

Pine savannas

Pine savannas also lie in the vicinity of the wet prairie mosaic, and their substrates typically consist of sand and rocks (Willard et al., 2001). They have short hydroperiods and are burned frequently (Platt, 1999). Pine savannas in the ENP are

occupied by *Pinus elliottii* var *densa, Quercus virginiana,* and contain Burseraceae, Poaceae, Asteraceae, and subtropical hammocks. Such areas (e.g., Lostman's Pines and Raccoon Point regions of Big Cypress National Preserve) are also present in the interior of the Everglades region of South Florida (Doren et al. 1993; Willard et al., 2001; Schmitz et al., 2002; Bernhardt and Willard, 2009; Hanan et al., 2010).

The Shark River Estuary

The Shark River Estuary is the biggest freshwater outlets in the ENP. During the wet season, water overflowing Lake Okeechobee and associated rainfall result in a southward sheet flow along a gentle slope of ~3 cm/km into SRS (Lodge, 2010). The water entering SRS flows through long-hydroperiod prairie sloughs into mangrove swamps at the river estuary and then into Whitewater Bay or the Gulf of Mexico along the southwestern coast of Florida. Along the Shark River Estuary, four study sites (SRM, SRS-6, SRS-5, and SRS-4) are located at 0 km, 4.1 km, 9.9 km, and 18.2 km from the mouth of the estuary, respectively. Site SRM, SRS-6, and SRS-5 receive strong influence from tidal activities, and site SRS-4 is mainly influenced by groundwater and freshwater runoffs (Castañeda-Moya, 2010).

Soil at site SRS-4 (Table 1, Fig. 1) has an atomic nitrogen to phosphorus ratio (N: P) of 105 (Chen and Twilley, 1999b), therefore it is very phosphorus limited. According to a multi-year (2005-2010) monitoring study of the Shark River transect (Castañeda-Moya, 2010), this site is flooded 165 days annually with a pore-water salinity of 4.6 ± 1.1 ppt. It is occupied by red mangroves (*Rhizophora mangle*) (67%

of total above ground biomass) with white mangroves (*Laguncularia racemosa*) as co-dominant species. It is the only site along the SRS transect where *Conocarpus erectus* is found and black mangroves (*Avicennia germinans*) are absent. The average mangrove canopy height at this site is less than 5 meters.

Soil at site SRS-5 (Table 1, Fig. 1) has an atomic nitrogen to phosphorus ratio (N: P) of 46 (Chen and Twilley, 1999b). This site is flooded 197 days annually with a pore-water salinity of 20.8 ± 3.1 ppt. *Rhizophora mangle* is the dominant species (87% of total above ground biomass) with very few other mangrove species. The average mangrove canopy height at this site is approximately 8 meters (Castañeda-Moya, 2010).

Soil at site SRS-6 (Table 1, Fig. 1) has an atomic nitrogen to phosphorus ratio (N: P) of 28 (Chen and Twilley, 1999b). This site is flooded 233 days annually with a pore-water salinity of 27 ± 2.6 ppt. *Laguncularia racemosa* is the dominant species (43% of total above ground biomass) with *Rhizophora mangle* and *Avicennia germinans* as co-dominant species (43% of total above ground biomass each). Site SRS-6 has the highest complexity index along the SRS transect, and the average mangrove canopy height is approximately 10 meters (Castañeda-Moya, 2010).

Site SRM (Table 1, Fig. 1) is located on the edge of Ponce de Leon Bay, at the mouths of Whitewater Bay and Shark River Estuary. It is flooded by tides 90% of the year with an average tidal range of 0.5 m (Castañeda-Moya et al., 2010). This site is situated in a fringing mangrove forest, where *Laguncularia racemosa* and *Rhizophora mangle* are co-dominant species (Chen and Twilley, 1999 a, b). Field observation

suggests the average mangrove canopy height at SRM is the highest (> 15m) among all 4 sites. Hurricane Wilma, the most recent major hurricane to cross SRS, made landfall as a category 3 storm near site SRM in 2005. Strong winds and storm surge from this hurricane caused damage to approximately 1,250 ha of mangrove forest along the west coast of the ENP, resulting in 90% mortality of trees with diameters at breast height greater than 2.5 cm (Whelan et al., 2009; Smith et al., 2009). The storm surge flooded site SRM with 3 - 4 m of water and deposited ~3 cm of marine sediment as far as 10 km inland (Castañeda-Moya et al., 2010).

Materials and methods

Twenty-five surface samples were analyzed from 11 sites with 5 broad vegetation types (Fig. 1). Location and vegetation composition at each site are briefly described in Table 1. Surface soil samples were collected by pushing aside surface vegetation to expose the surface of the peat and pushing a 15 cm diameter shovel into the ground to collect the upper 5 cm of sediments. The upper 1 cm of the sediments was later removed to avoid contamination. In the laboratory, all surface samples were scanned by a handheld Olympus Innov-X DELTA Premium X-ray fluorescence (XRF) analyzer to measure elemental concentrations (ppm) of 9 major chemical elements (Fig. 4).

Palynological analysis was performed on each surface sample. One commercial *Lycopodium* (L_c) tablet (~18,583 grains) was added to each sample (0.9 mL) as an exotic marker to calculate pollen concentration (grains/cm^3) (sum = L_c added * no. of grains counted / L_c counted / volume of sample). Samples were first washed with 10%

HCL and then distilled water. After this step, samples were boiled with 10% KOH for 15 min and then washed with distilled water for 2-3 times until the supernatant was clear to ensure the removal of humic compounds. After this pre-treatment, samples were passed through a 170 μm sieve to remove large organic fragments, and then reconcentrated with a 10 μm sieve. 10 mL acetolysis solution was then added to the test tubes and boiled for 2 minutes. Except for samples taken from wet prairies, the hydrofluoric acid treatment was omitted because samples contain mostly peat and limited amount of silicates. The main pollen taxa, non-pollen microfossils, and charcoal were counted and photographed with objective of 400x magnification (see Figure 5. for photos of all identified microfossils). The identification of pollen was based on published pollen illustrations by McAndrews et al. (1973) and Willard et al. (2004). Approximately 300 grains of pollen and spores were counted in most of the samples, and charcoal fragments were counted for all samples. The palynological results are reported in percentage (%) diagrams (Fig. 3).

Principal components analysis (PCA) was performed by the IBM SPSS version 22.0 on all surface samples to reveal the internal structure of 19 proxies (Fig. 4). The PCA results provide a basis to classify different pollen types into statistically meaningful groups, which can be interpreted in terms of different wetland sub-environment. In addition, Grimm's (1987) CONISS, which uses the method of incremental sum of squares and Edwards and Cavalli-Sforza's chord distance as dissimilarity coefficients, was applied to classify the surface pollen samples into groups using Tilia version 1.7.16.

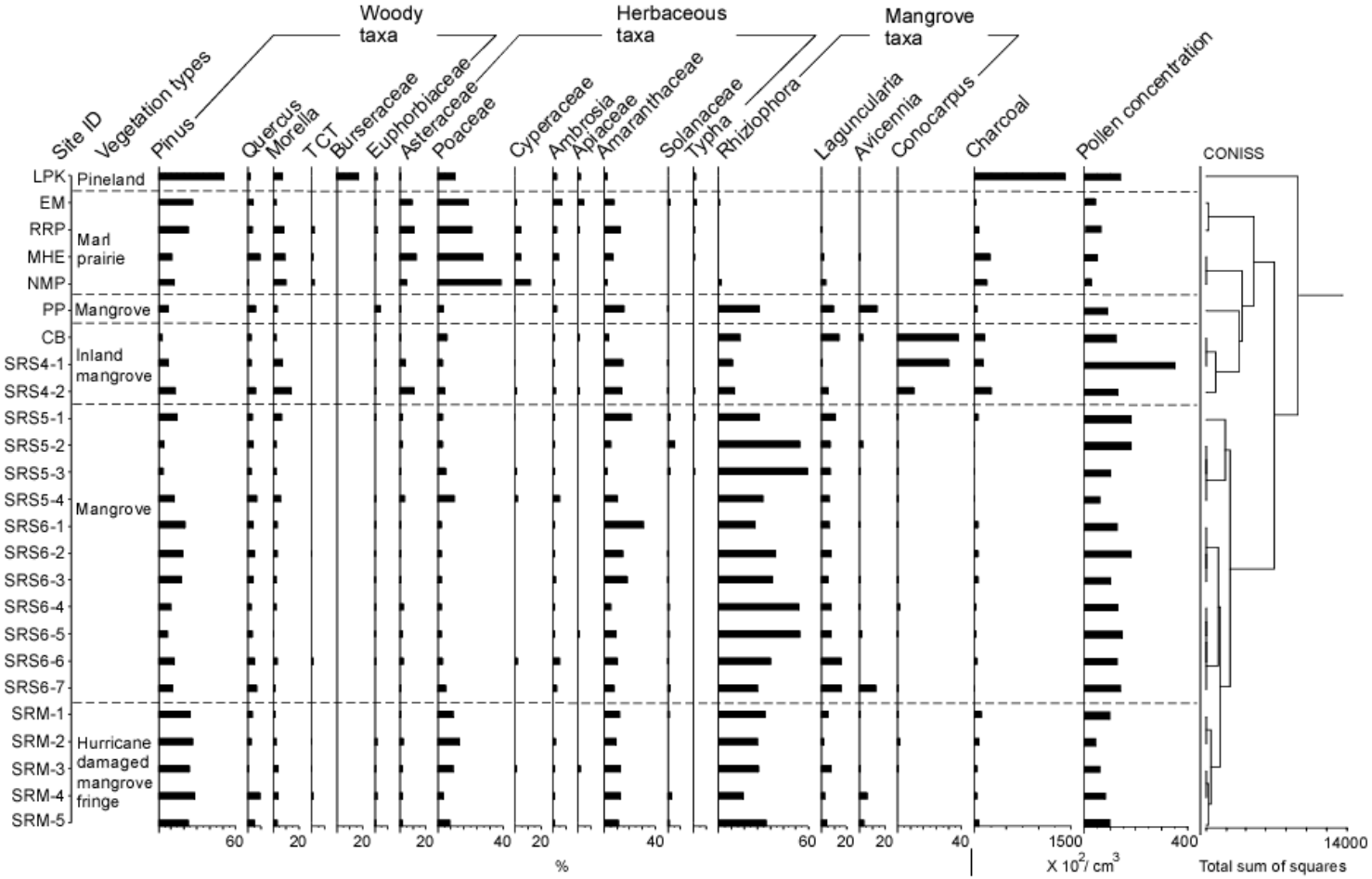

Figure 2. Pollen percentage diagram of 18 major pollen taxa for 25 surface samples. Vegetation types are classified by Grimm's (1987) CONISS. Pollen percentages are calculated based on the sum of all pollen taxa. The pollen concentration curve is added on the right to facilitate comparison.

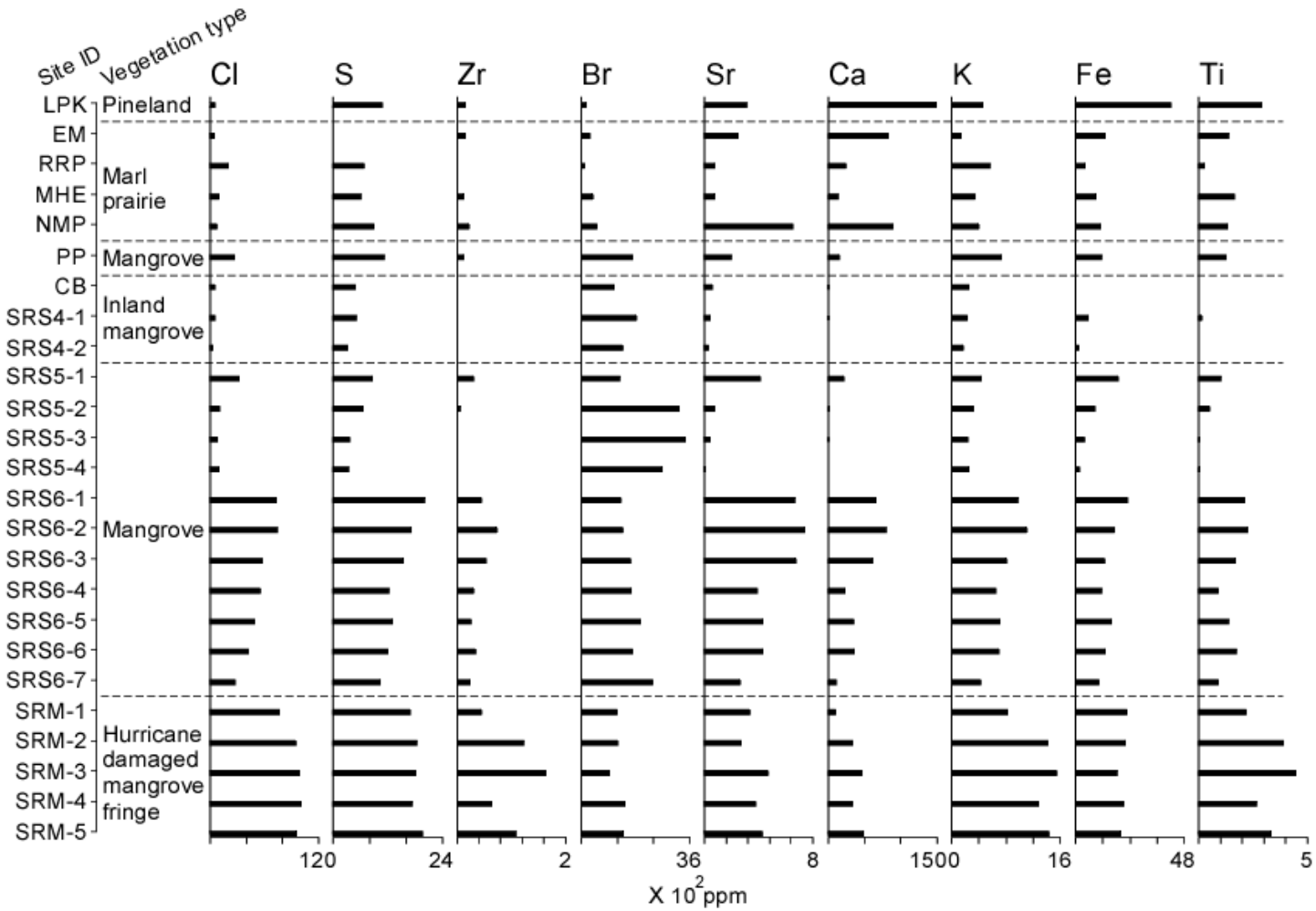

Figure 3. XRF diagram of 9 major elements for 25 surface samples. The samples are classified into same vegetation types as in Figure 2 to facilitate comparison.

Results and discussion

Five vegetation types are distinguishable from the surface pollen assemblages, which are marl prairies, pinelands, inland mangroves, mangrove forests, and hurricane damaged mangrove fringe (Fig. 2). Characteristic pollen assemblages of each type are summarized below.

The marl prairie group includes sample NO.1, 3, 4, and 6 taken at the park entrance marsh, Rock Reef Pass, Mohagony Hammock, and Nine Mile Pond along the main park road (Fig. 1, Table 1). Pollen concentrations are relatively low in wet prairie assemblages, with less than 6000 grains/cc sediment, compared to 15,000 grains/cc in mangrove assemblages. This may reflect greater oxidation of sediments associated with marl (Willard et al, 2001) and relatively dry substrates. Pollen assemblages (Fig. 2) are characterized by high percentages of herbaceous taxa (Poaceae >20%, Asteraceae >10%, Cyperaceae 5 -10%) and *Pinus* (10 – 30%), and low percentages of all other pollen taxa. In the interior part of ENP, *Cladium/Eleocharis* occupies the above-ground vegetation at most of marl prairie sites (Willard et al, 2001). However, their pollen only account for 5 -10% of the total pollen sum because the Cyperaceae pollens have very thin walls (exine), resulting in poor pollen preservation in the sedimentary record. Although sample 3 and 4 are taken from cypress forest, *Taxodium* is poorly represented in the pollen record. This is because the pollens of bald cypress are insect-pollinated, resulting in little pollen being shed from the flowers. Therefore, the pollen assemblages of cypress forest patches cannot be differentiated from surrounding wet prairie. However, the XRF

results suggest that the wet prairie samples (sample 1 and 6) have much higher content of Sr and Ca than the cypress forest samples (sample 3 and 4) (Fig. 3). The high content of Sr and Ca is due to the marl substrate of wet prairies.

The pineland group includes only sample NO.2 taken at Long Pine Key (Fig. 1, Table 1), which is a pine savanna imbedded in wet prairies. Pollen concentration of this sample is approximately 15,000 grains/ cubic centimeter, which is relatively high considering that the substrate at Long Pine Key is the same as surrounding marl prairies. The high pollen concentration of this sample is because *Pinus* (>50%), the dominant pollen taxon of this sample (Fig. 2), is a very prolific pollen producer. Other main pollen types include Burseraceae (a.k.a. gumbo-limbo, >15%), a fast growing tropical hardwood, and Poaceae (>10%). Concentration of charcoal fragments in this sample is very high (>150,000/ cubic centimeter). This result is in agreement with the short hydroperiod and frequent wildfires at pine savannas in the Everglades (Platt, 1999). Overall, the pollen assemblage of pineland is closely associated with the local vegetation and environment previously described (Doren et al. 1993; Willard et al., 2001; Schmitz et al., 2002; Bernhardt and Willard, 2009; Hanan et al., 2010). The XRF result of this sample is similar to that of marl prairie with high content of Sr and Ca (Fig. 3). However, the content of Fe and Ti is the highest among all surface samples. Typically, Fe and Ti are indicators of surface runoff. The high content of these two elements found in this sample is probably because pine savanna in the Everglades grows on sandy and rocky substrates (Duever et al., 1984; Willard et al., 2001).

The inland mangrove group includes sample 7 taken from Coot Bay and sample 8 and 9 from site SRS-4 (Fig. 1, Table 1). Pollen concentrations are relatively high, ranging from 15,000 to 35,000 grains/cc. The most abundant pollen is that of *Conocarpus* (15 -35%) (Fig. 2). *Rhizophora* and Amaranthaceae are also common at these sites, ranging from 5 to 10% and 2 to 5% of the total pollen sum, respectively. The lower percentages of upland taxa (e.g. *Pinus* and *Quercus*) and higher pollen concentrations at Coot Bay and SRS-4 reflect the relatively longer hydroperiod at these sites due to their closer distance to The Gulf of Mexico and the Florida Bay. The local vegetation at Coot Bay is occupied by *Conocarpus,* and site SRS-4 is the only site along the Shark River transect where *Conocarpus* is found (Castañeda-Moya, 2010). Therefore, the surface pollen assemblages at these sites are in close association with the local vegetation. The XRF results show low contents of all measured elements in inland mangrove samples (Fig. 3). This is probably because the substrate at these sites contains mostly nutrient-barren peat with little influences from tidal flooding and freshwater runoff.

The mangrove forest group includes only sample NO.5 taken at Paurotis Pond, a mixed mangrove forest, and sample 10-20 taken from sites SRS-5 and SRS-6 (Fig. 1, Table 1). Pollen concentrations of these samples range from 10,000 to 20,000 grains/cc. Pollen assemblages of this group are distinguishable by high abundance of *Rhizophora* pollen (20–55%); *Laguncularia*, Amaranthaceae, and *Pinus* are also common at these sites, ranging from 5 to 15%, 5 to 30%, and 10 to 30% of the total pollen sum, respectively (Fig. 2). Concentration of charcoal fragments in this group is

the lowest among all surface samples (<2000/cc). This probably reflects long hydroperiod at these sites since SRS-5 and SRS-6 are 9.9 and 4.1 miles from the Gulf of Mexico and regularly receive tidal flooding (Castañeda-Moya et al., 2010). Conspicuously, although the most predominant plant at site SRS-6 is *Laguncularia* (>40% of above ground biomass), the surface pollen assemblages from SRS-6 do not show a significant increase of *Laguncularia* pollen comparing with those from SRS-5. This is because the pollen of *Laguncularia* are insect-pollinated, resulting in *Laguncularia* being poorly represented in the pollen record. The XRF results show samples from site SRS-6 containing higher content of all measured elements comparing with samples from site SRS-5 (Fig. 3). This result is in agreement with the nutrient gradient along the Shark River Estuary showing that the limited nutrients are supplied by the Gulf of Mexico, rather than the upper watershed (Chen and Twilley, 1999 a, b). Therefore, it is reasonable to assume that site SRS-6 receives more nutrients from the ocean, hence containing higher content of all the chemical elements than site SRS-5, since site SRS-6 is closer to the Gulf of Mexico. This also explains the mangrove canopy height gradient along the Shark River Estuary, with taller mangrove trees occurring in sites closer to the ocean (Castañeda-Moya et al., 2010). Interestingly, XRF results of both site SRS-5 and SRS-6 show a progressive decrease of the elemental concentrations toward sites further away from the Shark River (SRS-5-1 toward SRS-5-4, and SRS-6-1 toward SRS-6-7) (Fig. 1, Table 1). This provides evidence that tidal flooding from the Shark River Estuary is directly related to the elemental concentration of the surface soil at surrounding mangrove forests.

The hurricane damaged mangrove fringe group includes all the samples from site SRM (sample 21-25), which is located at the mouth of Shark River Estuary (Fig. 1, Table 1). The mangroves at this site are severely damaged by Wilma, a category 3 hurricane, in 2005 (Smith et al., 2009). The impact of the hurricane can be clearly observed from the pollen diagram (Fig. 2). Surface pollen assemblages from site SRM have the lowest pollen concentrations comparing with other mangrove sites along the Shark River transect, despite the fact that site SRM contains the tallest mangrove trees of all mangrove sites (Fig. 2) (Simard et al., 2009). This irony is most likely related to low flowering rate at this site because of the massive mortality of mangrove trees caused by the hurricane. Additionally, a distinct increase of Poaceae pollen is observed in the pollen diagram. The direct landfall of catastrophic hurricanes has been documented to kill canopy trees in *Rhizophora*-dominant forests and give opportunities for shade-intolerant herbaceous plants to colonize (Smith et al, 1994, 2009; Baldwin et al, 1995, 2001; Vegas-Villarrúbia and Rull, 2002; Hogarth, 2007; Piou et al, 2006; Thaxton et al, 2007). Our results are in agreement with these studies. The XRF results show that samples from site SRM contain higher content of most measured elements comparing with samples from other mangrove sites (Fig. 3). Overall, the XRF results of the surface samples from our Shark River transect show a progressively increasing elemental concentration toward sites closer to the ocean; hence it is in agreement with previous studies (Chen and Twilley, 1999 a, b).

On the biplot of principal component loadings for the percentages of 18 pollen taxa and concentration of charcoal (Fig. 4, Table 2), the first two principal

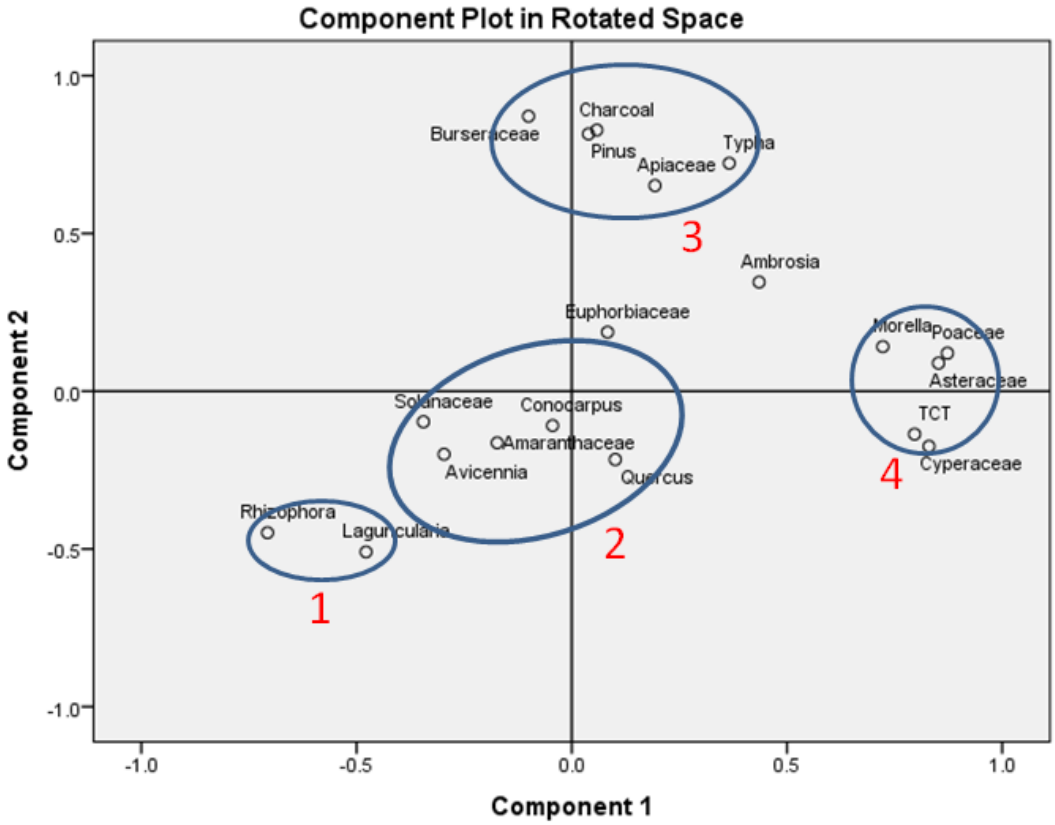

Figure 4. PCA biplot showing coordinates of charcoal and 18 pollen taxa from pollen diagram of surface samples plotted along component 1 and component 2. The results suggest that they can be divided into 4 primary groups, which are interpreted as: 1) Coastal Mangroves, 2) inland mangrove swamp, 3) Pine savanna, and 4) Marl prairie.

components account for 24.3% and 18.5% of the variance, respectively. Burseraceae, *Pinus*, Apiaceae, *Typha*, and charcoal have the highest positive loadings on principal component 1, whereas *Rhizophora* and *Laguncularia* have the most negative loadings. On the second principal component, *Morella*, Poaceae, Asteraceae, TCT, and Cyperaceae have the highest positive loadings, whereas *Rhizophora* and *Laguncularia* has the most negative loadings. Thus, the results of the PCA suggest that the pollen taxa and charcoal can be divided into 4 primary groups: (1) Coastal Mangrove group including *Rhizophora* and *Laguncularia*, (2) Inland mangrove group including

Table 2. Rotated Component Matrix of the Principal Component Analysis performed on the charcoal and 18 pollen taxa from pollen diagram of surface samples. Rotation Method is Varimax with Kaiser Normalization. Rotation converged in 3 iterations.

	Component	
	1	2
Pinus		.815
Quercus		
Morella	.723	
TCT	.796	
Euphorbiaceae		
Asteraceae	.852	
Poaceae	.873	
Cyperaceae	.830	
Ambrosia	.435	
Apiaceae		.652
Amaranthaceae		
Solanaceae		
Typha		.722
Burseraceae		.872
Rhizophora	-.707	-.448
Laguncularia	-.478	-.509
Avicennia		
Conocarpus		
Charcoal		.828

Conocarpus, Avicennia, Solanaceae, Amaranthaceae, and *Quercus*, (3) Pineland group including *Pinus*, Burseraceae, *Typha*, Apiaceae, and charcoal, and (4) Marl prairie group including Poaceae, Cyperaceae, TCT, Asteraceae, and *Morella*. These four groups are quite well-defined with no overlap among them (Fig. 4). The PCA results show that the internal structure of the pollen assemblages is statistically in agreement with the local vegetation of the sample sites described above (Fig. 2, Table 1).

Conclusion

This research applies Grimm's (1987) CONISS and PCA to the modern pollen data from the Everglades National Park, south Florida. The results show that the wetland sub-environments can be identified with empirical pollen data with the aid of statistical methods. By comparing vegetation groups classified by numerical and surface pollen analyses with the local vegetation at sampling locations, 25 surface pollen assemblages from the ENP are classified into five vegetation groups, which are marl prairie, pineland, inland mangroves, mangrove forests, and hurricane damaged mangrove fringe. These groups broadly correspond with various local vegetation types around the sampling sites. This study indicates that palynological data from sediment cores from the Everglades can be used for paleoenvironmental reconstructions.

Figure 5a. Common trees and shrubs: 1-2. *Pinus*, 3. Moraceae, 4. Burseraceae, 5. *Morella*, 6-7. *Quercus*, 8. TCT, 9-12. Euphorbiaceae, 13-15. Rubiaceae, 16-17. *Salix*

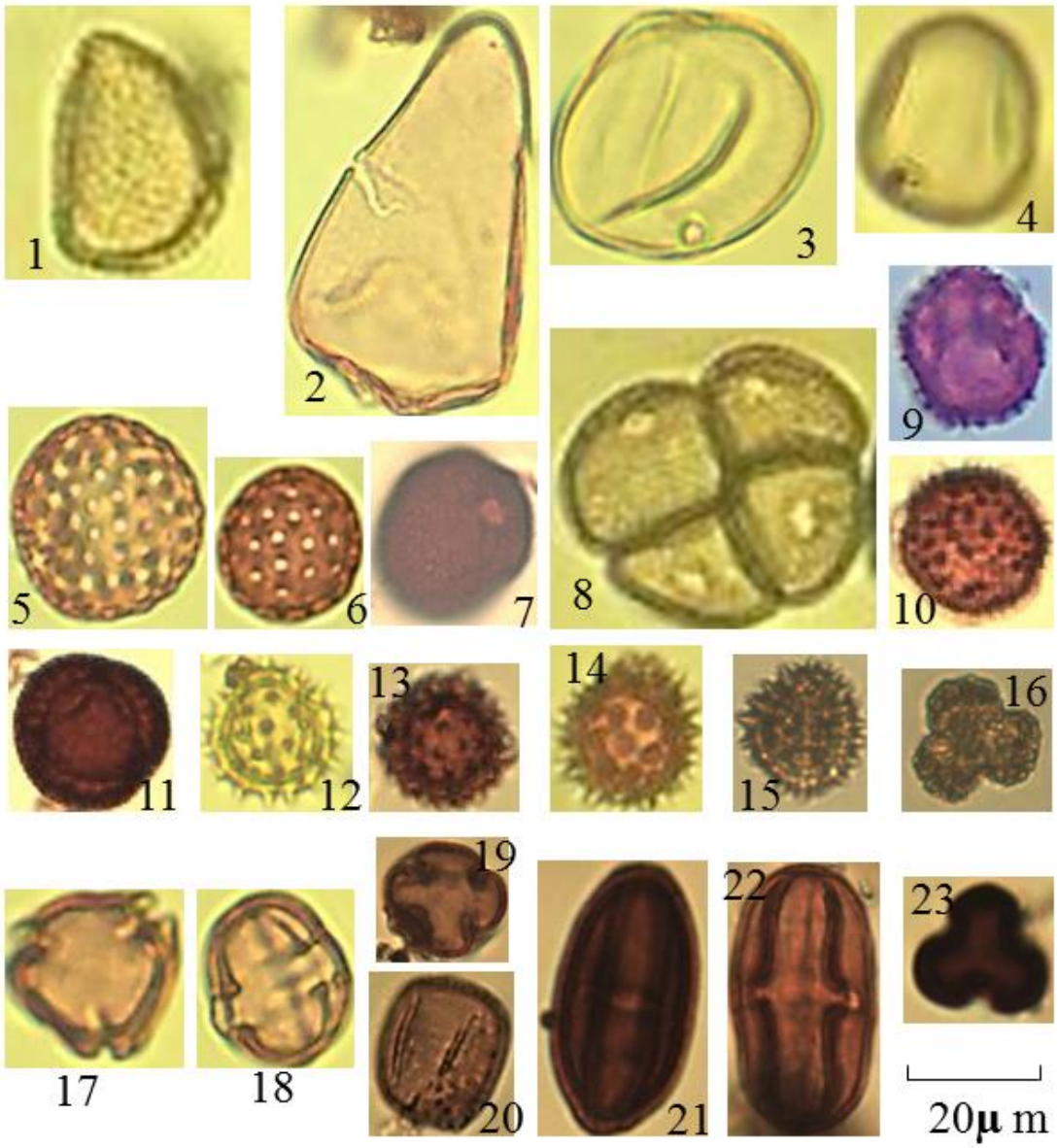

Figure 5b. Common herbaceous taxa: 1-2. Cyperaceae, 3-4. Poaceae, 5-6. Amaranthaceae, 7-8. *Typha*, 9-10. *Sagittaria*, 11 *Ambrosia* (Asteraceae short-spine), 12-16. Asteraceae (high-spine), 17-18. Solanaceae, 19-20. *Batis maritima* (Bataceae), 21-23. Apiaceae

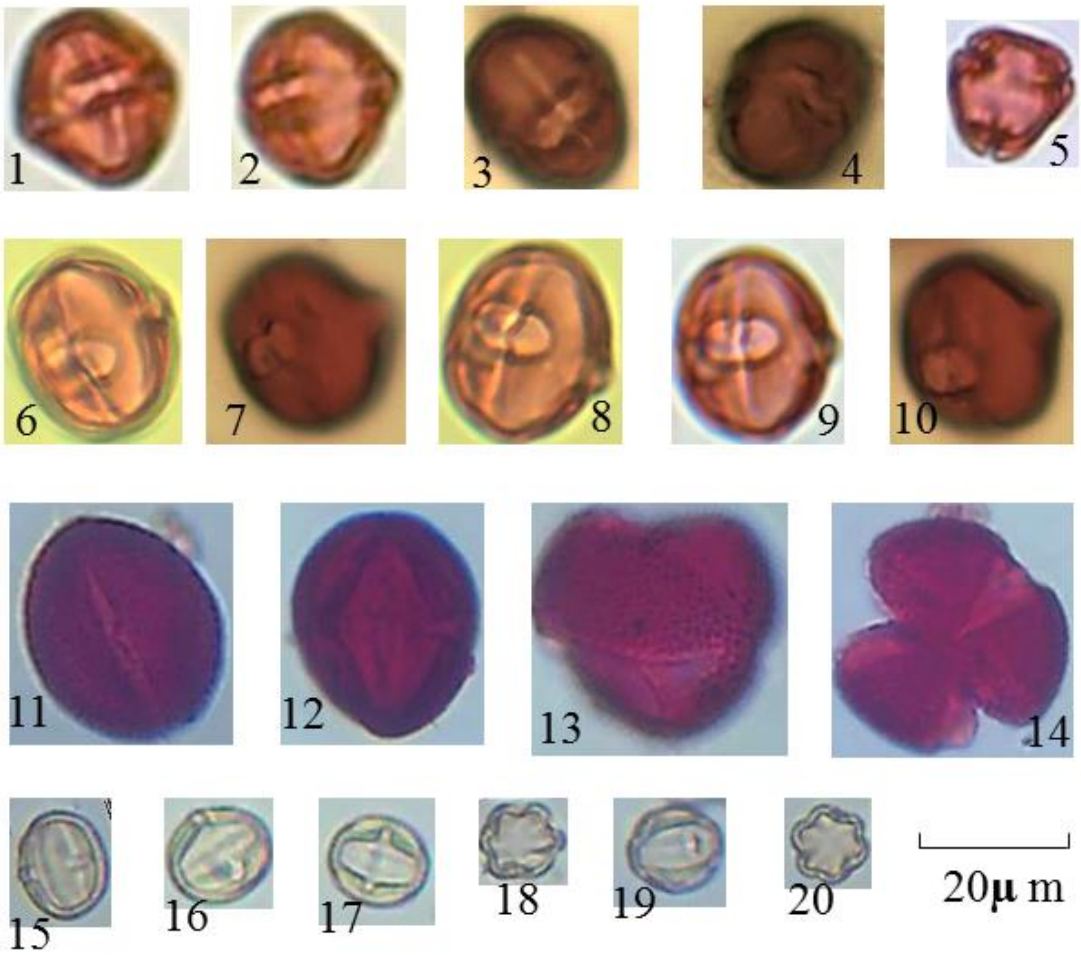

Figure 5c. Mangrove taxa: 1-5. *Rhizophora mangle*, 6-10. *Laguncularia racemosa*, 11-14. *Avicennia germinans*, 15-20. *Conocarpus erecta*

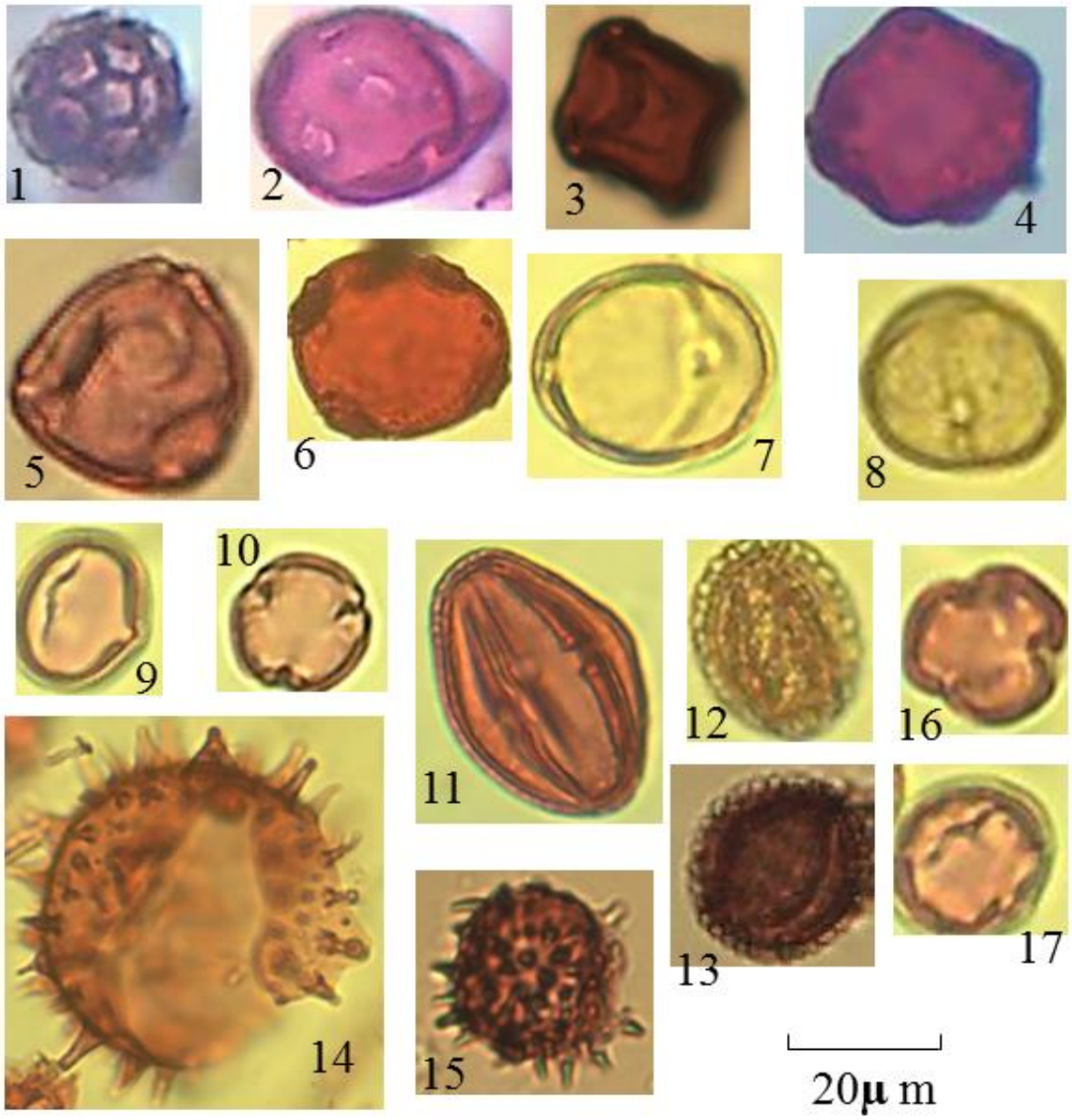

Figure 5d. Other pollen taxa: 1. *Alternanthera philoxeroides* (Amaranthaceae), 2. *Liquidambar*, 3. *Alnus*, 4. *Ulmus*, 5. *Corylus*, 6. Haloragaceae, 7-8. *Nyssa*, 9-10. *Dalbergia*, 11. Flacourtiaceae, 12-13. *Ilex*, 14-15. Malvaceae, 16-17. *Brysonima*

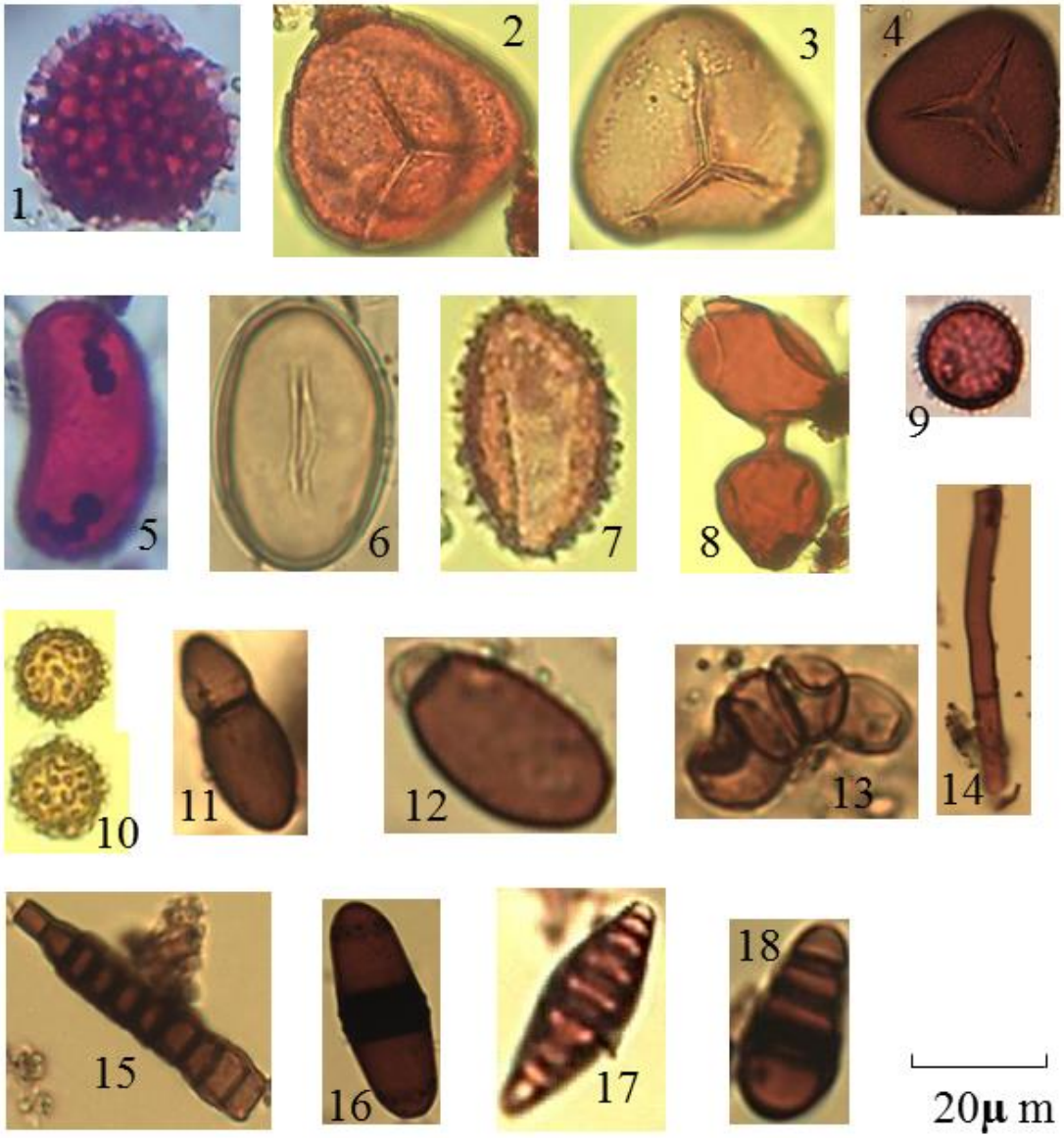

Figure 5e. Spores: 1. *Lycopodium*, 2-3. *Salvinia minima*, 4. *Pteridium*, 5-7. Polypodiaceae, 8. *Glomus*, 9-18. unidentified fungal spores

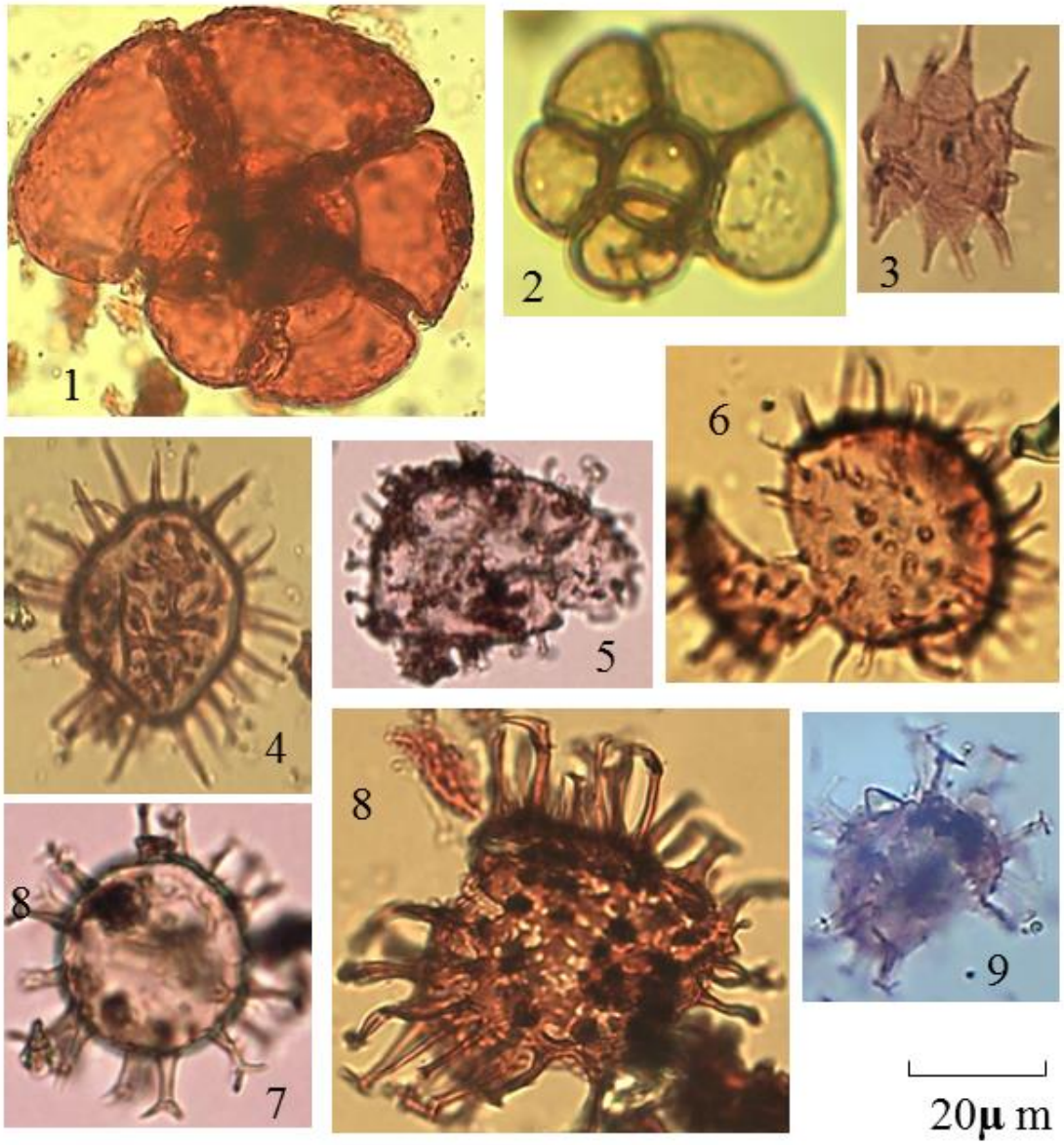

Figure 5f. Non-pollen/spore microfossil: 1-2. test linings of *foraminifera*, 3-9. test linings of unidentified Dinoflagellates

References

Baldwin, A.H., W.J. Platt, K.L. Gathen, J.M. Lessman, and T.J. Rauch, 1995. Hurricane damage and regeneration in fringe mangrove forests of southeast Florida, USA. Journal of Coastal Research 21, 169-183.

Baldwin, A.H., M.S. Egnotovich, M.A. Ford, and W.J. Platt, 2001. Regeneration in fringe mangrove forests damaged by Hurricane Andrew. Plant Ecology 57, 151-164.

Bernhardt, C.E., Willard, D.A., 2009. Response of the Everglades ridge and slough landscape to climate variability and 20th-century water management. Ecological Applications 19, 1723–1738.

Castañeda-Moya, E.,2010. Doctoral Dissertation: Landscape patterns of community structure, biomass and net primary productivity of mangrove forests in the Florida coastal Everglades as a function of resources, regulators, hydroperiod, and hurricane disturbance. Department of Oceanography and Coastal Sciences, Louisiana State University.

Castañeda-Moya, E., Twilley, R.R., Rivera-Monroy, V,H., Zhang, K.Q., Davis III, S.E., and Ross, M.S., 2010. Sediment and Nutrient Deposition Associated with Hurricane Wilma in Mangroves of the Florida Coastal Everglades. Estuaries and Coasts 33, 45-58.

Chappell, J.M.A., and Grindrod, J., 1985. Pollen analysis: a key to past mangrove communities and successional changes in North Australian coastal environments, In: Bardsley, K.N., Davie, J.D.S., Woodroffe, C.D. (Eds.), Coasts and Tidal Wetlands of the Australian Monsoon Region. Australian National University, Canberra, pp. 225-236.

Chen, R., and Twilley, R.R., 1999a. A simulation model of organic matter and nutrient accumulation in mangrove wetland soils. Biogeochemistry 44, 93-118.

Chen, R., and Twilley, R.R., 1999b. Patterns of mangrove forest structure and soil nutrient dynamics along the Shark River Estuary, Florida. Estuaries 22, 955-970.

Donders, T.H., Wagner, F., Dilcher, D.L., Visscher, H., 2005. Mid- to late-Holocene El Niño-Southern Oscillation dynamics reflected in the subtropical terrestrial realm. PNAS 102, 10,904–10,908.

Doren, R.F., Platt,W.J., and Whiteaker, L.D., 1993. Density and size structure of slash pine stands in the everglades region of south Florida. Forest Ecology and Management 59, 295-311.

Duever, M.J., Meeder, J.F., Duever, L.C., 1984. Ecosystems of the Big Cypress Swamp. In: Ewel, K.C., Odum, H.J. (Eds.), Cypress Swamps. University of Florida Press, Gainesville, FL, pp. 294-303.

Ellison, J.C., 2008. Long-term retrospection on mangrove development using sediment cores and pollen analysis: A review. Aquatic Botany 89, 93–104.

Florida Coastal Everglades (FCE), Long Term Ecological Research (LTER) Network: http://fce.lternet.edu/ (Accessed 24 December 2014)

Gleason, P.J. and Stone, P.A., 1994. Age, origin and landscape evolution of the Everglades peatland, In: S.M. Davis and J.C. Ogden (Eds.), Everglades, the Ecosystem and its Restoration. St. Lucie Press, Delray Beach, FL, pp. 149-198.

Grimm, E. C. 1987. CINISS: A FORTRAN 77 program for stratigraphically constrained cluster analysis by method of incremental sum of square. Computer and Geoscience 13:13–35.

Hanan, E.J., Ross, M.S., Ruiz, P.L., et al., 2010. Multi-Scaled Grassland-Woody Plant Dynamics in the Heterogeneous Marl Prairies of the Southern Everglades. Ecosystems 13, 1256-1274.

Hogarth, P.J., 2007. The biology of mangroves and seagrasses, second edition, Oxford University Press

Kiage, L.M., and Liu, K.B., 2009. Palynological evidence of climate change and land degradation in the Lake Baringo area, Kenya, East Africa, since AD 1650. Palaeogeography, Palaeoclimatology, Palaeoecology 279, 60-72.

Liu, K.B., Lu, H.Y., and Shen, C.M., 2008. A 1,200-year proxy record of hurricanes and fires from the Gulf of Mexico coast: Testing the hypothesis of hurricane-fire interactions. Quaternary Research 69, 29-41.

Liu, K.B., Li, C., Bianchette, T.A., McCloskey, T.A., Yao, Q., and Weeks, E., 2011. Storm deposition in a coastal backbarrier lake in Louisiana caused by Hurricanes Gustav and Ike. Journal of Coastal Research, Special Issue 64, 1866-1870.

Lodge, T.E., 2010, The Everglades Handbook: Understanding the Ecosystem, second edition, Boca Raton, Florida: CRC Press.

McAndrews, J.H., Berti, A.A., and Norris, G., 1973. Key to the Quaternary pollen and spores of the Great Lakes region. Royal Ontario Museum

NOAA, 2011, National Oceanic and Atmospheric Administration, Hurricane Center, Historical Hurricane Tracks website: http://maps.csc.noaa.gov/hurricanes/# (Accessed 24 December 2014)

Platt, W.J. 1999. Southeastern pine savannas., In Anderson, R.C., Fralish, J.S., and Baskin, J., (Eds), The savanna, barren, and rock outcrop communities of North America. Cambridge University Press, Cambridge, England, pp. 23-51

Piou, C., Feller, I., Berger, U., and Chi, F., 2006. Zonation patterns of Belizean offshore mangrove forests 41 years after a catastrophic hurricane. Biotropica 38, 365-374.

Ross, M.S., Meeder, J.F., Sah, J.P., Ruiz, P.L., and Telesnicki, G.J., 2000. The southeast saline Everglades revisited: 50 years of coastal vegetation change. Journal of Vegetation Science 11, 101–112.

Schmitz, M., Platt, W.J., and DeCoster, J., 2002. Substrate heterogeneity and numbers of plant species in Everglades savannas (Florida, USA). Plant Ecology 160, 137-148.

Slocum, M.G., Platt, W.J., and Cooley, H.C., 2003. Effects of differences in prescribed fire regimes on patchiness and intensity of fires in subtropical savannas of Everglades National Park, Florida. Restoration Ecology 11, 91-102.

Simard, M., Zhang, K.Q., Rivera-Monroy, V.H., Ross, M.S., Ruiz, P.L., Castañeda-Moya, E., Twilley, R.R., and Rodriguez, E., 2006. Mapping height and biomass of mangrove forests in Everglades National Park with SRTM elevation data. Photogrammetric Engineering and Remote Sensing 72, 299-311.

Smith, T.J., Robblee, M.B., Wanless, H.R., and Doyle, T.W., 1994. Mangroves, Hurricanes, and Lightning Strikes. BioScience 44, 256-263.

Smith, T.J., Anderson, G.H., Balentine, K., Tiling, G., Ward, G.A., Whelan, K.R.T., 2009. Cumulative impacts of hurricanes on Florida mangrove ecosystems: Sediment deposition, storm surges and vegetation. Wetlands 29, 24-34.

Thaxton, J.M., S.J. DeWalt, and W.J. Platt, 2007. Spatial patterns of regeneration after Hurricane Andrew in two south Florida fringe mangrove forests. Florida Scientist 70, 148-156.

Vegas-Vilarrúbia, T., and Rull, V., 2002. Natural and human disturbance history of the Playa Medina mangrove community (eastern Venezuela). Caribbean Journal of Science 38, 66-76.

Wanless, H.R., Parkinson, R.W., Tedesco, L.P., 1994. Sea Level Control on Stability of Everglades Wetlands, In: Davis, S.M., and Ogden, J.C., (Eds). Everglades: the ecosystem and its restoration, St. Lucie Press, p. 199-222.

Webb, R.S., Anderson, K.H., Webb III, T., 1993. Pollen responsesurface estimates of Late-Quaternary changes in the moisture balance of the northeastern United States. Quaternary Research 40, 213-227.

Whelan, K.R.T., T.J.I. Smith, G.H. Anderson, and M.L. Ouellette. 2009. Hurricane Wilma's impact on overall soil elevation and zones within the soil profile in a mangrove forest. Wetlands 29, 16–23.

Willard, D.A., Weimera, L.M., and Riegel, W.L., 2001, Pollen assemblages as paleoenvironmental proxies in the Florida Everglades. Review of Palaeobotany and Palynology 113, 213-235.

Willard, D.A., Cooper, S.R., Gamez, D., and Jensen, J., 2004, Atlas of pollen and spores of the Florida Everglades. Palynology 28, 175-227.

Willard, D.A., and Bernhardt, C.E., 2011. Impacts of past climate and sea level change on Everglades wetlands: placing a century of anthropogenic change into a late-Holocene context. Climatic Change 107, 59-80.

Willard, D.A., and Cronin, T.M., 2007. Paleoecology and ecosystem restoration: case studies from Chesapeake Bay and the Florida Everglades. Front Ecol Environ 5, 491–498.

CHAPTER 4. PALYNOLOGICAL RECONSTRUCTION OF ENVIRONMENTAL CHANGES IN COASTAL WETLANDS OF THE FLORIDA EVERGLADES SINCE THE MID-HOLOCENE

Introduction

Most coastal ecosystems around the world are influenced by changes in sea-level (SL). For example, tidal gauges from south Florida show that the average rate of SL rise has increased to 3.8 mm/yr since 1930; this rate is 6 to 10 times higher than that of the past 3,500 years (0.4 mm/yr) and approaches the highest rate of SL rise (>5 mm/yr) during the mid-Holocene Climate Optimum (Wanless et al, 1994). Studies predict that the rapid RLS rise will continue during the 21st century (IPCC, 2014). Thus, an understanding of how coastal wetlands in regions like south Florida have changed in response to past SL fluctuations may assist investigation of responses of coastal ecosystems to ongoing SL rise (e.g., Wooller et al., 2004; Torrescano and Islebe, 2006; Monacci et al., 2009; Gonzalez etal., 2010).

Palynological studies have related changes in vegetation to hydrological and climatic changes. Some such studies have been conducted in south Florida (Donders et al., 2005; Willard and Bernhardt, 2011; van Soelen et al., 2012). These studies indicate that drier intervals have been influenced by southward shifts of the Inter-tropical Convergence Zone, and wetter intervals have been influenced by the positive phase of the North Atlantic Oscillation. Such climatic changes have been associated with shifts in hydroperiod and hence composition of wetland plant communities (Willard and Cronin, 2007; Bernhardt and Willard, 2009; Willard and Bernhardt, 2011). Similar vegetation shifts attributed to variation in climate have also

been suggested by other studies in south Florida and the Caribbean region (Islebe et al., 1996; Donders et al., 2005; van Soelen et al., 2012).

Peat-accumulating ecosystems are among the coastal communities associated with rises in sea level. Previous studies have documented the initiation of peat accumulating wetlands (Scholl et al. 1969; Robbin, 1984) and formation of mangrove communities in south Florida from macrofossil records (Parkinson, 1989; Wanless et al., 1994). However, no pollen record from the Everglades is older than 5,000 years, and a detailed continuous chronology of Holocene changes in wetland vegetation in the now extensive mangrove region of South Florida remains lacking. Therefore a multi-proxy paleoecological record, focused on the mid-Holocene time of rapid SL rise, should be useful in documenting changes and in generating hypotheses regarding processes involved in the formation of freshwater wetlands, their changes over time as SL rise occurs, and their relationship to formation of coastal/estuarine mangrove forests.

This study presents a 5,700 yr palynological record, retrieved from a mangrove-dominant estuarine wetland at the mouth of Shark River Estuary in Everglades National Park. We aim to: (1) document the origination of freshwater peat-accumulating wetlands, document changes occurring over time during the Holocene, and determine when they transition to brackish marsh/mangrove swamp at the Shark River Estuary; and (2) characterize the allogenic forcing controlling development of coastal wetlands at the Shark River Estuary.

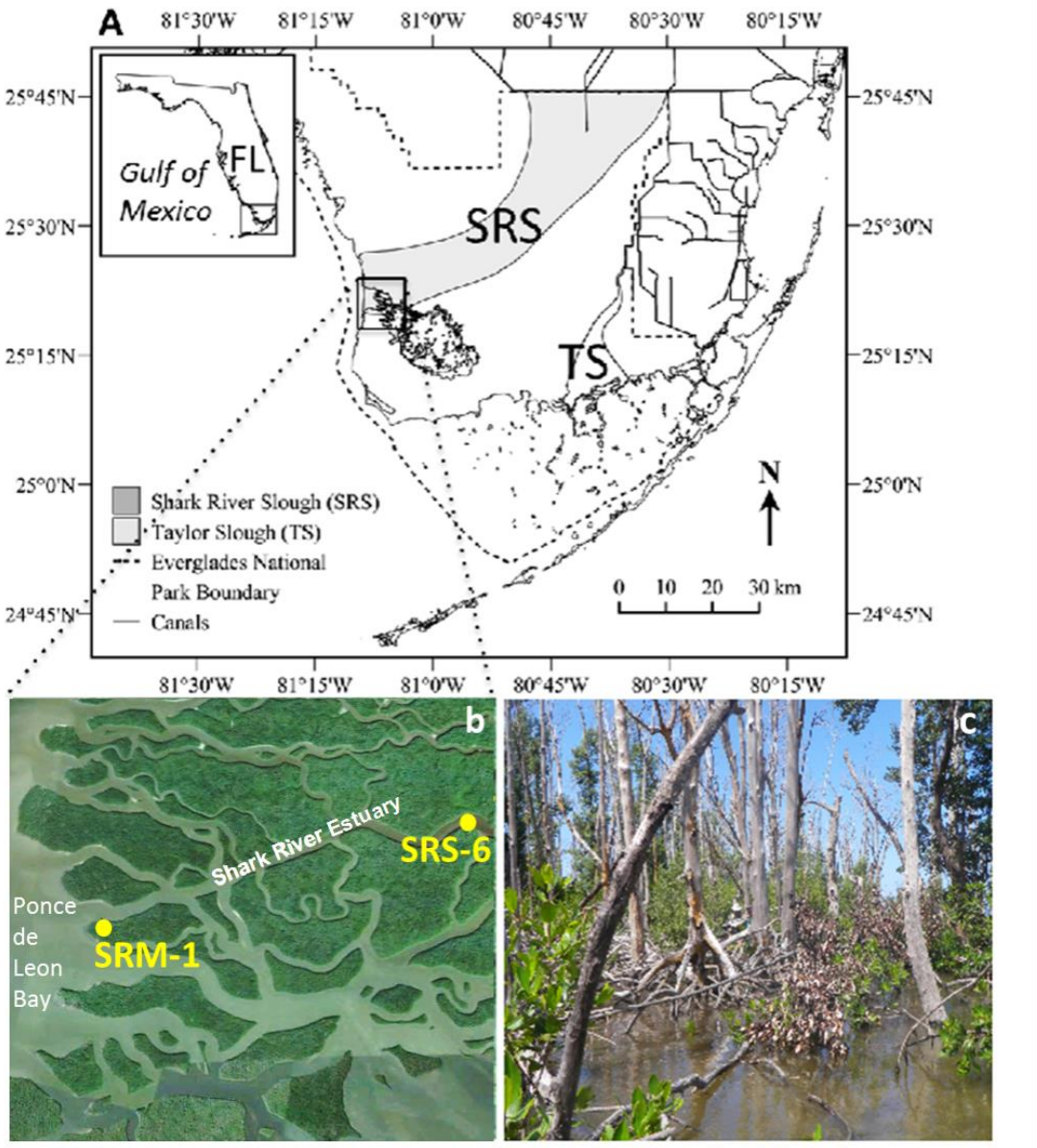

Figure 1. A) Location of the Shark River Slough (SRS) and Everglades National Park, South Florida (base map adapted from FCE LTER: http://fcelter.fiu.edu); B) Location of the Shark River Estuary, coring site (SRM) at the mouth of Shark River, and the SRS-6 site where hydroperiod and forest productivity has been monitored since 2002; C) Partial view of the SRM Mangrove forest impacted by Hurricane Wilma in 2005; photo taken at the time the cores was sampled.

Study area

The largest contiguous mangrove swamp in the continental USA occurs in the Florida Everglades. Approximately 144,000 ha of dense mangrove forests extend along the modern coast from Naples to Florida Bay (Simard et al., 2006; Lodge, 2010). Our

study was conducted at the western end of this region, at the mouth of the Shark River Estuary along the coast of southwestern Florida in the Everglades National Park (Monroe County). This region of the Florida peninsula is subtropical, having pronounced wet and dry seasons with 70–75% of the annual precipitation falling from June to September (Lodge, 2010; Beckage et al., 2003). Water overflowing Lake Okeechobee and associated rainfall result in a southward sheet flow along a gentle slope of ~3 cm/km into Shark River Estuary and to a lesser extent into Taylor Slough (Castañeda-Moya et al., 2013; Lodge, 2010; Rivera-Monroy et al., 2011). The water entering Shark River Estuary flows through long-hydroperiod prairie sloughs into a mangrove swamp at the river estuary and then into Whitewater Bay or the Gulf of Mexico along the southwestern coast of Florida (Lodge, 2010). Our study site (25°21’10”N, 81°6’52”W) is located on the edge of Ponce de Leon Bay, at the mouths of Whitewater Bay and Shark River Estuary (Fig. 1). It is situated in a fringing mangrove forest, where *Laguncularia racemosa* (white mangrove) and *Rhizophora mangle* (red mangrove) are co-dominant species (Chen and Twilley, 1999 a, b), and *Avicennia germinans* (black mangrove) is also present. This location (Fig. 1) was strongly affected by Hurricane Wilma, resulting in 90% mortality for trees with diameters at breast height greater than 2.5 cm (Smith et al., 2009).

The hydroperiod in the study site is influenced by both tidal cycles and freshwater discharge (Saha et al., 2012). A multi-year (2001-2004) monitoring study at a nearby location (SRS-6), ~4 km inland from the mouth of Shark River, shows that the mangrove forests are inundated by tides 90% of the year, with an average tidal range of

0.5 m (Castañeda-Moya et al., 2013). As a result of changes in hydrology along the Shark River, soil pore-water salinity inside the mangrove forests decreases significantly from 27 ± 2.6 ppt close to the mouth (i.e. SRS-6) to 4.6 ± 1.1 ppt 20 km upstream (Castañeda-Moya et al., 2013). Since the early 20th century, land-use changes linked to anthropogenic activities (agriculture and urbanization) have dramatically reduced the seasonality of freshwater flow throughout the Everglades (Light and Dineen, 1994) and have affected surface and groundwater flows in this coastal region (Saha et al. 2012).

SL-changes in south Florida have varied significantly over the past several thousand years. Previous studies of regional sea-level history indicate a rate of SL-rise of >5 mm/yr between 8,500 to 6,500 cal yr BP, when SL is at least 6.2 m lower than today and the shoreline is 30 km seaward of the present position (Wanless et al., 1994). Since 6,500 cal yr BP, the rate of SL-rise decreases to 2.3 mm/yr, and it continues to decline to 0.4 mm/yr after 3,500 cal yr BP, at which time SL is only 1 m below today's level (Wanless et al., 1994; Ross et al., 2009). Since AD 1930, the rate of SL-rise has increased to 3.8 mm/yr, and replacement of freshwater marshes by mangrove wetlands has been observed in the Everglades National Park as a result of salt water intrusion and salinity changes in groundwater (Wanless et al., 1994; Ross et al., 2000; Michot et al. 2011).

Materials and methods

A 5.25 m core (SRM-1) was retrieved at the study site in May 2010 using a Russian peat borer. The 50 cm core segments were measured, photographed, and wrapped in the field, and stored in a cold room (4 ℃) at the Global Change and

Coastal Paleoecology Laboratory at Louisiana State University. The core was scanned using an X-ray fluorescence (XRF) analyzer at 2 cm intervals to measure elemental concentrations (ppm) of 32 chemical elements. XRF analysis is widely used in coastal studies and the behaviors of most key elements are well established through previous studies (van Solen et al., 2012; Ramirez-Herrera et al., 2012). Loss-on-ignition (LOI) analyses were performed at contiguous 1 cm intervals to establish the ratio of organic versus inorganic sediment through the core (Dean, 1974).

Fourteen samples from core SRM-1 are used for AMS ^{14}C measurements. Ten samples consisting of leaf fragments and pieces of wood are selected under a dissecting microscope and sent to the NOSAMS Laboratory at Woods Hole Oceanographic Institution (Table 1, Fig. 2). In addition, approximately 10 grams of sediments taken at 374 and 446 cm are submitted to Beta Analytic Inc., in Miami, Florida, for AMS ^{14}C measurements. At the dating facility these sediments are passed through a 180 μm sieve to separate the <180 μm fine organic fraction from the >180 μm coarse organic fraction. Both fractions are dated separately to compare dating results using different materials (Table 1). An age-depth model is developed by using BACON version 2.2 (Blaauw and Christen, 2013), a Bayesian age-depth modeling software using R as an interface. Most priors are using default settings (acc.shape=1.5, res=5, mem.strength=4, and mem.mean=0.7). One of the prior distributions (acc.mean) is set to be ten as suggested by Bacon model. Combined with an estimated starting date of -55 cal yr BP at 0 cm for the first section, these accumulation rates then form the age-depth model, which is reported as calibrated years BP (cal yr BP).

Table 1. Radiocarbon dating results for core SRM-1. Dates in parentheses are rejected due to extreme age reversal.

Sample ID	**Depth (cm)**	**Material**	**Conventional C^{14} age (yr BP)**	**2-σ Calibrated range (Cal yr BP)**
OS-960a2	56	Leaf	145 ±25	0 - 280
OS-83953	139	Leaf	1180 ±30	990 - 1180
OS-90704	179	Leaf	1940 ±30	1820 – 1970
OS-95704	243	leaf	2860 ±30	2880 – 3070
OS-83943	246	Wood	155 ±25	(Rejected)
OS-90685	246	Wood	> Modern	(Rejected)
OS-93264	260	Leaf	2240 ±30	2150 - 2340
OS-96061	300	Bark	3540 ±35	3700 – 3910
Beta-345774	374	Organic silt	4160 ±30	4780 - 4830
Beta-346208	374	Roots	2940 ±30	3000 - 3210
OS-96060	440	Leaf	1090 ±20	(Rejected)
Beta-345775	446	Organic silt	5800 ±30	6500 - 6670
Beta-346209	446	Roots	4060 ±30	4760 - 4800
OS-84455	448	Plant debris	6620 ±260	6940 – 7980

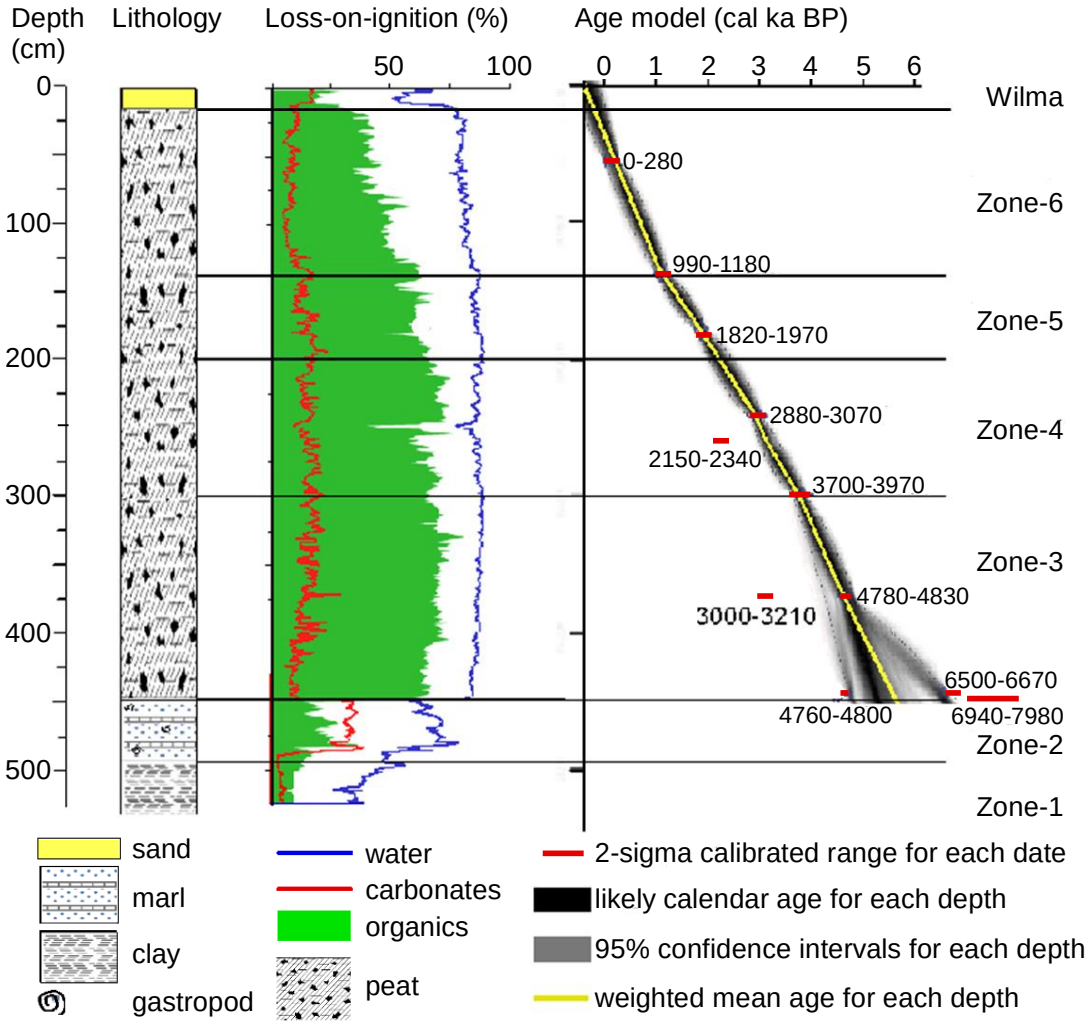

Figure 2. Lithology, loss-on-ignition diagram, and the age-depth model for the core. Loss-on-ignition diagram presents the % wet weight for water, and % dry weight for organics and carbonates. The age-depth model is developed by BACON and based on 11 calibrated C^{14} ages. The yellow curve shows the 'best' estimated age for each depth based on the weighted mean age. The surface (0 cm) of the core is assigned as -55 cal yr BP because it is identified as the Hurricane Wilma deposit (2005). Further information about radiocarbon dates is shown in Table 1 and Supplementary information.

Sixty-five samples of 0.9 to 1.8 mL are taken at 5 to 10 cm intervals for palynological analysis. Samples are processed using standard procedures (Liu et al., 2011; Kiage and Liu, 2009). One commercial *Lycopodium* (L_c) tablet (~ 18,583 grains) is added to each sample as an exotic marker to calculate the of pollen concentration (grains/cm^3). Hydrofluoric acid treatment and acetolysis are omitted to minimize the degradation of microfossils during processing. More information about the processing of pollen samples and calculation of the pollen concentration is described in **Chapter 3**. The identification of pollen is based on pollen illustrations by McAndrews et al. (1973), Willard et al. (2004), and Chmura et al. (2006). Approximately 300 pollen grains and spores, including both terrestrial and aquatic taxa, were counted in most samples, which were used as the pollen sum for the calculation of pollen percentages. Additional microfossils, including foraminifera linings, dinoflagellates tests, fungal spores, and charcoal fragments (>10 μm in size), were also counted. The pollen (and other) data are to be forwarded to the Neotoma Paleoecology Database.

Results

Core SRM-1 consists of 4 different sediment types. The stratigraphy is displayed in Fig 2, and the following sediment units can be recognized: basal clay (525-485 cm), marl (485-450 cm), peat (450-10 cm), and calcareous clastic sediments (10-1 cm).

Among the 10 AMS ^{14}C dates obtained from NOSAMS, three anomalously young dates (OS-83943, OS-90685, and OS-96060) were rejected due to extreme stratigraphic reversal (Table. 1). The date measured at 448 cm (6,940-7,980 cal yr BP) may also be erroneous (i.e., too old) because it comes from the base of the peat where

it directly overlies the marl, which increases the possibility of it being affected by carbonate error. For the two pairs of dates at 374 cm and 446 cm determined by Beta Analytic, the coarse organic fractions yield much younger dates than the fine organic fractions by ~1,200 to ~1,800 years (Table. 1). We suspect that the coarse organic fraction might be contaminated, as visual inspection of sieve residues revealed intrusive (younger) rootlets (See **Supplementary Information**). In order to be objective, all dates except for the three rejected ones (out of 14) were used to construct the age-depth model using BACON software (Fig. 2). The results confirm our interpretation that the "best" age-depth model (yellow curve, Fig. 2) based on the weighted mean age of each sample is very close to intercepting ^{14}C dates at 56 (178 cal yr BP), 139 (1138 cal yr BP), 179 (1872 cal yr BP), 243 (2,947 cal yr BP), 300 (3,777 cal yr BP), and 374 (4,658 cal yr BP) cm, and the bottom date has great uncertainties ranging from 4,760 to 7,980 cal yr BP (95% confidence intervals) (Fig. 2). We use the "best" age-depth model based on the weighted mean age for each sample to construct the chronologies for all the proxy records discussed in this paper, thus indicating a basal date for the peat of approximately 5,700 cal yr BP at 450 cm.

We divided core SRM-1 into 6 stratigraphic zones based on pollen composition, sediment stratigraphy, and chemical characteristics. Zone 3 is further subdivided into three subzones. The calcareous clastic sediments with low loss-on-ignition values at the top of the core (Fig. 2) are included in Zone 6. The palynological results are reported in percentage (%) and influx (grains/cm^2/yr) diagrams (Figs. 3 and 4). Each zone is described below.

Zone 1 (525-485 cm; >5,700 cal yr BP)

Clastic sediments below 450 cm in core SRM-1 were deposited prior to ~5700 cal yr BP, based on the age model. These sediments consist of homogeneous clay. Loss-on-ignition results indicate that these fine-grained sediments have the lowest contents of water (<50% wet weight), organic matter (<20% dry weight) and carbonates (<15% dry weight) of any zone in the core (Fig. 2). XRF data show that the elemental concentrations of Zr (>100 ppm), S (5,000-40,000 ppm), K (>3,000 ppm), Ti (>2,000 ppm), Fe (>10,000 ppm), and most of other heavy metals in Zone 1 are at least 5 to 10 times higher than values in the rest of the core (Fig. 5). Pollen is totally absent in samples taken from Zone 1 (Figs. 3 and 4).

Zone 2 (485-450 cm; >5,700 cal yr BP)

Calcareous sediments from 485-450 cm in core SRM-1 were also deposited prior to ~5700 cal yr BP, as indicated by the age model. Located above the basal clay but underlying the peat deposits, these sediments consist of silt, limestone fragments, and shell hashes of the freshwater snail *Helisoma trivolvis* sp. (Fig. 2). Zone 2 has higher percentages of water (50-70%) and organic matter (20-30%) than the clay in Zone 1, and the highest content of carbonates (30-35%) in the whole core (Fig. 2). XRF results reveal that the concentrations of Ca (30,000-100,000 ppm) and Sr (150-400 ppm) reach their highest values in Zone 2 (Fig. 5).

Pollen influx values are between 1,000 to 3,000 grains/cm^2/yr (Fig. 4), and charcoal is abundant (20,000-60,000 fragments per cc). The dominant taxon, *Salix*, accounts for > 50% of the pollen sum in some samples (Fig. 3). Sub-dominant taxa

include Poaceae (20%) and two trees, *Pinus* and *Quercus* (10-20%). Other major taxa (defined as those occurring at >5% in at least one level) include Amaranthaceae, *Sagittaria,* and *Typha*. Notably, *Pinus*, *Quercus*, and *Salix* pollen reach their highest percentages in the core in the middle of Zone 2, before decreasing toward the top of the zone, as Poaceae and Amaranthaceae increase.

Zone 3 (450-300 cm; 5,700 to 3,800 cal yr BP)

Zone 3 (450-300 cm) consists of continuous peat deposits. Our age model indicates that these peats were deposited between ~5,700 to 3,800 cal yr BP (Fig. 2). This peat layer displays high contents of organic matter (>50%) and water (>75%) and the lowest concentration of all detected chemical elements. The loss-on-ignition and XRF values are generally similar throughout this zone (Figs. 2 and 5).

Zone 3 is divided into three subzones based on changes in percentages and concentrations of the main pollen taxa. Subzone Zone-3a (~5,700 to 5,250 cal yr BP) contains mostly upland taxa, including *Salix* (up to 20%) and *Pinus* (up to 25%). In addition, some *Morella* and Rubiaceae (up to 20%) also are present, as are some herbs, such as *Typha* (up to 10%), Solanaceae (up to 5%), and Asteraceae (up to 10%). Mangrove pollen first appears in subzone 3a, but percentages are low (<5%).

A change in the pollen assemblage is notable in subzone 3b (~5,250 to 4,300 cal yr BP). At the outset, the pollen assemblage records the concurrent disappearance of *Salix* and Rubiaceae, decreases in *Morella* and *Quercus*, as well as a marked decline in *Pinus* (< 25%). In addition, abundances of Poaceae and Asteraceae decrease, and Amaranthaceae increases markedly (often >50%, and up to 90%).

In subzone 3c (~4,300 to 3,800 cal yr BP), Cyperaceae increases in abundance, while Amaranthaceae decreases precipitously in both percentage and concentration values. Freshwater *Sagittaria* also increases, reaching its highest percentage (10%) in subzone 3c.

Zone 4 (300 to 200 cm; 3800 to 2200 cal yr BP)

Our age model suggests that the uniform peat in Zone 4 was deposited between ~3,800 to 2,200 cal yr BP. The organic matter (>50%) and water (>75%) contents in this zone remain consistently high, while the concentrations of all detected chemical elements remain the lowest throughout the zone.

The overall pollen influx (< 2,000 grains/cm^2/yr) is low (Fig. 4). At the beginning of the zone, the dominant pollen types are Amaranthaceae (>50%) and Poaceae (30%), but other herbaceous taxa (i.e., Apiaceae, Solanaceae, Asteraceae, *Typha*) are rare (<5%) or absent (*Ambrosia*, Cyperaceae, and *Sagittaria*). *Pinus* and *Quercus* are uncommon (<10%) throughout the zone. The abundance of mangrove pollen (especially *Rhizophora*) is low at the beginning of the zone, but increases towards the top of the layer (Fig. 4). Near the top of this zone, *Rhizophora* becomes dominant, comprising as much as 50% of the pollen. Foraminifera linings make their first appearance in the upper part of the zone. Charcoal concentrations decrease from <10,000 fragments per cc at the bottom of Zone 4 to insignificant levels at the top of the zone.

Zone 5 (200 to 140 cm; 2,200 to 1,150 cal yr BP)

Sediments in Zone 5 was deposited between ~2,200 and 1,150 cal yr BP (Fig. 2). The loss-on-ignition and XRF results are very similar to those in Zones 4 and 3.

The pollen assemblage in Zone 5 is characterized by the lowest pollen influx values (< 1,000 grains/cm^2/yr) above 485 cm (Fig. 4), and the increasing dominance of mangrove taxa. Amaranthaceae and Poaceae percentages are very low, and the percentages of all other herbaceous and upland species (*Pinus* and *Quercus*) reach their minima for the entire core. *Rhizophora* pollen continues to increase. Mangrove pollen reaches 50% of the pollen sum in the middle of Zone 5 (Fig. 3). Dinoflagellates and foraminifera linings appear at higher concentrations more consistently. Concentrations of charcoal fragments were generally insignificant in Zone 5.

Zone 6 (140 to 0 cm; 1150 cal yr BP to present)

The peat deposit at the bottom of this zone has an age of ~1,150 cal yr BP (Fig. 2). The water (>75%) content in this zone remains high, but the organic matter decreases to <50% in most samples.

The pollen influx values (2,000 – 4,000 grains/cm^2/yr) of zone 6 are the highest among all six zones. Mangroves are the dominant pollen taxa in Zone 6. *Rhizophora* comprises >50%; other mangrove genera (*Laguncularia*, *Avicennia*, and *Conocarpus*) also are present (Fig. 4). Amaranthaceae and Poaceae continue to decrease, as do the percentages of all other herbaceous taxa. *Pinus* and *Quercus* are present, and for the first time, *Taxodium* is abundant. Dinoflagellate and foraminifera linings occur at high concentrations. Charcoal fragments are absent in most samples in this zone.

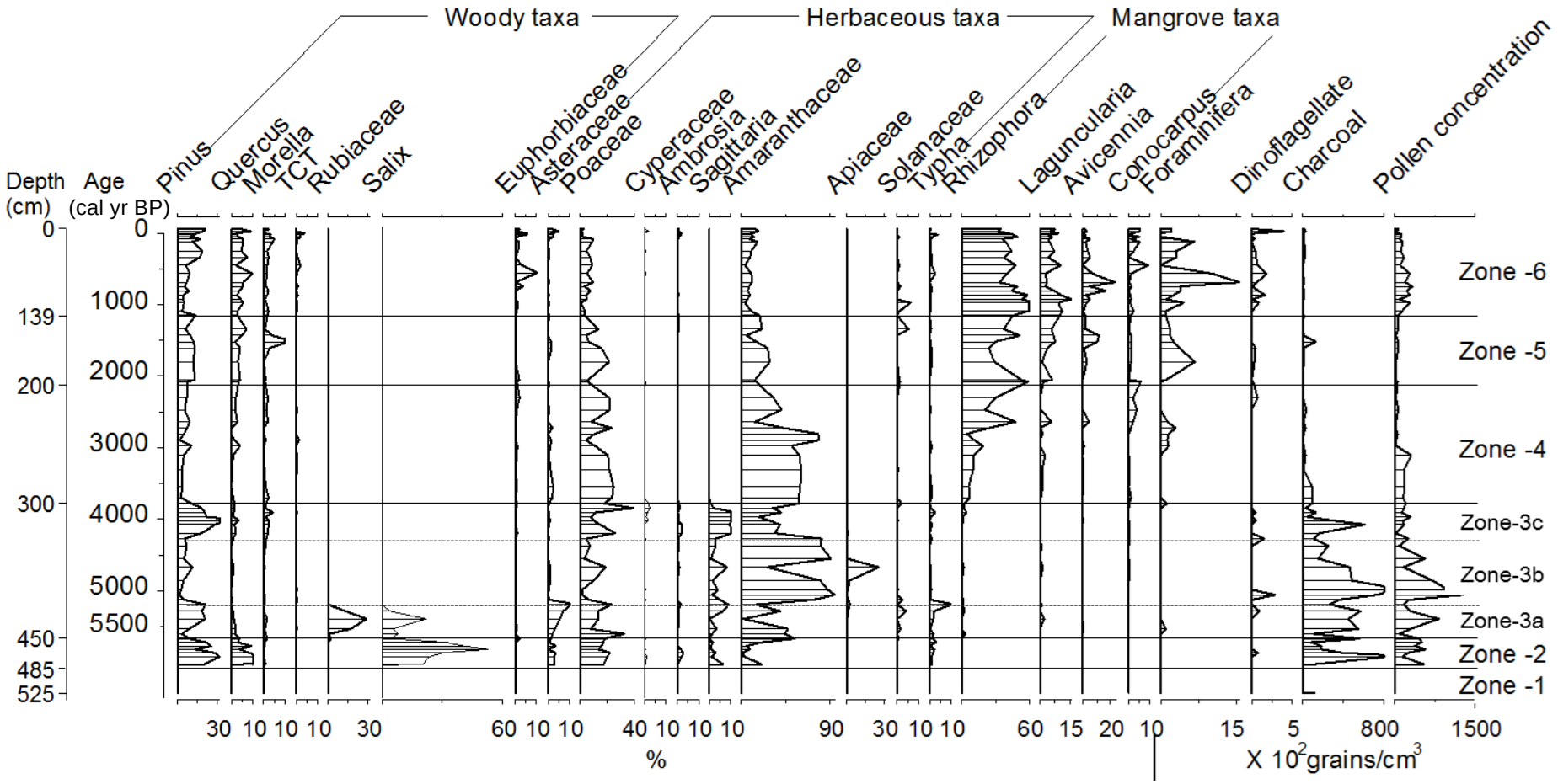

Figure 3. Pollen percentage diagram for core SRM-1. The concentration curves for marine planktons, charcoal, and pollen are added on the right to facilitate comparison. Dates on Y-axis are calibrated yr BP. TCT is the acronym for Taxodiaceae- Cupressaceae- Taxaceae.

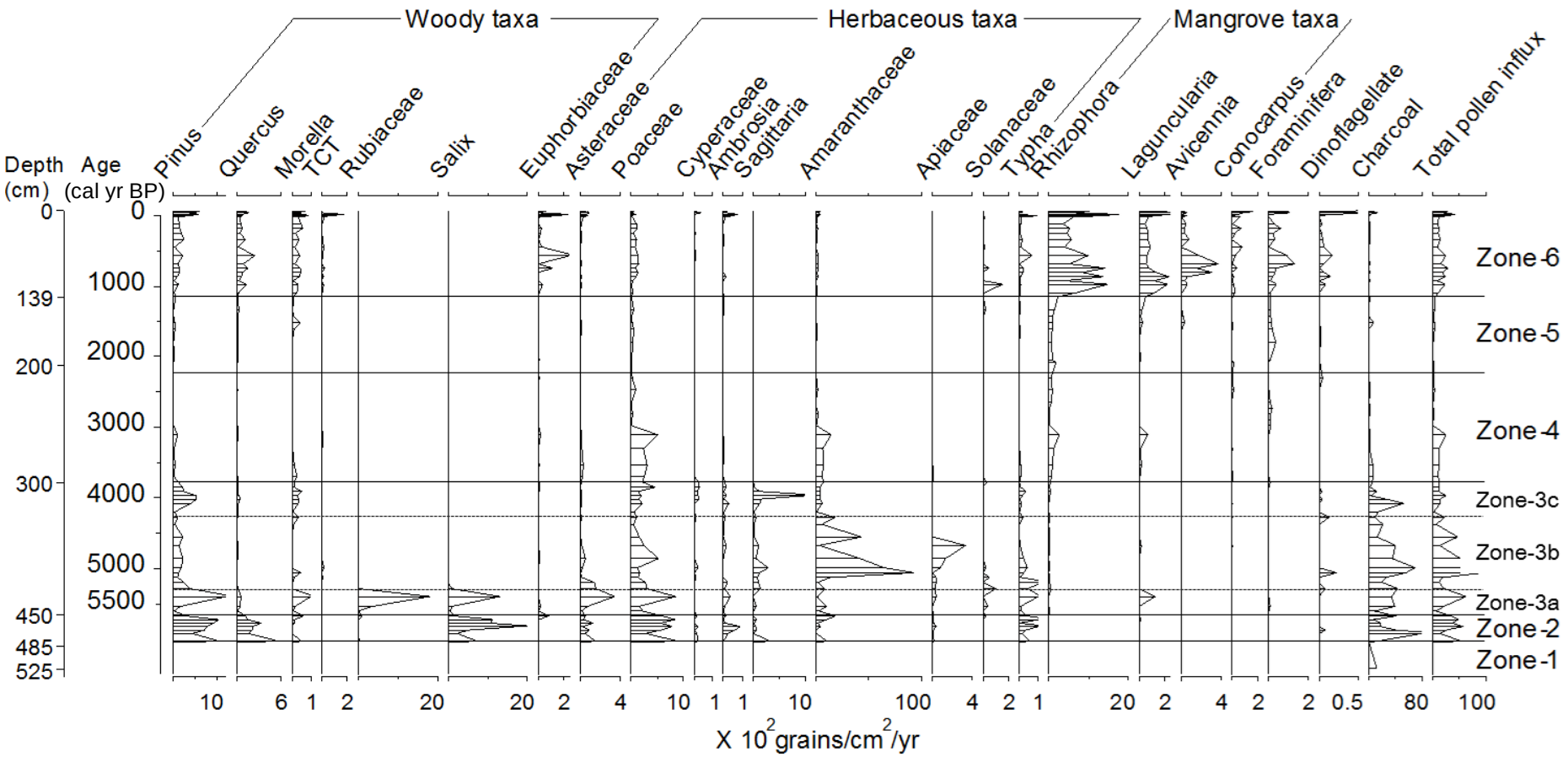

Figure 4. Pollen influx diagram for core SRM-1. The influx curves for marine plankton and charcoal are added on the right to facilitate comparison. Dates on Y-axis are calibrated yr BP. TCT is the acronym for Taxodiaceae- Cupressaceae- Taxaceae.

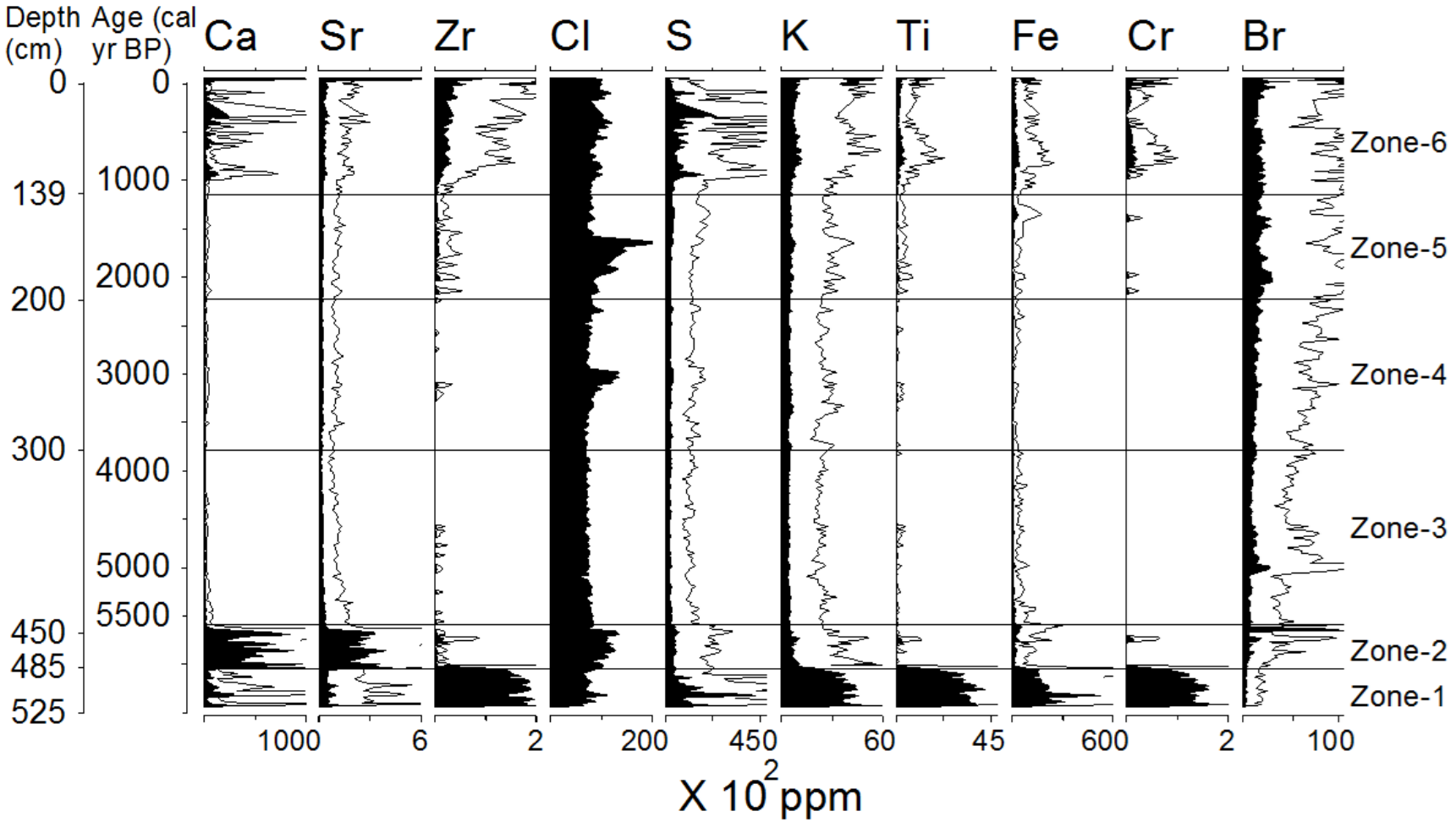

Figure 5. XRF results from core SRM-1. Dates on the Y-axis are calibrated yr BP. The black silhouettes represent the actual concentration of the elements, and the transparent curves represent 5X exaggerated values.

The top 10 cm

The top 10 cm of the core consists of calcareous clastic sediments deposited by storm surges generated by Hurricane Wilma (Castañeda-Moya et al., 2010; Ramirez-Herrera et al., 2012). The contents of water (50-70% vs >80%) and organic matter (20-25% vs 40-60%) in these sediments are significantly lower than those in the underlying peat, but carbonate content is much higher (30-35% vs 10-15%). The concentrations of Ca, Sr, and Zr in the top 10 cm are 10 to 100 times higher than in the underlying peat (Figs. 5, 6).

Discussion

The early Holocene dry upland landscape (>5,700 cal yr BP)

The basal sections of the core (Zones 1 and 2) were deposited prior to ~5,700 cal yr BP. At that time, the climate in south Florida was drier than today (Lodge, 2010; Donders et al., 2005; van Soelen et al., 2010). Zone 1 (486-525cm) is composed of fine silicates (clastic clay) devoid of pollen. The very high concentrations of metals such as Ti, Fe, and Cr in these sediments of Zone 1 are most likely the result of acidic leaching; such sediments are commonly found in Florida (Hine and Belknap 1986) and the Caribbean region underlying more recent mangrove peat (Wooller et al., 2007; Macintyre et al., 2004). Overall, the proxy record for Zone 1 indicates an arid or frequently dried out terrestrial environment that was not inundated long enough to promote marl or peat accumulation and to preserve pollen. The absence of pollen precludes knowledge of the vegetation types present.

Short-hydroperiod prairie (> 5,700 cal yr BP)

Zone 2 (451-485cm) consists of calcareous sediments that resemble those in marl prairies currently present in the Everglades. Such sediments now underlie large areas of peat from the northern Everglades to Whitewater Bay, Cape Sable, and Florida Bay (Gleason and Stone, 1994, Lodge, 2010). The formation of freshwater calcitic marl over subaerial substrate marks a transition from a dry and drained environment to a shallow seasonally flooded freshwater wetland environment (Gleason and Stone, 1994). Indeed, shell hashes of the freshwater snail *Helisoma trivolvis* found in Zone 2 are consistent with such environment. These evidences probably suggests a period during the mid-Holocene with a higher subsurface water table and increasing hydroperiod, but not yet wet enough to sustain peat accumulation.

The pollen assemblage of Zone 2 contains mostly a mixture of upland and herbaceous species. The composition of this pollen assemblage is consistent with a mixture of short-hydroperiod and longer-hydroperiod prairies, perhaps also with higher nonflooded areas (i.e., pine savannas) in the immediate vicinity. Such areas (e.g., Lostman's Pines and Raccoon Point regions of Big Cypress National Preserve; Long Pine Key in Everglades National Park) are present in the interior of the Everglades region of South Florida today (Doren et al. 1993; Willard et al., 2001; Schmitz et al., 2002; Bernhardt and Willard, 2009; Hanan et al., 2010). The freshwater marl-accumulating wetlands postulated as present in Zone 2 appear to have been subject to frequent fires. These habitats today have hydroperiods lasting less than 12 months and are thus dry seasonally, tending to burn more than once a decade, and

even every 1-2 years if located adjacent to pine savannas (Platt 1999; Schmitz et al., 2002; Slocum et al., 2003, Platt et al. 2015). Such high fire frequency would be consistent with the abundance of charcoal particles in pollen samples. The occurrence of *Pinus*, *Quercus*, Poaceae, and Asteraceae in the pollen assemblage further suggests that upland habitats were in the vicinity.

We suggest that the study site was most likely a short-hydroperiod prairie containing longer-hydroperiod willow thickets as "islands" prior to ~5,700 cal yr BP. These willow-dominant thickets may have been bounded by open water species like *Typha* and *Sagittaria*. These wetland habitats could have been surrounded by pine savanna and contained subtropical hammocks. Most importantly, the palynological data indicate not only that wetlands have been present for more than ~5,700 years in southwestern Florida, but also suggest that early wetland landscapes in interior southern Florida are likely to have resembled to some extent the fire-maintained landscapes occurring today in Big Cypress National Preserve and Everglades National Park (DeCoster et al. 1999; Schmitz et al., 2002, Slocum et al., 2003, 2007).

Dynamic freshwater wetlands (~5,700 to 3,800 cal yr BP)

Zones 3, 4, and 5 consist of peat that dates back to ~5,700 cal yr BP. Our study site in the southwestern region of the Everglades lies atop the permeable Tamiami limestone where the water table is very sensitive to changes in hydrological conditions (Gleason and Stone, 1994). The formation of peat instead of marl in Zone 3 (~5,700 to 3,800 cal yr BP) suggests deeper water levels and longer, 12-month hydroperiods in at least some local areas such as the coring site. Historically, water

availability in the southern Everglades is determined by local rainfall and drainage through sheet flow of water from Lake Okeechobee (Donders et al., 2005; Lodge, 2010; Michot et al., 2011; Saha et al., 2012). Some evidence indicates that intensification of the El Niño-Southern Oscillation (ENSO) during the mid-Holocene increased precipitation in south Florida (Donders et al., 2005). Therefore, formation of peat throughout Zone 3 is consistent with the hypothesis that the mid-Holocene intensification of ENSO might have marked the onset of more modern-day precipitation regimes in the Everglades (Rodbell et al, 1999; Koutavas et al, 2002).

Our study suggests that freshwater wetlands in south Everglades were dynamic and changing on time scales of millennia during the mid-Holocene. Subzone Zone-3a is between ~5,700 to 5,250 cal yr BP, when numerous upland taxa (*Salix*, *Pinus*, Rubiaceae, *Quercus*, and *Morella*) and herbaceous taxa (Poaceae, *Typha*, Solanaceae, and Asteraceae) consistently appear in the pollen assemblage (Figs. 3 and 4). This pollen assemblage, which persisted until ~5,250 cal yr BP, suggests that 12-month hydroperiod *Salix* (willow)-dominant sloughs or perhaps *Cephalanthus* (buttonbush; Rubiaceae) and imbedded in long- or short-hydroperiod prairies occupied by grasses or sedges continued to persist after moisture levels increased over those associated with Zone 2 (Hanan et al., 2010).

The shift to an herbaceous-dominant landscape marks the onset of Zone-3b, between ~5,250 to 4,300 cal yr BP. At the outset, the pollen assemblage records the concurrent decline in upland taxa (*Salix*, Rubiaceae, *Pinus*, *Morella*, and *Quercus*), and a marked increase in Amaranthaceae (Figs. 3 and 4). In addition, pollen

percentages for *Sagittaria* and Apiaceae reach their maximum in Zone 3, suggesting widespread freshwater wetlands with 12-month hydroperiods near the coring site during this subzone.

Amaranthaceae abundance increases with disturbances. In present-day south Florida wetland habitats, such increases have been noted after natural lightning-ignited fires (Slocum et al. 2003, 2010) and hurricanes (Armentano et al. 1995), when open space is generated and colonized by species like *Amaranthus australis* (Schmitz et al., 2002). Increases of Amaranthaceae in other pollen diagrams have also been attributed to periods of drought (Willard et al, 2001; Willard and Cronin, 2007). Therefore the shift to an herbaceous community in this subzone suggests frequent major fires, perhaps in conjunction with periods of droughts; such intense fires have burned out willow thickets in the present-day Everglades (Beckage et al., 2003, Slocum et al., 2007). This is supported by the increase in micro-charcoal particles (Figs. 3 and 4). Such periodic droughts and intense fires may have characterized this subzone (~950 years).

Subzone 3c (~4,300 to 3,800 cal yr BP) reflects the formation of open water sloughs. After 4,300 cal yr BP, *Sagittaria* reaches its highest concentration throughout the core, and Cyperaceae reappears. At the same time, upland taxa reappear or increase, accompanied by a decrease in Amaranthaceae, suggesting that the long-hydroperiod prairies changed to open water and/or sedge-sloughs (perhaps *Eleocharis*-dominant) due to the rising water table. This change, which would have reduced fire frequency, is supported by the continuing decrease of charcoal fragments.

XRF results show no signs of marine influence in Zone 3 (Fig. 5), as common marine indicators (Ca, Sr, and Zr) are rare or absent. During the mid-Holocene, sea level in southwestern Florida was at least 6 m lower than the present level (Parkinson, 1989), and the shoreline was probably 30 km seaward relative to today (Wanless et al., 1994), implying that marine influence was minimal or non-existent in the southwestern Everglades from ~5,700 to 3,800 cal yr BP.

Freshwater to marine transition (~3,800 to 2,200 cal yr BP)

Zone 4 (~3,800 to 2,200 cal yr BP) represents a transitional stage from freshwater to brackish marsh. At around 4,000 cal yr BP, the sea level was at least 5 m lower than at present, with a regional sea level rise of ~0.6 mm/yr in southern Florida (Wanless et al., 1994). The resultant marine transgression gradually reduced the site-to-sea distance. This transition is clearly recorded by the palynological data (Fig. 3). Linings of foraminifera start to appear with greater regularity at the top of this zone, while mangrove taxa increase in abundance beginning at ~3800 cal yr BP, indicating increased seawater flooding (Scott et al., 2003; Sabatier et al., 2008; González et al., 2010). Additionally, the abundance of Amaranthaceae and microscopic charcoal fragments diminishes, while *Sagittaria* and *Typha* pollen decline to trace values during this period, indicating a changing environment (less fresh water and fewer fires) with more marine influence (Willard et al., 2001; Willard and Cronin, 2007). These palynological data clearly show a period of marine transgression from ~3800 to 2200 cal yr BP. Similar environmental histories have been documented in southern Florida (Donders et al., 2005; van Soelen et al., 2010, 2012), suggesting that

the freshwater marshes in the southwestern Everglades were receiving more and more marine influence during the late Holocene. Today, similar brackish marshes occur between mangrove forests and freshwater marshes in the Everglades, including the Shark River Estuary (Willard et al., 2001). Using these as a modern analog, it could be inferred that during ~3800 to 2200 cal yr BP, the Shark River Estuary was probably occupied by grasses and *Amaranthus*, with some scrub red mangroves and occasional black and white mangroves. Salt-intolerant species like *Sagittaria* were no longer present. The frequency of fire was probably much reduced due to lower fuel loads (less graminoids biomass) and a 12-month hydroperiod, but with low salinity (Ross et al., 2000).

The development of mangrove scrubs (~2200 to 1150 cal yr BP)

In Zone 5 (~2,200 to 1,150 cal yr BP), all mangrove species reach high percentages and gradually exceed the marsh pollen taxa. Previous palynological studies from mangrove areas have documented that 50% to 95% *Rhizophora* pollen in total pollen assemblages indicates a well-developed red mangrove forest (Chappell and Grindrod, 1985; Woodroffe et al., 1985; Behling et al., 2001; Ellison, 2008). Some studies have shown that the abundance of mangrove pollen production is positively correlated with canopy height (Gill and Tomlinson, 1977; Versteegh et al., 2004; Van Campo and Bengo, 2004; Scourse et al., 2005). Although *Rhizophora* exceeds 50% of the total pollen sum in most samples in Zone 5 (Fig. 3), we assume it represents low-stature *Rhizophora* scrubs, because the pollen influx values of *Rhizophora* remained low during this period. Thus, Zone 5 represents a transition

from brackish marsh to mangrove forest. During this period, even though the shoreline was still undergoing transgression, the relatively stable sea level enabled mangroves to colonize the southern Everglades estuarine area. The multi-proxy data from the beginning of Zone 3 to the end of Zone 5 thus show a multi-millennial transition from freshwater to marine influences at the site. Similar replacement of freshwater marshes by low-stature mangrove scrubs has been observed at some inland sites in the southeastern Everglades since AD 1930 (Ross et al., 2000; Castañeda-Moya et al., 2013). The significantly shorter transitional time span involved in the recent transitions can probably be attributed to the current rapid SL rise rate of 3.8 mm/yr, compared with 2.3 to 0.4 mm/yr during the mid- to late-Holocene (Wanless et al., 1994; Ross et al., 2009). If the current rapid rate of SL rise continues, present coastal zonation of the Everglades can be anticipated to be altered in similar ways, but much more rapidly than occurred during the late-Holocene.

The establishment of coastal mangrove forests (~1,150 cal yr BP to present)

The multi-proxy record of Zone 6 (~1,150 cal yr BP to present) suggests an established coastal environment with predominately marine influences. Marine microfossils (foraminifera and dinoflagellates) are found in most levels in this zone. Indeed, high concentrations of Ca, Sr, and S characterize a coastal environment with increased allochthonous sediment input in this period (Davison, 1988; Ramirez-Herrera et al., 2012). Moreover, Zr, the main constituent for Florida beach sand (Miller, 1945), starts to consistently appear at ~1,150 cal yr BP (Fig. 6).

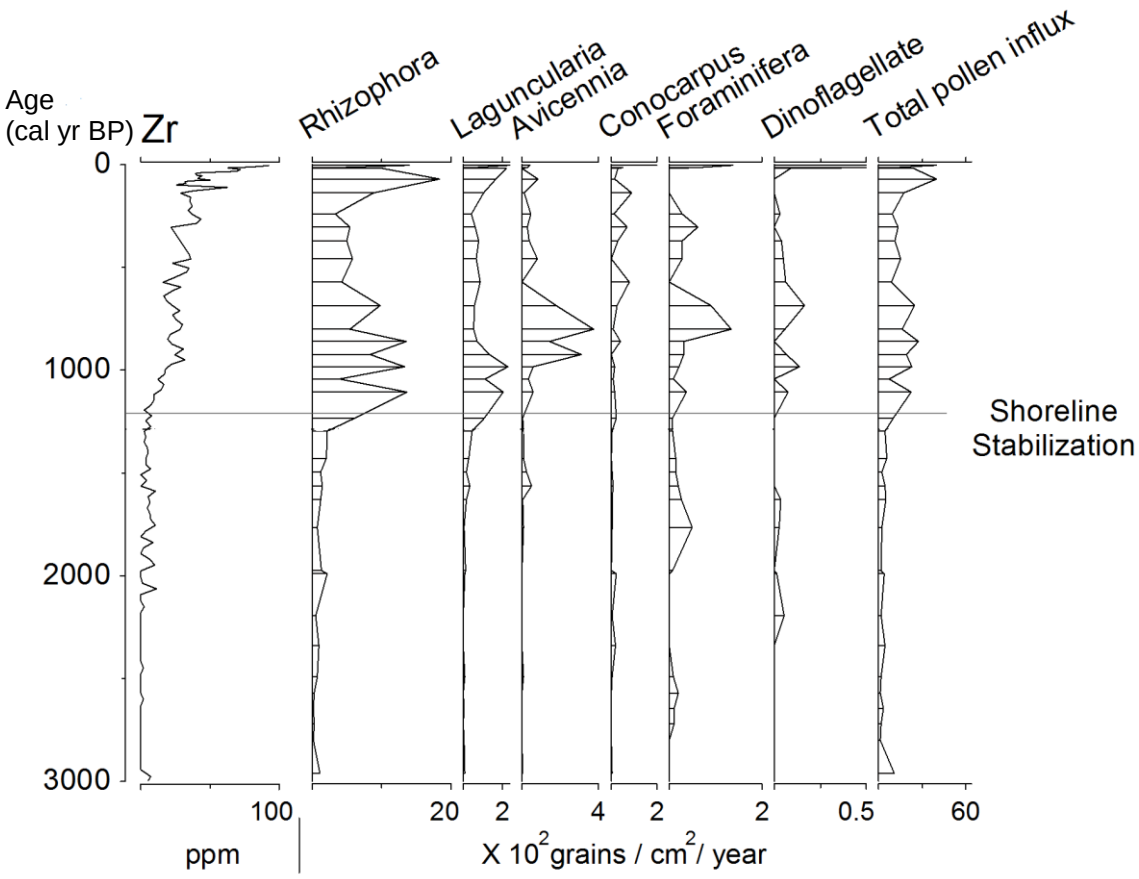

Figure 6. Zr concentration and influx values of selected microfossils for core SRM-1. The influx values of all mangrove species increase simultaneously with the concentration of Zr, indicating the establishment of mangrove forest and shoreline stabilization.

Because tides (and episodic storms) are the only source that consistently carries marine sediments into the fringing wetlands, this chemical signature suggests that the coring site started to receive sand through tidal exchange at that time. Concurrently, the pollen influx diagram shows a significant increase in all mangrove species (Fig. 6). This relative shift in pollen dominance suggests that a mixed mangrove forest similar to today's in structure and composition was established at the mouth of the Shark River Estuary around 1,150 cal yr BP. Because mangroves are generally found within the inter-tidal zones (Behling et al., 2001; Ellison, 2008; Urrego et al., 2009; Monacci et al., 2009), we propose that the modern coastal mangrove ecosystem was formed at

approximately the same time. Previous studies suggest that the modern coastal mangrove ecosystem in southwestern Florida was established about 3500 to 3000 cal yr BP (Parkinson, 1989; Gleason and Stone, 1994; Wanless et al., 1994). Our pollen and XRF data suggest a different mangrove development and history. Although *Rhizophora* is the first to arrive at the study site, *Avicennia* and *Laguncularia* are always present locally or in the vicinity in the last 3,000 years (Fig. 6). At approximately 1,150 cal yr BP, the tidal zone reached its modern position, and the modern shoreline occupied by mixed mangrove forest was formed at the mouth of the Shark River Estuary (Fig. 6).

Conclusion

Our 5700-yr multi-proxy record from the southwestern Everglades has yielded arguably the oldest basal peat date and longest paleoecological record for the region. High-resolution data allowed us to reconstruct a series of changes in coastal wetlands at the mouth of Shark River Estuary since the mid-Holocene. We have five major conclusions regarding paleoecological changes occurring in wetlands that should be especially applicable to ongoing changes in the Everglades resulting from SL rise.

(1) Palynological data indicate that wetlands have been present in the southwestern Everglades since the mid-Holocene. Initial wetland habitats, which originated more than 5,700 years ago from terrestrial, non-flooded habitats, most likely resembled present-day short-hydroperiod graminoid-dominant marl prairies with imbedded longer-hydroperiod sloughs occupied by willow (*Salix*) and possibly buttonbush (*Cephalanthus*); these wetlands have been surrounded by upland habitats, possibly

pine savannas. These patterns suggest that as new wetlands originate from non-wetland habitats such as pine savannas, they should be similar in species composition, ecological fire regimes, and landscape organization to habitats currently present in the Everglades, to the extent that rapid formation of such wetlands does not interfere with colonization processes. We note that because of the current overwhelming presence of human ecosystems in areas most likely to become wetlands, most wetlands formed from SL rise will not resemble short- and long-hydroperiod prairies, nor will fire be a major environmental process unless management efforts are made to restore historical fire regimes.

(2) Our study site became part of the Shark River Slough basin, with a continuous deposition of peat around 5,700 cal yr BP. During the period from ~5,700 to 3,800 cal yr BP, there was little evidence of marine influence. Initially, once peat began accumulating, plant communities comprising short- and long-hydroperiod prairies with imbedded sloughs and surrounded by uplands persisted, but after ~5,250 cal yr BP these habitats were replaced by long-hydroperiod prairies that were herb-dominant and lasted about 1,000 yr. As a response to increasing, but perhaps more seasonal precipitation, sloughs imbedded in frequently-burned long-hydroperiod prairies/marshes containing *Sagittaria* and *Typha* (and most likely sawgrass, *Cladium mariscus ssp. jamaicense*, whose pollen does not tend to be preserved) were formed. These herbaceous-dominant habitats burned, perhaps intensely, at periodic intervals, setting the stage for the abundance of disturbance-stimulated taxa like *Amaranthus* to increase after fires. These data suggest that freshwater wetlands in the southwestern

Everglades date back to the mid-Holocene and were dynamic, changing almost continuously on millennial timescales. Our pollen record also suggests that as rapid SL rise occurs, gradual change is less likely and more extensive changes become compressed into much shorter time scales.

(3) The multi-proxy data show a clear transition from a freshwater to a coastal/estuarine environment, as well as shoreline transgression beginning around 4,000 cal yr BP due to SL rise. From ~3,800 to 2,200 cal yr BP, mangrove taxa and marine planktons increased in the sedimentary record as a result of increased marine influence caused by rising sea level. This pattern also indicates a shift from a freshwater to a brackish wetland as marine influence (e.g., tidal inundation) increased. Over the next 1,050 years, relatively stable sea levels allowed the colonization of mangroves, causing a shift to mangrove-dominant forest in the southwestern Everglades. These changes occurred as the shoreline was still going through a transgression process. Compressing the changes with rapid SL rise, especially if hurricane frequency and intensity also increase, may result in rapid inland shifts of marine influences (e.g., salinity). Thus changes from freshwater to saline habitats are likely to be even more accelerated, resulting in further reductions in the likelihood that fresh-water species and short- and long-hydroperiod habitats might be able to move inland.

(4) At around 1150 cal yr BP, a mixed mangrove forest was established at the present-day Shark River estuary. Accelerated SL rise should both generate new habitat suitable for mangroves, but also remove current shoreline habitats. Thus, accelerated

SL rise should result in mangrove forests that do not reach the ages that they used to when shorelines were transgressing more slowly or were stable. Such dynamics should result in a dynamic non-equilibrium front of developing mangrove forest that moves inland, but is lost on the oceanward side at rates dependent on SL rise and hurricane frequency and intensity.

(5) Results from this study suggest that the modern mangrove-dominant shoreline at the mouth of the Shark River is more than 2,000 years younger than previously estimated (Parkinson, 1989; Gleason and Stone, 1994; Wanless et al., 1994; Lodge, 2010). Since the Shark River Slough is the largest freshwater outlet in the Everglades, its unique hydrological and ecological settings might have caused this inconsistency when comparing with other mangrove timelines proposed for other study sites. Therefore more regional paleoenvironmental works are needed to verify the mangrove development history along the diverse southwest Florida coastlines.

References

Armentano, T.V., Doren, R.F., Platt, W.J., and Mullins. T., 1995. Effects of Hurricane Andrew on coastal and interior forests of southern Florida. Journal of Coastal Research 21,111-144.

Barr, J.G., Engel, V., Smith, T.J., and Fuentes, J.D., 2012. Hurricane disturbance and recovery of energy balance, CO2 fluxes and canopy structure in a mangrove forest of the Florida Everglades. Agricultural and Forest Meteorology 153, 54-66.

Beckage, B., Platt, W.J., Slocum, M.G., and Panko, B., 2003. Influence of the El Niño-Southern Oscillation on the fire regimes of the Florida Everglades. Ecology 84, 3124-3130.

Behling, H., Cohen, M.C.L., and Lara, R.J., 2001. Studies on Holocene mangrove ecosystem dynamics of the Braganc, a Peninsula in north-eastern Para´, Brazil, Palaeogeogr. Palaeoclimatology 167, 225–242.

Bernhardt, C.E., Willard, D.A., 2009. Response of the Everglades ridge and slough landscape to climate variability and 20th-century water management. Ecol Appl 19, 1723–1738.

Blaauw, M., and Christen, J.A., 2013. Bacon Manual , http://chrono.qub.ac.uk/blaauw/ (Accessed 24 December 2014)

Castañeda-Moya, E., Twilley, R.R., and Rivera-Monroy, V.H., Zhang, K.Q., Davis, S.E., and Ross, M., 2010. Sediment and Nutrient Deposition Associated with Hurricane Wilma in Mangroves of the Florida Coastal Everglades. Estuaries and Coasts 33, 45-58.

Castañeda-Moya, E., Twilley, R.R., and Rivera-Monroy, V.H., 2013. Allocation of biomass and net primary productivity of mangrove forests along environmental gradients in the Florida Coastal Everglades, USA. Forest Ecology and Management 307, 226-241.

Chappell, J.M.A., and Grindrod, J., 1985. Pollen analysis: a key to past mangrove communities and successional changes in North Australian coastal environments, In: Bardsley, K.N., Davie, J.D.S., Woodroffe, C.D. (Eds.), Coasts and Tidal Wetlands of the Australian Monsoon Region. Australian National University, Canberra, pp. 225–236.

Chen, R., and Twilley, R.R., 1999a. A simulation model of organic matter and nutrient accumulation in mangrove wetland soils. Biogeochemistry 44, 93-118.

Chen, R., and Twilley, R.R., 1999b. Patterns of mangrove forest structure and soil nutrient dynamics along the Shark River Estuary, Florida. Estuaries 22, 955-970.

Chmura, G.L., Stone, P.A., and Ross, M.S., 2006. Non-pollen microfossils in Everglades sediments. Review of Palaeobotany and Palynology 141, 103-119.

Davison, W., 1988. Interactions of iron, carbon and sulphur in marine and lacustrine sediments. Geological Society, London, Special Publications 40, **131-137.**

Dean, W.E.Jr., 1974. Determination of carbonate and organic matter in calcareous sediments and sedimentary rocks by loss on ignition: Comparison with other methods. Journal of Sedimentary Petrology 44, 242–248.

DeCoster, J., Platt, W.J., and Riley, S.A., 1999. Pine savannas of Everglades National Park: An endangered ecosystem, *In* Jones, D.T. and Gamble W.B., (Eds.), Florida's Garden of Good and Evil, Proceedings of the 1998 Joint Symposium of the Florida Exotic Pest Plant Council and the Florida Native Plant Society. South Florida Water Management District, West Palm Beach, Florida, pp 81-88.

Donders, T.H., Wagner, F., Dilcher, D.L., Visscher, H., 2005. Mid- to late-Holocene El Niño-Southern Oscillation dynamics reflected in the subtropical terrestrial realm. Proceedings of the National Academy of Sciences 102, 10,904–10,908.

Doren, R.F., Platt,W.J., and Whiteaker, L.D., 1993. Density and size structure of slash pine stands in the everglades region of south Florida. Forest Ecology and Management 59, 295-311.

Ellison, J.C., 2008. Long-term retrospection on mangrove development using sediment cores and pollen analysis: A review. Aquatic Botany 89, 93–104.

Gaiser, E.E., McCormick, P.V., Hagerthey, S.E., and Gottlieb, A.D., 2011. Landscape Patterns of Periphyton in the Florida Everglades. Critical Reviews in Environmental Science and Technology 41, 92-120.

Gill, A.M., and Tomlinson, P.B. 1977. Studies on the Growth of Red Mangrove (Rhizophora mangle L.) 1. Habit and General Morphology. Biotropica 1, 1-9.

Gleason, P.J. and P.A. Stone, 1994. Age, origin and landscape evolution of the Everglades peatland, In: S.M. Davis and J.C. Ogden (Eds.), Everglades, the Ecosystem and its Restoration. St. Lucie Press, Delray Beach, FL, pp. 149-198.

Gonzalez, C., L. E. Urrego, J. I. Martinez, J. Polania, and Y. Yokoyama, 2010. Mangrove dynamics in the southwestern Caribbean since the 'Little Ice Age': A history of human and natural disturbances. *Holocene 20*, 849–861.

Hanan, E.J., Ross, M.S., Ruiz, P.L., et al., 2010. Multi-Scaled Grassland-Woody Plant Dynamics in the Heterogeneous Marl Prairies of the Southern Everglades. Ecosystems 13, 1256-1274.

Hine, A.C., and Belknap, D.F., 1986. Recent geological history and modem sedimentary processes of the Pasco, Hemando and Citrus County coastline: west central Florida: Gainesville, Fl. University of Florida, Florida Sea Grant Report, 79:166

Intergovernmental Panel on Climate Change (IPCC) (2014), Climate Change 2013: The Scientific Basis. Contribution of Working Group I to the Fifth Assessment Report of the Intergovernmental Panel on Climate Change, edited by S. Solomon et al., Cambridge Univ. Press, New York.

Islebe, G., Hooghiemstra, H., Brenner, M., Curtis, J., and Hodell, D., 1996. A Holocene vegetation history from lowland Guatemala. The Holocene, 6, 265–271.

Kiage, L.M., and Liu, K.B., 2009. Palynological evidence of climate change and land degradation in the Lake Baringo area, Kenya, East Africa, since AD 1650. Palaeogeography, Palaeoclimatology, Palaeoecology 279, 60-72.

Koutavas, A., Lynch-Stieglitz, J., Marchitto Jr., T.M. and Sachs, J.P., 2002. El Niño-like pattern in ice age tropical Pacific sea surface temperature. Science 297, 226–230.

Light, S.S., and J.W. Dineen, 1994. Water control in the Everglades: A historical perspective, Everglades: The Ecosystem and Its Restoration, In S.M. Davis and J.C. Ogden (Eds), St. Lucie Press, Delray Beach, Florida, pp. 47-84.

Liu, K.B., Lu, H.Y., and Shen, C.M., 2008. A 1,200-year proxy record of hurricanes and fires from the Gulf of Mexico coast: Testing the hypothesis of hurricane-fire interactions. Quaternary Research 69, 29-41.

Liu, K.B., Li, C., Bianchette, T.A., McCloskey, T.A., Yao, Q., and Weeks, E., 2011. Storm deposition in a coastal backbarrier lake in Louisiana caused by Hurricanes Gustav and Ike. Journal of Coastal Research, Special Issue 64, 1866-1870.

Lodge, T.E., 2010, The Everglades Handbook: Understanding the Ecosystem, second edition, Boca Raton, Florida: CRC Press.

Macintyre, I.G., Toscano, M.A., Lighty, R.G., and Bond, G.B., 2004. Holocene history of the mangrove islands of Twin Cays, Belize, Central America. Atoll Research Bulletin 510, 1-16.

McAndrews, J.H., Berti, A.A., and Norris, G., 1973. Key to the Quaternary pollen and spores of the Great Lakes region: Royal Ontario Museum, Life Science Miscellaneous Publication, vol.64.

Michot, B., Meselhe, E.A., Riyera-Monroy, V.H., Coronado-Molina, C., and Twilley, R.R., 2011. A tidal creek water budget: Estimation of groundwater discharge and overland flow using hydrologic modeling in the Southern Everglades. Estuarine Coastal and Shelf Science 93, 438-448.

Miller, R., 1945. The heavy minerals of Florida beach and dune sands. American Mineralogist 30, 65–75.

Monacci, N.M., Meier-Grünhagen, U., Finney, B.P., Behling, H., and Wooller, M.J., 2009. Mangrove ecosystem changes during the Holocene at Spanish Lookout Cay, Belize. Palaeogeography, Palaeoclimatology, Palaeoecology 280, 37–46.

Parkinson, R.W., 1989. Decelerating Holocene Sea-Level Rise and Its Influence on Southwest Florida Coastal Evolution: A Transgressive/Regressive Stratigraphy. Journal of Sedimentary Petrology 59, 960-972.

Platt, W.J. 1999. Southeastern pine savannas., In Anderson, R.C., Fralish, J.S., and Baskin, J., (Eds), The savanna, barren, and rock outcrop communities of North America. Cambridge University Press, Cambridge, England, pp. 23-51

Platt, W.J., S.L. Orzell, and M.G. Slocum. 2015. Seasonality of fire weather strongly influences fire regimes in south Florida savanna-grassland landscapes. PLoS ONE 10(1): e0116952.

Ramírez-Herrera, M.T., Lagos, M., Hutchinson, I., Kostoglodov, V., Machain, M.L., et al., 2012. Extreme wave deposits on the Pacific coast of Mexico: tsunami or storms? A multi-proxy approach. Geomorphology 140, 360-371.

Rivera-Monroy, V.H., Twilley, R.R., Davis, S.E., Childers, D.L., Simard, M., et al., 2011. The Role of the Everglades Mangrove Ecotone Region (EMER) in Regulating Nutrient Cycling and Wetland Productivity in South Florida. Critical Reviews in Environmental Science and Technology 41, 633-669.

Robbin, D.M., 1984, A new Holocene sea level curve for the upper Florida Keys and Florida reef tract, in Gleason, P.J. (Eds.), Environments of South Florida, Present and Past II (2nd ed.): Miami Geological Society, p. 437–458.

Rodbell, D. T., Seltzer, G. O., Anderson, D. M., Abbott, M. B., Enfield, D. B., and Newman, J. H., 1999. An 15,000-Year Record of El Niño-Driven Alluviation in Southwestern Ecuador. Science 283, 516–520.

Ross, M.S., O'Brien, J.J., Ford, R.G., Zhang, K.Q., and Morkill, A.. 2009. Disturbance and the rising tide: the challenge of biodiversity management on low-island ecosystems. Frontiers in Ecology and Environment 7, 471-478.

Ross, M.S., Meeder, J.F., Sah, J.P., Ruiz, P.L., and Telesnicki, G.J., 2000. The southeast saline Everglades revisited: 50 years of coastal vegetation change. Journal of Vegetation Science 11, 101–112.

Sabatier, P., Dezileau, L., Condomines, M., Briqueu,L., Colin, C., Bouchette, F., Le Duff, M., and Blanchemanche, P., 2008. Reconstruction of paleostorm events in a coastal lagoon (Herault, South of France). Marine Geology 251, 224-232.

Saha, A.K., Moses, C.S., Price, R.M., Engel, V., Smith, T.J., and Anderson, G., 2012. A Hydrological Budget (2002-2008) for a Large Subtropical Wetland Ecosystem Indicates Marine Groundwater Discharge Accompanies Diminished Freshwater Flow. Estuaries and Coasts 35, 459-474.

Schmitz, M., Platt, W.J., and DeCoster, J., 2002. Substrate heterogeneity and numbers of plant species in Everglades savannas (Florida, USA). Plant Ecology 160, 137-148.

Scott, D.B., Collins, E.S., Gayes, P.T., Wright, E., 2003. Records of prehistoric hurricanes on the South Carolina coast based on micropaleontological and sedimentological evidence, with comparison to other Atlantic Coast records. Geological Society of America Bulletin 115, 1027-1039.

Scourse, J., Marret, F., Versteegh, G.J.M., Jansen, J.H.F., Schefuss, E., and van der Plicht, J., 2005. High-resolution last deglaciation record from the Congo fan reveals significance of mangrove pollen and biomarkers as indicators of shelf transgression. Quaternary Research 64, 57-69.

Simard, M., Zhang, K.Q., Rivera-Monroy, V.H., Ross, M.S., Ruiz, P.L., Castañeda-Moya, E., Twilley, R.R., and Rodriguez, E., 2006. Mapping height and biomass of mangrove forests in Everglades National Park with SRTM elevation data. Photogrammetric Engineering and Remote Sensing 72, 299-311.

Slocum, M.G., Platt, W.J., and Cooley, H.C., 2003. Effects of differences in prescribed fire regimes on patchiness and intensity of fires in subtropical savannas of Everglades National Park, Florida. Restoration Ecology 11, 91-102.

Slocum, M.G., Platt, W.J., Beckage, B., Panko, B., and Lushine, J.B., 2007. Decoupling natural and anthropogenic fire regimes: a case study in Everglades National Park, Florida. Natural Areas Journal 27, 41-55.

Slocum, M.G., Platt, W.J. Beckage, B., Orzell, S.L., and Taylor, W., 2010. Accurate Quantification of Seasonal Rainfall and Associated Climate-Wildfire Relationships. Journal of Applied Meteorology and Climatology 49, 2559-2573.

Smith, T.J., Anderson, G.H., Balentine, K., Tiling, G., Ward, G.A., Whelan, K.R.T., 2009. Cumulative impacts of hurricanes on Florida mangrove ecosystems: Sediment deposition, storm surges and vegetation. Wetlands 29, 24-34.

Torrescano, N., and Islebe, G.A., 2006. Tropical forest and mangrove history from southeastern Mexico: a 5000 yr pollen record and implications for sea level rise. Vegetation History and Archaeobotany 15, 191-195.

Urrego, L.E., Bernal, G., and Polanía, J., 2009. Comparison of pollen distribution patterns in surface sediments of a Colombian Caribbean mangrove with geomorphology and vegetation. Review of Palaeobotany and Palynology 156, 358–375.

Van Campo, E., and Bengo, M.D., 2004. Mangrove palynology in recent marine sediments off Cameroon. Marine Geology 208, 315-330.

van Soelen, E.E., Lammertsma, E.I., and Cremer, H., 2010. Late Holocene sea-level rise in Tampa Bay: Integrated reconstruction using biomarkers, pollen, organic-walled dinoflagellate cysts, and diatoms. Estuarine, Coastal and Shelf Science 86, 216–224.

van Soelen, E.E., Brooks, G.R., Larson, R.A., Damsté, J.S.S., and Reichart, G.J., 2012. Mid- to late-Holocene coastal environmental changes in southwest Florida, USA. The Holocene, 1-10.

Versteegh, G.J.M., Schefuss, E, Dupont, L., Marret, F., Damste, J.S.S., and Jansen, J.H.F., 2004. Taraxerol and Rhizophora pollen as proxies for tracking past mangrove ecosystems. Geochimica Et Cosmochimica Acta 68, 411-422.

Wanless, H.R., Parkinson, R.W., Tedesco, L.P., 1994. Sea Level Control on Stability of Everglades Wetlands, In: Davis, S.M., and Ogden, J.C., (Eds). Everglades: the ecosystem and its restoration, St. Lucie Press, p. 199-222.

Whelan, K.R.T., T.J.I. Smith, G.H. Anderson, and M.L. Ouellette. 2009. Hurricane Wilma's impact on overall soil elevation and zones within the soil profile in a mangrove forest. Wetlands 29, 16–23.

Willard, D.A., Weimera, L.M., and Riegel, W.L., 2001, Pollen assemblages as paleoenvironmental proxies in the Florida Everglades. Review of Palaeobotany and Palynology 113, 213-235.

Willard, D.A., Cooper, S.R., Gamez, D., and Jensen, J., 2004, Atlas of pollen and spores of the Florida Everglades. Palynology 28, 175-227.

Willard, D.A., and Bernhardt, C.E., 2011. Impacts of past climate and sea level change on Everglades wetlands: placing a century of anthropogenic change into a late-Holocene context. Climatic Change 107, 59-80.

Willard, D.A., and Cronin, T.M., 2007. Paleoecology and ecosystem restoration: case studies from Chesapeake Bay and the Florida Everglades. Front Ecol Environ 5, 491–498.

Woodroffe, C.D., Thom, B.G., Chappell, J., 1985. Development of widespread mangrove swamps in mid- Holocene times in northern Australia. Nature 317, 711–713.

Wooller, M.J., Behling, H., Smallwood, B.J., Fogel, M., 2004. Mangrove ecosystem dynamics and elemental cycling at Twin Cays, Belize, during the Holocene. Journal of Quaternary Science 19, 703–711.

Wooller, M.J., Morgan, R., Fowell, S., Behling, H., and Fogel, M., 2007. A multiproxy peat record of Holocene mangrove palaeoecology from Twin Cays, Belize.

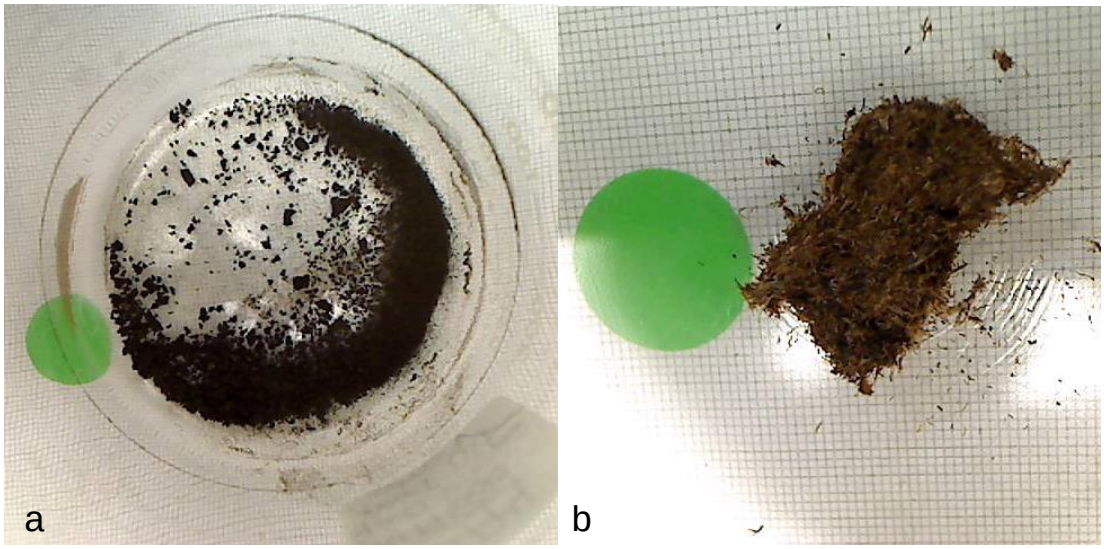

Supplement Figure 1. Ten grams of bulk sediment samples were taken at 445-446 cm from core SRM-1 and submitted to Beta Analytic Inc., in Miami, Florida, for AMS ^{14}C dating. The sample is sieved and separated into: (a) organic silt fraction containing decomposed or broken debris of leaves or wood; (b) plant fiber fraction containing predominantly elongated plant fibers that resembled rootlets or root hairs. The green dot is 24mm in diameter.

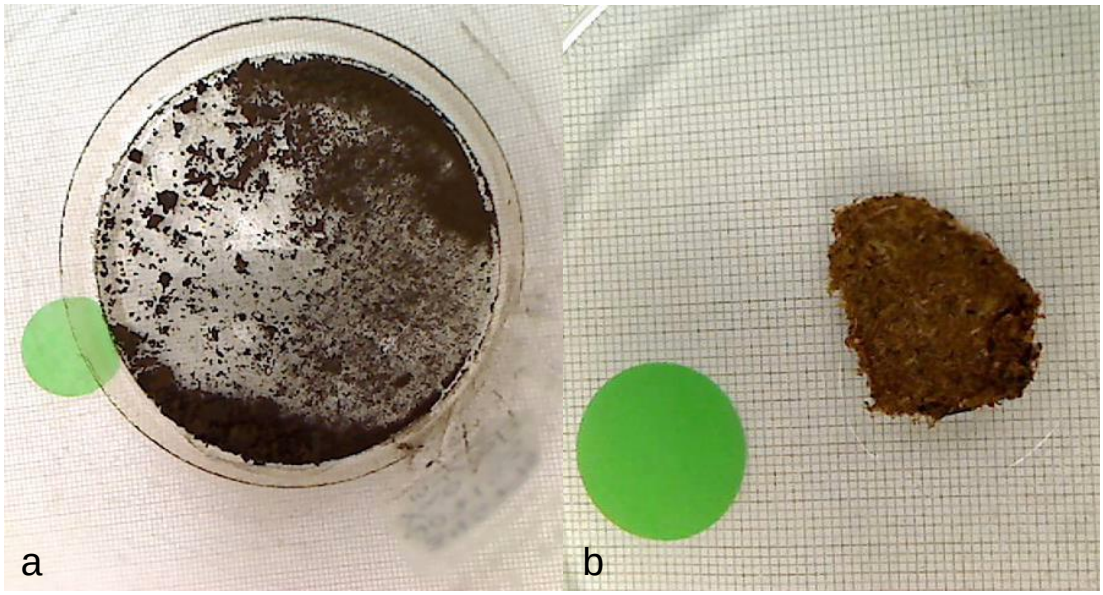

Supplement Figure 2. Ten grams of bulk sediment samples were taken at 373-374 cm from core SRM-1 and submitted to Beta Analytic Inc., in Miami, Florida, for AMS ^{14}C dating. The sample is sieved and separated into: (a) organic silt fraction containing decomposed or broken debris of leaves or wood; (b) plant fiber fraction containing predominantly elongated plant fibers that resembled rootlets or root hairs. The green dot is 24mm in diameter.

CHAPTER 5. A PALEOECOLOGICAL RECORD OF HISTORICAL HURRICANE EVENTS FROM THE FLORIDA EVERGLADES

Introduction

Paleotempestology, a relatively young field in the geosciences (Liu, 2004, 2007), provides a means to reconstruct the occurrence of paleohurricane events from the proxy record. The most useful proxy is overwash sand layers preserved in sediment cores retrieved from coastal lakes and marshes (Liu and Fearn, 1993, 2000; Donnelly et al., 2001; Liu, 2004). The principle underlying this research methodology is that when storm surges generated by intense hurricanes overtop the sand barriers, sand will be washed over into the backbarrier lakes and marshes, forming an overwash sand layer in the sedimentary record which can later be identified by loss-on-ignition (LOI) analyses and other sedimentological techniques (Liu, 2004; Dean, 1974). By means of radiometric (^{137}Cs, ^{210}Pb, and ^{14}C) dating of these cores, a paleohurricane record can be established.

In addition to LOI, X-ray fluorescence (XRF) analysis has also been successfully used in paleotempestological studies (Liu et al, 2014). XRF analysis measures the concentration of the common chemical elements on the periodic table and is widely used in coastal studies to identify the origin of different sediment sources (van Soelen et al., 2012; Ramirez-Herrera et al., 2012). Paleotempestological studies from Gulf Coast locations have yielded millennial records of recurrent major hurricane strikes and vegetation changes during the late-Holocene (Liu and Fearn, 1993, 2000; Liu et al., 2008). However, no paleohurricane proxy record exists in south Florida. In this paper, we demonstrate that XRF analysis can be used along with other proxies to identify

paleohurricane events in sand-limited coastal wetland environments based on a peat core retrieved in the Everglades National Park (ENP). This core captures 5700 years of sedimentary record and the distinctive carbonate-rich clastic layer left by Hurricane Wilma (2005) at the top of the core (Fig. 6) (Castañeda-Moya et al, 2010). We aim to (1) identify the sedimentary signature of Hurricane Wilma (2005) by multi-proxy analyses (LOI, XRF, pollen); and (2) use this intense storm as a modern analog to reveal other paleohurricane events in the sedimentary record based on statistical analyses of XRF and LOI results. This study will fill an important data gap in the paleotempestology data network between the Gulf of Mexico coast and the Atlantic coast of the U.S. by recording the paleohurricane activities for South Florida. This study is also expected to contribute to the methodological advancement of paleotempestology by exploring the application of geochemical proxies in non-limnic, sand-limited tropical coastal and mangrove-dominant wetlands.

Study area

Our study site (25°21'10"N, 81°6'52"W) is located on the edge of Ponce de Leon Bay, at the mouths of Whitewater Bay and Shark River Estuary (Fig. 1). It is situated in a fringing mangrove forest, where *Laguncularia racemosa* (white mangrove) and *Rhizophora mangle* (red mangrove) are co-dominant species (Chen and Twilley, 1999 a and b). Previous studies in the south Florida region indicate that wetland peat began accumulating over a platform of limestone bedrock at least by 5,000 ^{14}C yr BP (Gleason and Stone, 1994), whereas mangrove forests appear to have established on this thick peat layer along coastal margins about 3,500 ^{14}C yr BP, when sea-level stabilized

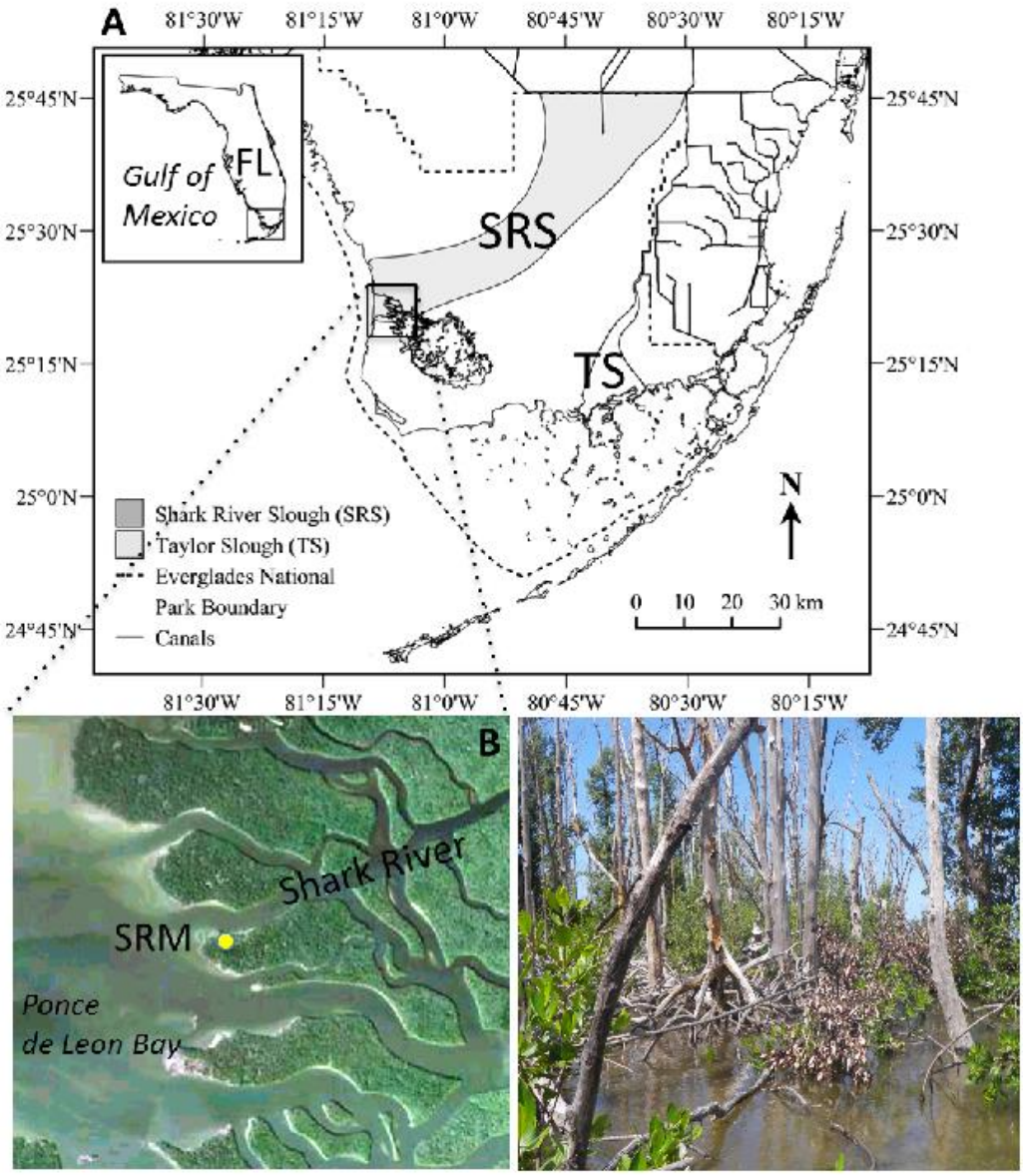

Figure 1. A) Location of the Shark River Slough (SRS) and Everglades National Park, South Florida; B) Dot indicates coring site (SRM) at the mouth of Shark River; C) Mangrove forest impacted by Hurricane Wilma in 2005 at the sampling location (base map adapted from FCE LTER, http://fcelter.fiu.edu.)

(Parkinson, 1989; Wanless et al., 1994). Historically, water overflowing Lake Okeechobee and associated rainfall results in a southward sheet flow along a gentle slope of ~3 cm/km down Shark River Slough into Shark River Estuary (Lodge, 2010). Since the early 20th century, anthropogenic activities (agriculture and urbanization) have dramatically reduced the seasonality of freshwater flow throughout the

Everglades (Light and Dineen, 1994) and have affected surface and groundwater flows in this coastal region (Saha et al. 2012).

During the last 160 years, 46 major (category 3-5 according to the Saffir-Simpson scale) hurricanes have crossed south Florida with an average return interval of 3.5 years (NOAA, 2013). During the 20th century, two category 5 hurricanes directly struck the Everglades in 1935 and 1992 (Elsner and Kara, 1999). Wilma, the most recent major hurricane to cross our study site, made landfall as a category 3 storm in 2005 (Castañeda-Moya et al, 2010). Strong winds and storm surge from this hurricane caused damage to approximately 1,250 ha of mangrove forest along the west coast of the ENP, resulting in 90% mortality of trees with diameters at breast height greater than 2.5 cm (Whelan et al., 2009; Smith et al., 2009). The storm surge flooded the study site with 3 - 4 m of water and deposited 3 cm of marine sediment as far as 10 km inland (Castañeda-Moya et al., 2010).

Materials and methods

Sedimentary record

A 525 cm core (SRM-1) was retrieved at the study site in May 2010 using a Russian peat borer. The top 445 cm of the core was used for proxy studies because it contains the depositional history of the peat-forming coastal wetlands in the Everglades. X-ray fluorescence (XRF) analysis is performed on the peat sediments at 2 cm intervals, and the elemental concentrations (ppm) of 9 common chemical elements (Ca, Sr, S, Fe, Cl, K, Ti, Zr, Br) are reported in this study. Loss-on-ignition (LOI) analysis was performed at the same intervals to establish core stratigraphy

(Dean, 1974). Samples were heated at 105 ℃ to calculate %water (wet weight), 550 ℃ for %organics (dry weight), and 1000 ℃ for %carbonates (dry weight). In total, the 445 cm of deposits were divided into 223 sediment layers, and each layer is represented by a set of LOI and XRF data. Five samples of 1.8 mL sediments were taken from the top 40 cm of the core at 5 to 10 cm intervals for palynological analysis. Samples were processed using standard procedures (Liu et al., 2011, Kiage and Liu, 2009). More information about the processing of pollen is described in **Chapter 3**. Approximately 300 grains of pollen and other microfossils (foraminifera and dinoflagellates) were counted in all samples. Identification of the microfossils was based on published pollen illustrations by McAndrews et al. (1973) and Chmura et al. (2006).

Fourteen samples from core SRM-1 were used for AMS ^{14}C measurements (Table 1, Fig. 2). Ten samples consisting of leaf fragments and wood pieces selected under a dissecting microscope were sent to the NOSAMS Laboratory at Woods Hole Oceanographic Institution. In addition, approximately ten grams of bulk sediments each were taken at 374 and 446 cm from core SRM-1 and submitted to Beta Analytic Inc., in Miami, Florida for duplicated AMS ^{14}C measurements. The age model is developed with BACON version 2.2 (Blaauw and Christen, 2013). More information about the chronology of core SRM is described in **Chapter 4**. The ages described in this paper are reported as calibrated years before present (cal yr BP).

Table 1. Radiocarbon dating results for core SRM-1. Dates in parentheses are rejected due to extreme age reversal.

Sample ID	**Depth (cm)**	**Material**	**Conventional C^{14} age (yr BP)**	**2-σ Calibrated range (Cal yr BP)**
OS-960a2	56	Leaf	145 ±25	0 - 280
OS-83953	139	Leaf	1180 ±30	990 - 1180
OS-90704	179	Leaf	1940 ±30	1820 – 1970
OS-95704	243	leaf	2860 ±30	2880 – 3070
OS-83943	246	Wood	155 ±25	(Rejected)
OS-90685	246	Wood	> Modern	(Rejected)
OS-93264	260	Leaf	2240 ±30	2150 - 2340
OS-96061	300	Bark	3540 ±35	3700 – 3910
Beta-345774	374	Organic silt	4160 ±30	4780 - 4830
Beta-346208	374	Roots	2940 ±30	3000 - 3210
OS-96060	440	Leaf	1090 ±20	(Rejected)
Beta-345775	446	Organic silt	5800 ±30	6500 - 6670
Beta-346209	446	Roots	4060 ±30	4760 - 4800
OS-84455	448	Plant debris	6620 ±260	6940 – 7980

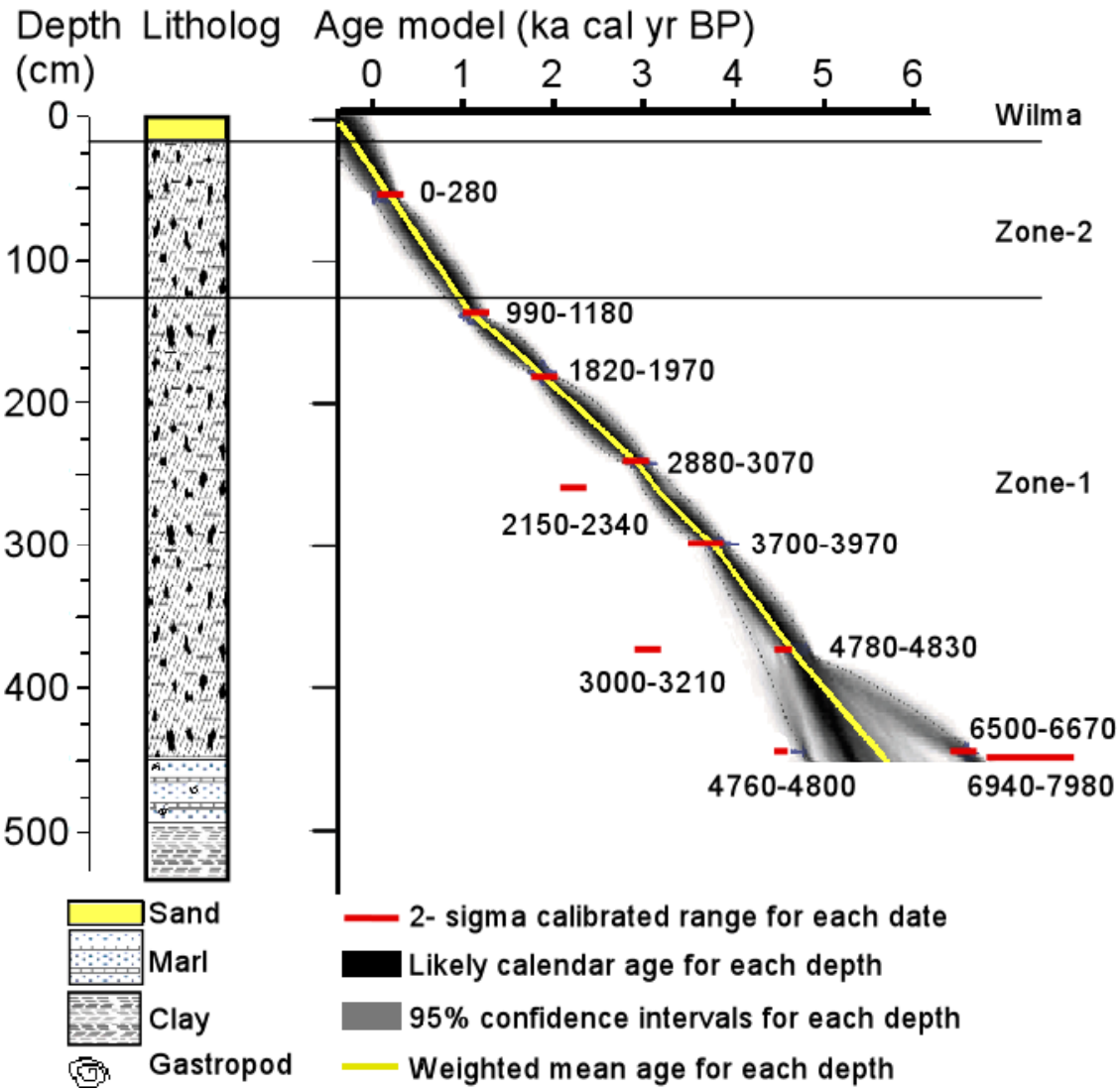

Figure 2. Lithology and the age-depth model for the core. The age-depth model is developed by BACON and based on 11 calibrated C^{14} ages (2-σ Calibrated range). The yellow curve shows the 'best' estimated age for each depth based on the weighted mean age. The surface (0 cm) of the core is assigned as -55 cal yr BP because it is identified as the Hurricane Wilma deposit (2005). Further information about radiocarbon dates is shown in Table 1.

Statistical analysis

By using the IBM SPSS version 22.0, principal components analysis (PCA) is performed on all the LOI and XRF datasets to reveal their internal statistical structure. The PCA results provide a basis to classify the stratigraphic samples into statistically meaningful groups, which can be interpreted in terms of the regular peat deposits or paleohurricane deposits. In addition, discriminant analysis (*sensu* Liu and Lam, 1985, Lu and Liu, 2005), an inferential statistical technique, was performed using the same program to classify the LOI and XRF datasets with reference to the *a priori* groups suggested by the PCA results. These predicted group memberships demonstrate which sediment layers share the same LOI and XRF signatures as Hurricane Wilma deposits and therefore permit the identification of paleo-storm deposits based on their sedimentological and geochemical properties.

Results

Radiocarbon dating

Among the 14 AMS ^{14}C dates obtained from NOSAMS and Beta Analytic, three anomalously young dates retrieved at 246 cm and 440 cm are rejected due to extreme stratigraphic reversal (Table. 1). The surface (0 cm at -55 cal yr BP) and 11 valid ^{14}C dates are used to construct the age-depth model by BACON v2.2 (Fig. 2). The result shows that the "best" age-depth model (yellow curve) based on weighted mean age of each depth is very close to a polynomial line intercepting ^{14}C dates at 56 (178 cal yr BP), 139 (1138 cal yr BP), 179 (1872 cal yr BP), 243 (2947 cal yr BP), 300 (3777 cal yr BP), and 374 (organic silt) (4658 cal yr BP) cm. We pick a bottom date of

approximately 5700 cal yr BP at 450 cm based on estimation of the "best" age-depth model. More detailed information about the radiocarbon dating of core SRM is described in **Chapter 4**.

Core Stratigraphy

Core SRM-1 consists of 4 different sediment types. The bedrock substrates consist of homogeneous clay (525-485 cm) and marl (485-445 cm) and they are older than the oldest dated sediments in the core (Fig. 2). Above the basal sediments are more than 4 m of contiguous peat (445-10 cm) (Fig. 2). At the top of the core is 10 cm of calcareous clastic sediments (10-1 cm) (Fig. 6). We divided the peat sediments (445-10 cm) into 2 stratigraphic zones, based on their sediment stratigraphy and chemical characteristics revealed by LOI and XRF analyses (Fig. 3).

Zone 1 (445-125 cm, 5700-1150 cal yr BP)

Loss-on-ignition results indicate that the peat sediments in Zone-1 have very high contents of water (>80% wet weight) and organic matter (>50% dry weight) and low concentration of carbonates (15-20% dry weight) (Fig. 3). XRF data show that the elemental concentrations of Ca (< 1000 ppm), Sr (< 30 ppm), S (< 5000 ppm), Fe (< 2000 ppm), K (< 600 ppm), Ti (< 100 ppm), and Zr (< 10 ppm) are relatively low (Fig. 3). The LOI and XRF values are generally stable within this zone, except for sediment layers at approximately 250-255 cm and 165-175 cm where there are abrupt increases in Cl (>15000 ppm) (Fig. 3).

Zone 2 (125-10 cm, 1150 cal yr BP to present)

The values of %water of Zone-2 remain very high (>80% wet weight), and the

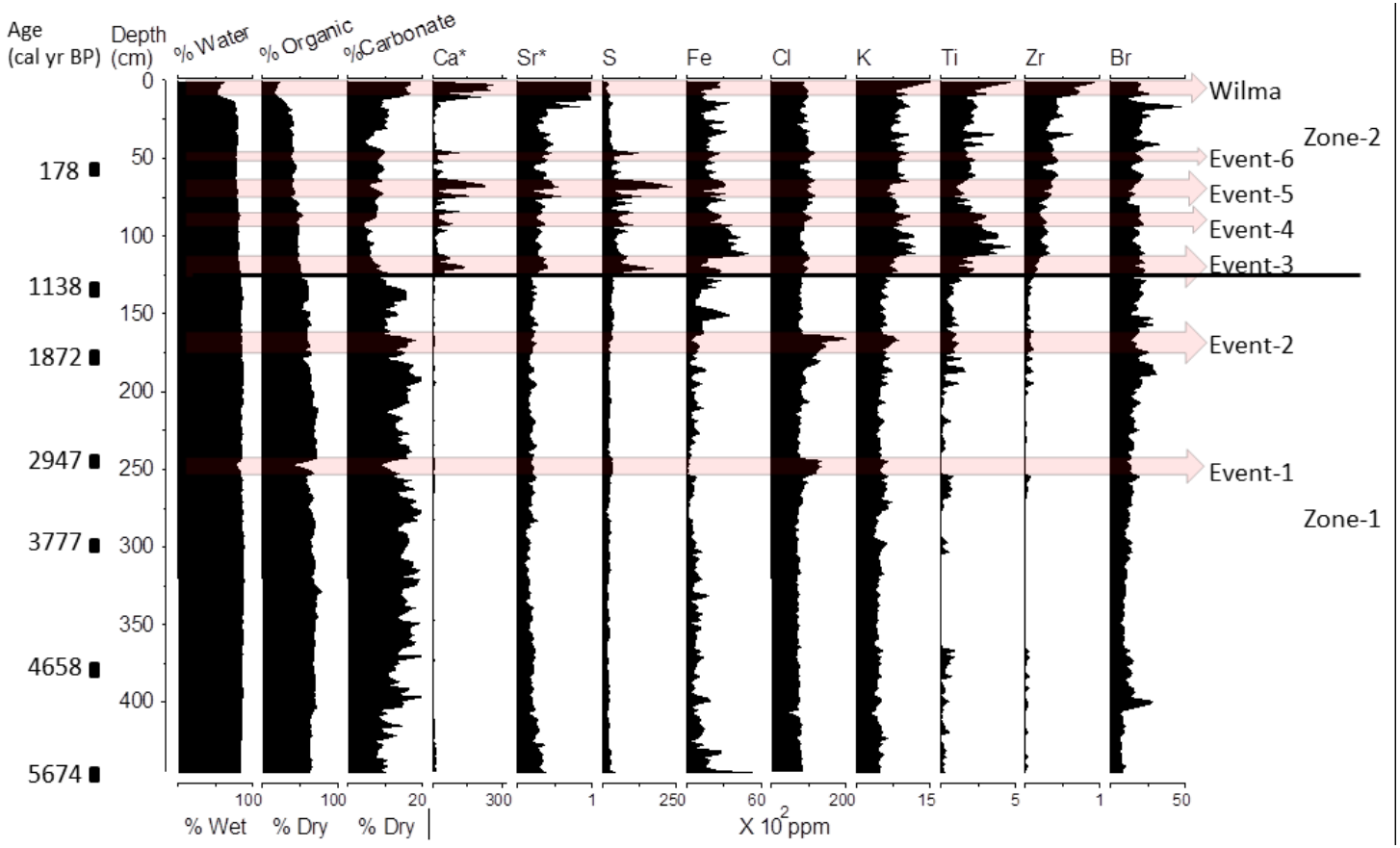

Figure 3. Loss-on-ignition and XRF diagram of core SRM-1. Loss-on-ignition diagram presents the % wet weight for water, and % dry weight for organics and carbonates. Six Intercepted radiocarbon dates and estimated bottom age of the core are based on the single 'best' model on Figure 2 (yellow curve). The arrows indicate the occurrence of hurricane Wilma (2005) and six inferred hurricane events (47-53, 67-79, 85-97, 115-121, 165-175, and 250-255 cm). (* In order to show the variations of Ca and Sr of the sediments below 10 cm, the maximum concentrations of Ca of Sr are set to be 30000 and 100 ppm instead of 100000 and 600 ppm.)

elemental concentrations of Ca, Sr, S, Fe, K, Ti, and Zr in these sediments are higher than Zone 1 (Fig. 3). Especially at approximately 50, 70 and 120 cm, three peat levels exhibit very high values of Ca (>15,000 ppm), Sr (>50 ppm), and S (>10,000 ppm) comparing with the rest of the sediments in the core. The elemental concentrations of Cl and Br remain relatively stable (Fig. 3).

The top 10 cm

The top 10 cm of the core consists of calcareous clastic sediments, as indicated by LOI, XRF, and visual analyses. The contents of water (50-70% vs >80%) and organic matter (20-25% vs 40-60%) in these sediments are significantly lower than those in the underlying peat, but carbonate content is much higher (30-35% vs 10-15%). The concentrations of Ca, Sr, and Zr in the top 10 cm are 10 to 100 times higher than in the underlying peat (Fig. 3). The palynological analysis reveals higher percentages and influx values of *Conocarpus*, *Pinus*, *Quercus*, and Amaranthaceae (Fig. 3). Additionally, dinoflagellate and foraminifera linings both appear at high concentrations.

Numerical analysis of proxy data

The PCA plots of 12 proxies (elemental concentration Ca, Sr, S, Fe, Cl, K, Ti, Zr, Br, and percentages of water, organics and carbonates) and 223 sediment layers are shown in Figure 4. On the biplot of principal component loadings for the 12 proxies (Fig. 4a, Table 2), the first two principal components account for 34% and 33.9% of the variance, respectively. Fe, S and Br have the highest positive loadings exclusively on principal component 1, whereas %Carbonate has the most negative loadings. On

the second principal component, Ca and Sr have the highest positive loadings, whereas %Water has the most negative loading. Therefore, among the 12 total proxy measurements, only %Water, %Carbonate, Ca, Sr, S, Fe and Br are considered relevant proxies and used for statistical analysis of the 223 peat sediment layers.

On the biplot of principal component loadings for the 223 sediment layers (Fig. 4b), the first 2 principal components account for 72.8% and 20.1% of the variance, respectively. Sediment layers deposited by hurricane Wilma (W1-W7) and 15 other sediment layers at various depths (47, 53, 67, 69, 73, 75, 79, 85, 91, 93, 97, 113, 115, 119, 121cm) have the highest scores on component 2 and lowest scores on component 1. Samples from Zone-1 (previous described) score lowest on component 2 and highest on component 1. The rest of sediment layers in Zone-2 have moderate scores on component 1 and 2. Thus, the results of the PCA ordination analysis suggest that the 223 sediment layers can be divided into 3 primary groups: (1) Zone-1; (2) non-hurricane deposits in Zone-2; (3) hurricane deposits (hurricane Wilma deposits and 15 other sediment layers). These three groups are quite well-defined with little overlap among them (Fig. 4b).

Discriminant analysis was used to validate the classification of the 3 primary groups and to generate probability estimates for statistical inference. Most of the samples (98.2%) are correctly classified into their respective *a priori* groups (Table 3). Figure 5 shows the 3 groups of surface samples plotted against discriminant functions 1 and 2, which account for 72.3% and 27.7% of the variance, respectively. Again, the 3 groups and their centroids are clearly distinct from each other with a few overlaps

between groups. The high degree of correct classification suggests that the identification of the hurricane deposits is statistically robust (Fig. 5). These results indicate that the numerical analyses of multi-proxy records can be used to infer the paleohurricane events from the coastal Everglades.

Table 2. Rotated Component Matrix of the Principal Component Analysis performed on the 12 proxies from multi-proxy data of core SRM-1. Rotation Method is Varimax with Kaiser Normalization. Rotation converged in 3 iterations.

	Component	
	1	2
% Water		-.838
% Organic	-.655	-.654
%Carbonate	-.803	
Ca		.882
Sr		.957
S	.620	
Fe	.782	
Cl		
K	.729	.552
Ti	.766	.506
Zr	.559	.772
Br	.531	

Table 3. Classification results of the discriminant analysis performed on the 223 sediment layers from core SRM-1. 98.2% of original grouped cases correctly classified. a. Number of samples classified as that group. b. Percentage of samples classified as that group.

		Predicted Group Membership			
	Origin	1	2	3	Total
Original count [a]	1	172	0	0	172
	2	4	28	0	32
	3	0	0	14	14
% [b]	1	100.0	.0	.0	100.0
	2	12.5	87.5	.0	100.0
	3	.0	.0	100.0	100.0

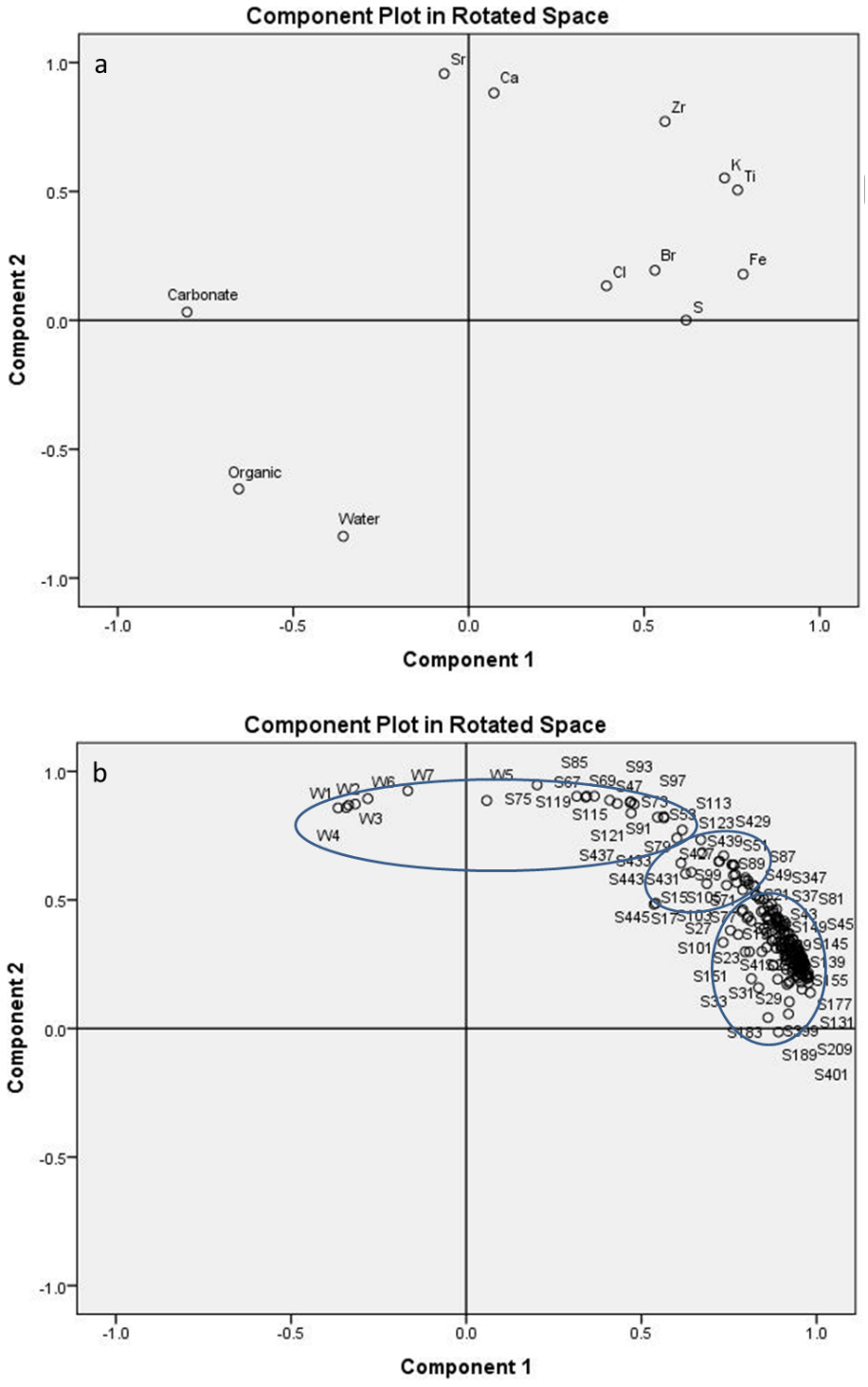

Figure 4. a) PCA biplot showing coordinates of the 12 proxies plotted along component 1 and component 2. b) PCA biplot showing coordinates of the 223 sediment layers plotted along component 1 and component 2. W1-W7 represents 7 sediment layers deposited by Hurricane Wilma. Other sample ID shows the depth of the sediment layer in the core (e.g. Sample S100 is at 100 cm from the top of the core). PCA ordination analysis delineates 15 sediment layers (47, 53, 67, 69, 73, 75, 79, 85, 91, 93, 97, 113, 115, 119, and 121 cm) into the same primary group with hurricane Wilma deposits (W1-W7).

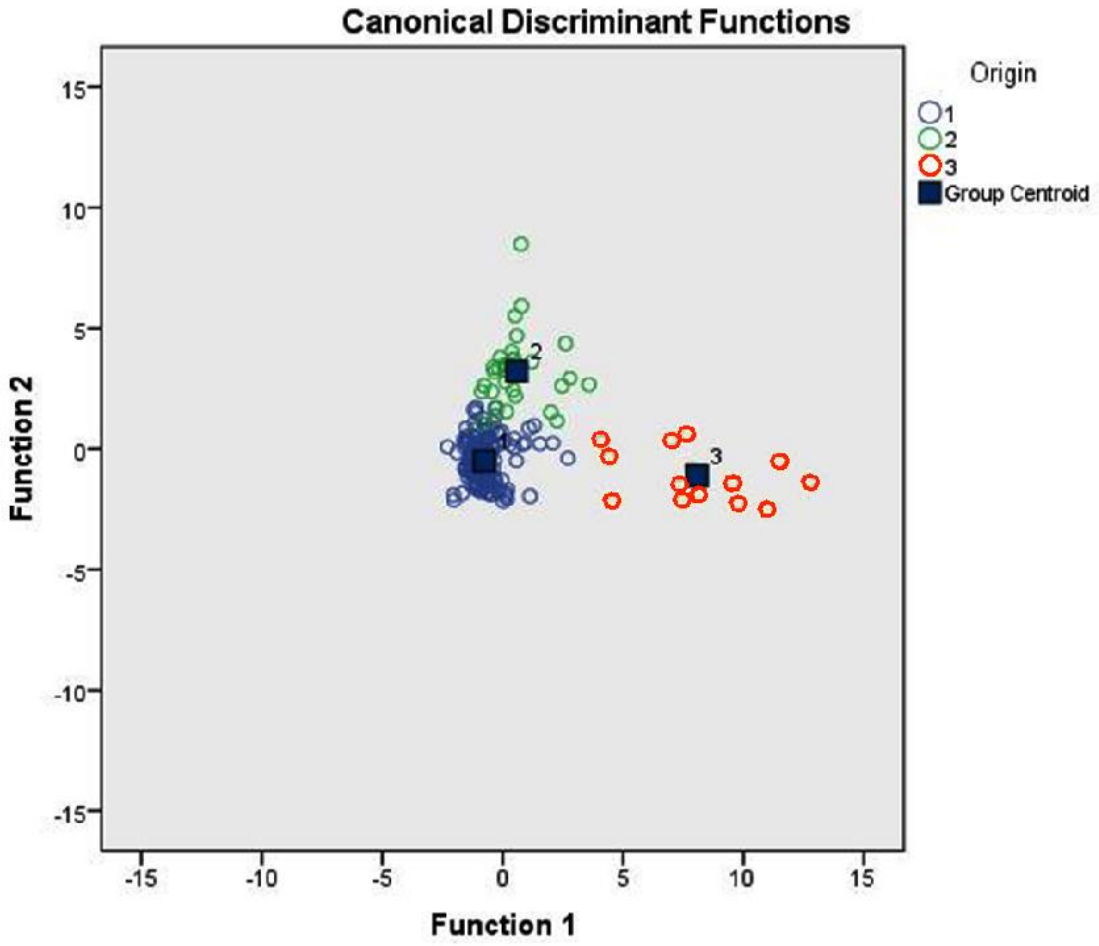

Figure 5. The 223 sediment layers plotted against canonical discriminant functions 1 and 2 and their classification into three primary groups corresponding to (1) Zone-1; (2) non-hurricane deposits in Zone-2; (3) hurricane deposits (hurricane Wilma deposits and 15 other sediment layers).

Discussion

Sedimentary signatures of Hurricane Wilma (2005)

The top 10 cm of the calcareous clastic sediments in core SRM-1 has been identified as hurricane deposits from Hurricane Wilma in 2005 by a previous study (Castañeda-Moya et al., 2010). Figure 6 summarizes the sedimentary, chemical, and palynological characteristics of this storm deposit. This clastic layer has higher concentrations of marine planktons (foraminifera and dinoflagellates), carbonates, and Zr, and the content of Ca and Sr is significantly higher than the underlying peat

(up to 100 times). High contents of Ca and Sr have been described as indicators of marine incursions in previous studies from southwestern Florida (van Soelen et al., 2012) and elsewhere (Ramirez-Herrera et al., 2012). In addition, the principal source of Zr, zircon ($ZrSiO_4$), is a common constituent of Florida beach sands (Miller, 1945; van Soelen et al., 2012). Thus, high concentration of these minerals indicates that the top 10 cm of the core came from an allochthonous marine sediment source, most likely located along the nearshore shelf of southern Florida (i.e., Ponce de Leon Bay), where carbonate mud, shell fragments, and silica sand accumulate (Lodge, 2010). Pollen analysis indicates that deposits from Hurricane Wilma contain high percentages of regional pollen taxa (*Conocarpus, Pinus, Quercus*, and Amaranthaceae) (Fig. 6). However, these plants are absent at the coring site, a fringe mangrove forest (Chen and Twilley, 1999b). Some studies indicate that offshore sediments from a delta system contain pollen transported throughout the entire drainage system rather than local coastal areas (Chmura et al., 1999). These results suggest that during a high-energy overwash event, pollen deposited offshore would be transported to the coastal mangrove forest along with the clastic marine sediments. Thus, the pollen assemblage in the Wilma deposit carries a regional rather than local pollen signal. Overall, the sedimentary, chemical, and palynological results suggest that deposits from Hurricane Wilma have distinctive characteristics that can be used as a modern analog to help identify past hurricane deposits in this region.

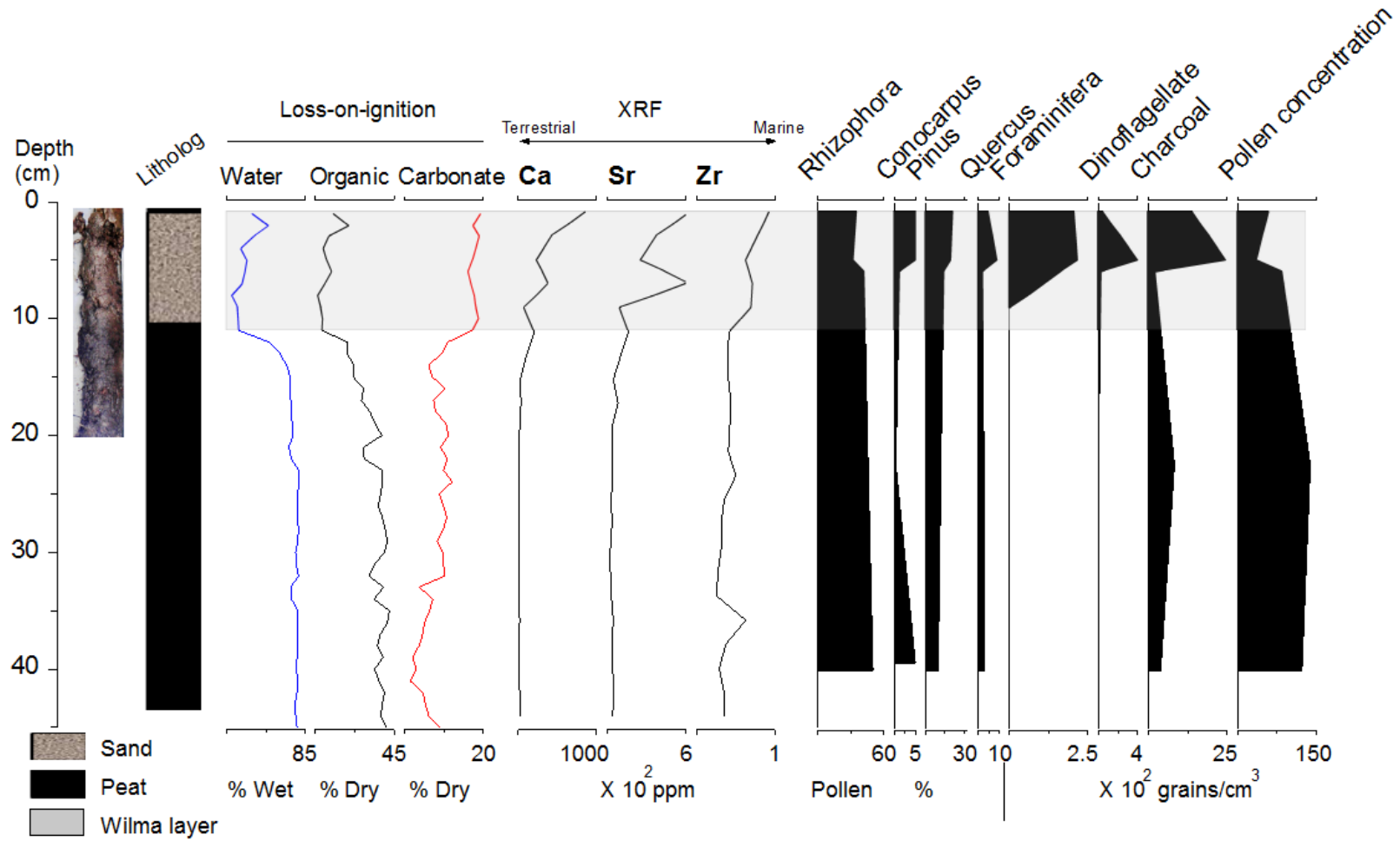

Figure 6. Lithologic, chemical, and palynological characteristics of Hurricane Wilma storm deposit (top 10 cm) compared with the underlying wetland peat. From left to right is the photo of the sediments, lithology, loss-on-ignition data, XRF data, and pollen diagram.

Paleo-hurricane events

After identifying the most relevant proxies (%Water, %Carbonate, Ca, Sr, S, Fe, and Br), PCA ordination analysis and discriminant analysis delineate 15 other sediment layers as potential hurricane deposits (Fig. 4, 5). These potential hurricane layers fall into 4 stratigraphic units, which are inferred as 4 paleo-hurricane events (Fig. 3). There are event 3 around 950 cal yr BP (115-121 cm), event 4 around 580 cal yr BP (85-97 cm), event 5 around 350 cal yr BP (69-79 cm), and event 6 around 120 cal yr BP (47-53 cm). Each paleo-hurricane event is represented by a sediment layer that is 7 to 10 cm thick due to fast deposition rate and sediment mixing during a storm surge. The age of each paleo-hurricane event is based on the median age of the storm deposit.

Similar to the Wilma deposit, sediment layers of events 3, 4, 5, and 6 contain high values of Ca and Sr (Fig. 3, 6), which are clear evidence of marine clastic sediments (Ramirez-Herrera et al., 2012). When compared with the Wilma signature, however, all paleo-event layers contain less Ca and Sr, but a higher concentration of S. In general, mangrove soils are slightly acidic (pH <6.0) due to the accumulation of hydrogen sulfide (H_2S) and ferrous sulfide (FeS), which are formed by sulfur-reducing bacteria and other bacteria under anaerobic soil conditions (Arkesteyn, 1980; Burgin and Hamilton, 2008). In an acidic environment, Ca and Sr are gradually dissolved and mobilized at greater depths of the core. This process explains the lower Ca and Sr values detected in event layers 3 to 6; as a result, these elements can no longer be used as hurricane indicators in sediments older than 1 ka. By contrast, sulfur,

another common marine indicator, occurs in high concentrations in event layers 3 to 6 but is inconspicuous in the Wilma layer. Sulfur occurs in marine sediments mainly as pyrite (Davison, 1988). The reason why the Wilma layer does not show a relatively higher concentration of S is probably because surface sediments in the Shark River region are slightly oxidized (100-150 mv) (Castañeda-Moya et al., 2013), forming sulfate (SO_4) as pyrite is oxidized when exposed to O_2 (Arkesteyn, 1980). Sulfate is highly soluble in water, which makes it difficult to detect by the hand-held XRF device. At deeper soil depths, where anoxic conditions are predominant, the sulfate in hurricane deposits is reduced and becomes detectable again. This post-diagenetic biogeochemical transformation in the mangrove sediments sulfur cycles could explain the higher concentration of S detected in hurricane layer 3 to 6 than in the Wilma layer, particularly given its recent deposition.

Although classified as regular peat deposits in Zone-1 by PCA and discriminant analysis, sediment layers at approximately 250-255 cm and 165-175 cm are inferred as paleo-hurricane event 1 (3000 cal yr BP) and event 2 (1700 cal yr BP) because of high levels of Cl (Fig. 3). There are evidences showing that the sea-level in southwestern Florida was at least 6 m lower than the present level and the shoreline was probably 30 km seaward relative to today's at ~3500 cal yr BP (Parkinson, 1989; Wanless et al., 1994). Considering the relatively stable rate of sea-level rise (0.4 mm/yr) during the late Holocene (3000–2500 cal yr BP) across the western North Atlantic (Wanless et al., 1994; Ross et al., 2009; Behling et al., 2001), we infer that our study site currently at the mouth of the Shark River Estuary was still at some

distance inland from the former shoreline in the period from ~3000 to 1700 cal yr BP (245 – 165 cm in the core). Therefore, extremely high-energy events could have introduced large quantities of seawater to the coring site and caused salt accumulation, resulting in high concentrations of Cl in the sediment layers of events 2 and 1. But at that time the study site was still located beyond the distance reachable by clastic sediments carried as bed load by storm surge waters; hence the absence of a distinct clastic sediment layer and the low concentrations of Ca, Sr, and S associated with these early events. The absence of Cl in events 3 to 6 is probably due to regular tidal flushing.

Previous observational and modeling studies suggest that the effects of storm surges can extend up to 10 km inland in the coastal Everglades (Wanless et al., 1994; Lodge, 2010, Castañeda-Moya et al., 2010). The absence of sedimentary or geochemical evidence of storm deposition in the lower part of the core suggests that the site was not sensitive to storm surges prior to ~3000 cal yr BP due to the larger site-to-sea distance. Our proposed storm record for the coring site is also consistent with other studies indicating increased hurricane activity along the Gulf Coast during the late-Holocene (Liu and Fearn, 1993, 2000; van Soelen et al., 2012; Lane et al., 2011).

Environmental reconstruction

Although visual inspection does not show any differences between peat deposits in Zone-1 and Zone-2, **Chapter 4** describes that sediments in Zone-2 receive much more marine influence than sediments in Zone-1. XRF analysis shows that sediments

in Zone-2 (1150 cal yr BP to present) have much higher contents of Ca, Sr, S, Fe, K, Ti, and Zr than sediments in Zone-1 (5700-1150 cal yr BP). A significant increase in the pollen influx values of all mangrove species indicate that the modern mangrove coastline was established at site SRM at ~1150 cal yr BP (**Chapter 4**). These evidences correspond with results from PCA and discriminant analysis that Zone-1 and Zone-2 are delineated into different primary groups (Fig. 4b, 5).

Conclusion

This multi-proxy record from the southwestern Everglades has yielded high-resolution data allowing us to detect the occurrence of paleo-hurricane events in coastal wetlands at the mouth of Shark River Estuary during the late Holocene. By using the sedimentary signature of Hurricane Wilma as a modern analog and statistical analyses of the multi-proxy record, six major hurricane events are inferred at ~3000, 1700, 950, 580, 350, and 120 cal yr BP. The numerical analysis also confirms that the modern mangrove coastline was formed at the mouth of the Shark River by ~1150 cal yr BP, as the shoreline became stabilized

This study produces the first multi-proxy record of paleo-hurricane activities for South Florida, which is vital for the study of global climate change and forecasting future impacts of tropical cyclones. The study also introduces an application of numerical analysis to paleotempestology studies. Further paleoecological studies are needed to produce a high-resolution pollen record for the better understanding of the post-storm process of forest succession and habitat recovering in the Everglades landscape.

References

Arkesteyn, G.J.M.W., 1980. Pyrite oxidation in acid sulphate soils: The role of microorganisms. Plant and Soil 54, 119-134.

Behling, H., Cohen, M.C.L., and Lara, R.J., 2001. Studies on Holocene mangrove ecosystem dynamics of the Braganc, a Peninsula in north-eastern Para´, Brazil, Palaeogeogr. Palaeoclimatology 167, 225–242.

Blaauw, M., and Christen, J.A., 2013. Bacon Manual , http://chrono.qub.ac.uk/blaauw/ (Accessed 24 December 2014)

Burgin, A.J., and Hamilton, S.K., 2008. NO_3^- driven SO_4^{2-} production in freshwater ecosystems: Implications for N and S cycling. Ecosystems 11, 908-922.

Castañeda-Moya, E., Twilley, R.R., and Rivera-Monroy, V.H., Zhang, K.Q., Davis, S.E., and Ross, M., 2010. Sediment and Nutrient Deposition Associated with Hurricane Wilma in Mangroves of the Florida Coastal Everglades. Estuaries and Coasts 33, 45-58.

Castañeda-Moya, E., Twilley, R.R., and Rivera-Monroy, V.H., 2013. Allocation of biomass and net primary productivity of mangrove forests along environmental gradients in the Florida Coastal Everglades, USA. Forest Ecology and Management 307, 226-241.

Chen, R., and Twilley, R.R., 1999a. A simulation model of organic matter and nutrient accumulation in mangrove wetland soils. Biogeochemistry 44, 93-118.

Chen, R., and Twilley, R.R., 1999b. Patterns of mangrove forest structure and soil nutrient dynamics along the Shark River Estuary, Florida. Estuaries 22, 955-970.

Chmura, G.L., A.N. Smirnov, and I. A. Campbell, 1999. Pollen Transport through Distributaries and Depositional Patterns in Coastal Waters. Palaeogeography, Palaeoclimatology, Palaeoecology 149, 257-270.

Chmura, G.L., Stone, P.A., and Ross, M.S., 2006. Non-pollen microfossils in Everglades sediments. Review of Palaeobotany and Palynology 141, 103-119.

Davison, W., 1988. Interactions of iron, carbon and sulphur in marine and lacustrine sediments. Geological Society, London, Special Publications 40, 131-137.

Donnelly, J.P., Bryant, S.S., Butler, J., Dowling, J., Fan, L., Hausmann, N., Newby, P., Shuman, B., Stern, J., Westover, K., and Webb, T., III, 2001. 700 yr sedimentary record of intense hurricane landfalls in southern New England. Bulletin of the Geological Society of America 113, 714-27.

Ellison, J.C., 2008. Long-term retrospection on mangrove development using sediment cores and pollen analysis: A review. Aquatic Botany 89, 93–104.

Elsner, J.B., Kara, A.B., 1999. Hurricanes of the North Atlantic: Climate and Society. Oxford Univ. Press, New York. 488 pp.

Gleason, P.J. and P.A. Stone, 1994. Age, origin and landscape evolution of the Everglades peatland, In: S.M. Davis and J.C. Ogden (Eds.), Everglades, the Ecosystem and its Restoration. St. Lucie Press, Delray Beach, FL, pp. 149-198.

Kiage, L.M., and Liu, K.B., 2009. Palynological evidence of climate change and land degradation in the Lake Baringo area, Kenya, East Africa, since AD 1650. Palaeogeography, Palaeoclimatology, Palaeoecology 279, 60-72.

Lane, P., Donnelly, J.P., and Woodruff, J.D., 2011. A decadally resolved paleohurricane record archived in the late Holocene sediments of a Florida sinkhole. Marine Geology 287, 14–30.

Light, S.S., and J.W. Dineen, 1994. Water control in the Everglades: A historical perspective, Everglades: The Ecosystem and Its Restoration, In S.M. Davis and J.C. Ogden (Eds), St. Lucie Press, Delray Beach, Florida, pp. 47-84.

Liu, K.B., 2004. Palaeotempestology: principles, methods and examples from Gulf coast lake sediments. In Murnane, R. and Liu, K-b., editors, Hurricanes and typhoons: past, present and future. New York: Columbia University Press, 13-57.

Liu, K.B., 2007. Paleotempestology. In: Elias, S.A. (Ed.), Encyclopedia of Quaternary Science. Elsevier, Oxford, pp. 1978–1986.

Liu, K.B., and Fearn, M.L., 1993. Lake sediment record of late Holocene hurricane activities from coastal Alabama. Geology 21, 793-796.

Liu, K.B., and Fearn, M.L., 2000. Reconstruction of prehistoric landfall frequencies of catastrophic hurricanes in northwestern Florida from lake sediment records. Quaternary Research 54, 238-245.

Liu, K.b., and Lam, N.S.N., 1985. Paleovegetational reconstruction based on modern and fossil pollen data: an application of discriminant analysis. Annals of the Association of American Geographers 75, 115-30.

Liu, K.B., Lu, H.Y., and Shen, C.M., 2008. A 1,200-year proxy record of hurricanes and fires from the Gulf of Mexico coast: Testing the hypothesis of hurricane-fire interactions. Quaternary Research 69, 29-41.

Liu, K.B., Li, C., Bianchette, T.A., McCloskey, T.A., Yao, Q., and Weeks, E., 2011. Storm deposition in a coastal backbarrier lake in Louisiana caused by Hurricanes Gustav and Ike. Journal of Coastal Research, Special Issue 64, 1866-1870.

Lodge, T.E., 2010, The Everglades Handbook: Understanding the Ecosystem, second edition, Boca Raton, Florida: CRC Press.

Lu, H.Y. and Liu, K.b., 2003. Morphological variations of lobate phytoliths from grasses in China and the southeastern USA. Diversity and Distributions 9, 73-87.

McAndrews, J.H., Berti, A.A., and Norris, G., 1973. Key to the Quaternary pollen and spores of the Great Lakes region: Royal Ontario Museum, Life Science Miscellaneous Publication, vol.64.

Miller, R., 1945. The heavy minerals of Florida beach and dune sands. American Mineralogist 30, 65–75.

Monacci, N.M., Meier-Grünhagen, U., Finney, B.P., Behling, H., and Wooller, M.J., 2009. Mangrove ecosystem changes during the Holocene at Spanish Lookout Cay, Belize. Palaeogeography, Palaeoclimatology, Palaeoecology 280, 37–46.

NOAA, 2011, National Oceanic and Atmospheric Administration, Hurricane Center, Historical Hurricane Tracks website: http://maps.csc.noaa.gov/hurricanes/#

Parkinson, R.W., 1989. Decelerating Holocene Sea-Level Rise and Its Influence on Southwest Florida Coastal Evolution: A Transgressive/Regressive Stratigraphy. Journal of Sedimentary Petrology 59, 960-972.

Ramírez-Herrera, M.T., Lagos, M., Hutchinson, I., Kostoglodov, V., Machain, M.L., Caballero, M., Goguitchaichvili, A., Aguilar, B., Chaguéé-Goff, C., Goff, J., Ruiz-Fernández, A.C., Ortiz, M., Nava, H., Bautista, F., Lopez, G.I., and Quintana, P., 2012. Extreme wave deposits on the Pacific coast of Mexico: tsunami or storms? A multi-proxy approach. Geomorphology 140, 360-371.

Ross, M.S., O'Brien, J.J., Ford, R.G., Zhang, K.Q., and Morkill, A.. 2009. Disturbance and the rising tide: the challenge of biodiversity management on low-island ecosystems. Frontiers in Ecology and Environment 7, 471-478.

Saha, A.K., Moses, C.S., Price, R.M., Engel, V., Smith, T.J., and Anderson, G., 2012. A Hydrological Budget (2002-2008) for a Large Subtropical Wetland Ecosystem Indicates Marine Groundwater Discharge Accompanies Diminished Freshwater Flow. Estuaries and Coasts 35, 459-474.

Smith, T.J., Anderson, G.H., Balentine, K., Tiling, G., Ward, G.A., Whelan, K.R.T., 2009. Cumulative impacts of hurricanes on Florida mangrove ecosystems: Sediment deposition, storm surges and vegetation. Wetlands 29, 24-34.

Urrego, L.E., Bernal, G., and Polanía, J., 2009. Comparison of pollen distribution patterns in surface sediments of a Colombian Caribbean mangrove with geomorphology and vegetation. Review of Palaeobotany and Palynology 156, 358–375.

van Soelen, E.E., Brooks, G.R., Larson, R.A., Damsté, J.S.S., and Reichart, G.J., 2012. Mid- to late-Holocene coastal environmental changes in southwest Florida, USA. The Holocene, 1-10.

Wanless, H.R., Parkinson, R.W., Tedesco, L.P., 1994. Sea Level Control on Stability of Everglades Wetlands, In: Davis, S.M., and Ogden, J.C., (Eds). Everglades: the ecosystem and its restoration, St. Lucie Press, p. 199-222.

Whelan, K.R.T., T.J.I. Smith, G.H. Anderson, and M.L. Ouellette. 2009. Hurricane Wilma's impact on overall soil elevation and zones within the soil profile in a mangrove forest. Wetlands 29, 16–23.

CHAPTER 6. A PALYNOLOGICAL STUDY OF WETLAND DEVELOPMENT IN THE SHARK RIVER ESTUARY, EVERGLADES, FLORIDA, SINCE THE MID-HOLOCENE

Introduction

Because of their location at the transition zone between river and maritime environments, estuarine wetlands are complex and dynamic ecosystems subjected to both riverine influences (i.e. fresh water discharge and sediment input) and marine influences (i.e. sea-level changes, tides, and waves). These dynamic allogenic forces make these wetlands among the most productive natural habitats in the world.

The Everglades have some of the most productive mangrove estuaries in the world (Lodge, 2010), and they have been subjected to profound hydrological changes due to human activities in the south Florida since AD 1930 (Wanless et al, 1994). There are no consistent views regarding the long-term response of estuarine wetland to environmental changes. Since the processes that affect estuarine ecosystems operate at a centennial to millennial timescale, an historical perspective will help to understand the long-term estuarine vegetation dynamics in response to environmental changes. However, there are few paleoecological studies available from the Everglades, and no pollen record is older than 5000 cal yr BP (Willard and Bernhardt, 2011), a crucial time when vegetation started to flourish on the Florida platform. With these points in mind, we examined four sediment cores recovered from a 20 km transect along the Shark River Estuary in the Everglades National Park (ENP) (Fig.1), the largest freshwater outlet of the largest contiguous mangrove swamp in North America (Lodge, 2010).

At least 5,700 years of peat archives are recovered in our cores. In this paper, we present palynological, X-ray fluorescence (XRF), and loss-on ignition data of these archives. Our goal is to document the millennial-scale estuarine vegetation dynamics driven by climatic variations and sea-level rise in the Everglades. Our study provides the oldest pollen record to date from the Everglades and generates new paleoenvironmental data that will aid our understanding of contemporary coastal process in subtropical estuarine wetlands.

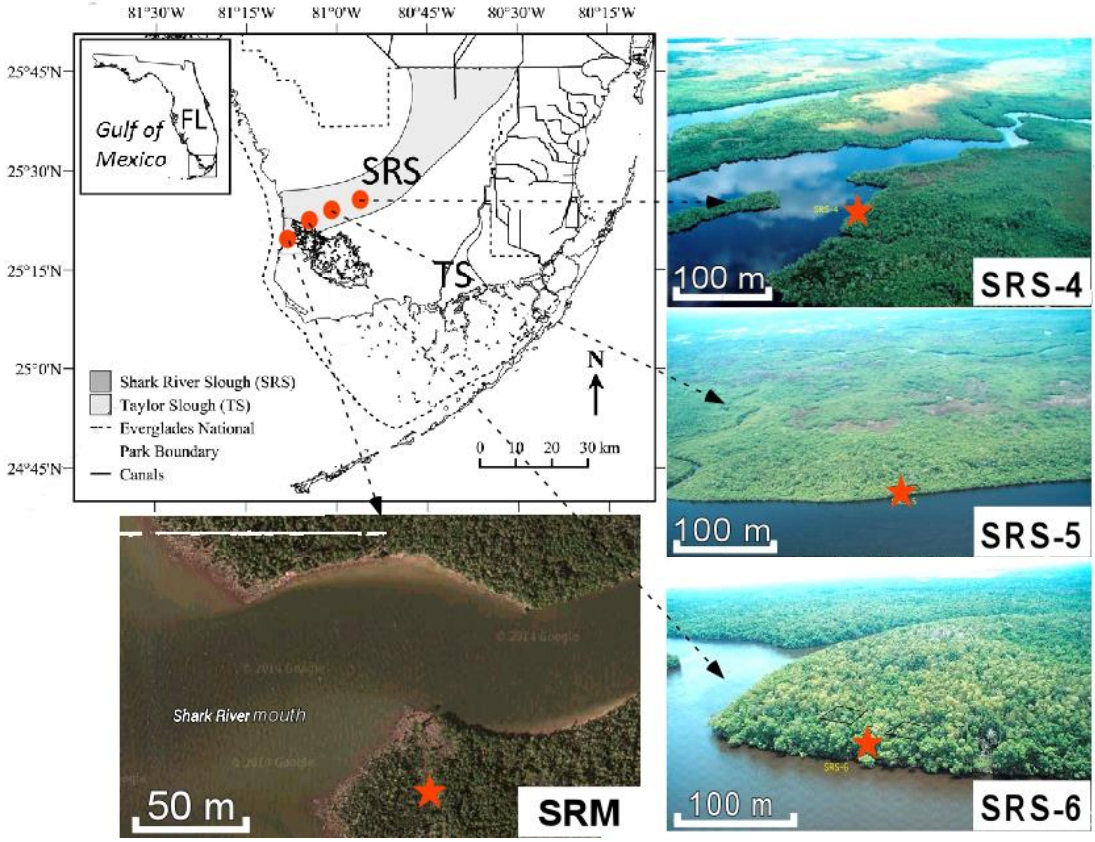

Figure 1. Location of the Shark River Slough (SRS) is on the top left side (base map adapted from FCE LTER: http://fcelter.fiu.edu). Pictures on the right side are the aerial photos of study site SRS-4, SRS-5, and SRS-6. Picture on the bottom left side is the satellite photo of site SRM. Red stars represent the exact coring location. Site numbers are tied to core ID described in Table 1.

Table 1. Key features of the pollen results of each core and description of the study sites. Latitudes and longitudes for sites are determined using global positioning systems. Composition of the above ground biomass of site SRS-4, SRS-5, and SRS-6 is retrieved from Castañeda-Moya (2010). Composition of the above ground biomass of site SRM is based on observation and field notes. Up arrow (↑) represents increase in pollen percentage. Down arrow (↓) represents decrease in pollen percentage.

Core ID	**GPS**	**Site description (above ground biomass)**	**Pollen zone (cal yr BP)**	**Modern analog**	**Pollen signature (total pollen sum)**
SRM	25 °21'10"	Heavily deforested by	I:	Marl prairie	*Pinus* 20-30%, *Quercus* 5-10%, *Salix* >30%, Poaceae 15-20%
	-81 °06'52"	Hurricane	> 5700		
		Avicennia fringe,	II:	Freshwater	↑: Amaranthaceae >50%, *Sagittaria* 5-15%, Pinus 10-30%, Rubiaceae 0-30%,
		Laguncularia/*Rhizophora*	5700-3800	marsh	Poaceae 5-20%,
		co-dominant	III:	Brackish	↑: Poaceae >15%, *Rhizophora* 0-50%
		no *Conocarpus*	3800-1140	marsh	↓: Amaranthaceae 35-75%
			IV:	Mangroves	↑: *Rhizophora* >50%, *Laguncularia* 5-15%, *Avicennia* 5-25%, *Conocarpus*>5%
			1140-present		↓: Amaranthaceae 5-15%, Poaceae <15%
SRS-6	25 °21'53"	*Laguncularia* >40%	I:	Marl prairie	Amaranthaceae >80%, Poaceae 0-10%
	-81 °04'41"	*Rhizophora* >25%	>4800		
		Avicennia >25%	II:	Freshwater	↑: Amaranthaceae >90%
		No *Conocarpus*	4800-3430	marsh	↓: *Sagittaria* 0-2%, *Pinus* 0-2%, Poaceae 0-2%
			III:	Brackish	↑: Mangroves, *Pinus* >10%, *Morella* 0-5%, Asteraceae 5-10%, Poaceae 5-10%
			3430-1060	marsh	↓: Amaranthaceae 30-75%, *Sagittaria* disappear
			IV:	Mangroves	↑: *Rhizophora* >20%, *Laguncularia* 5-30%, Pinus >15
			1060-present		↓: Amaranthaceae <30%

Table 1 cont.

SRS-5	25 °22'37" -81 °01'57"	Tall *Rhizophora* >80% few *Laguncularia* and *Avicennia* No *Conocarpus*	II: 4500-2380	Freshwater marsh	Amaranthaceae >50%, *Sagittaria* 5-15%, *Pinus* 10-60%, Poaceae >10%, Cyperaceae 2-5%
			III: 2380-860	Brackish marsh	↑: Mangroves, *Pinus* >15%, Poaceae 15-30%, *Quercus* >5%, Morella >5%, *Asteraceae* >3% ↓: Amaranthaceae 30-50%, *Sagittaria* 0-5%
			IV: 860-present	Mangroves	↑: *Rhizophora* >20%, *Laguncularia* 0-5% ↓: Amaranthaceae <25%
SRS-4	25 °24'34" -80 °57'51"	Scrub *Rhizophora* >60% *Laguncularia* > *Conocarpus*, no *Avicennia*	I: >4400	Marl prairie	*Pinus* >50%, Poaceae >15%, Amaranthaceae >30%
			II: 4400-2330	Freshwater marsh	↑: Amaranthaceae >50% ↓: *Pinus* 10-25%, Poaceae <15%,
			III: 2330-860	Brackish marsh	↑: Mangroves, *Pinus* >20%, Poaceae >15% ↓: Amaranthaceae 40-50%,
			IV: 860-present	Mangroves	↑: *Rhizophora* >10, *Laguncularia* 2-5, *Conocarpus* 0-25, *Morella* >15, Poaceae >20 ↓: Amaranthaceae 30-40%

Study area

Site description

The ENP is located at the southern tip of the Florida peninsula (Fig. 1), a permeable plateau of limestone sitting atop the Florida Platform. At ~25 °N, the climate of the ENP is mild with an average annual precipitation of 125 to 152 cm (Lodge, 2010). During the dry season (December-May), weather is pleasant with an average temperature between 25°C and 12°C. During the wet season (June-November), weather is hot and humid, with an average temperature around 32°C and humidity over 90%. The wet season coincides with the Atlantic Hurricane season; therefore tropical storms are common during the wet season. During the last 160 years, 46 major (category 3-5 according to the Saffir-Simpson scale) hurricanes have crossed the ENP with an average return interval of 3.5 years (NOAA, 2013).

The coastal area of the ENP, from Naples to Florida Bay, are covered by approximately 15,000 ha of dense mangrove forests (Simard et al, 2006).The interior part of the ENP contains 1,050,000 ha of sawgrass marshes, sloughs, wet prairies, and pinelands (Bernhardt and Willard, 2009). Previous study shows that these densely vegetated wetlands are phosphate-limited (Castañeda-Moya et al., 2010), and the limited nutrient is supplied by the Gulf of Mexico, rather than the upper watershed (Chen and Twilley, 1999 a, b).

The Shark River Estuary is the biggest freshwater outlets in the ENP. During the wet season, water overflowing Lake Okeechobee and associated rainfall result in a southward sheet flow along a gentle slope of ~3 cm/km into SRS. The water entering

SRS flows through long-hydroperiod prairie sloughs into mangrove swamps at the river estuary and then into Whitewater Bay or the Gulf of Mexico along the southwestern coast of Florida (Lodge, 2010).

The study area - the Shark River Estuary, encompassing 4 study sites along a transect, lies roughly between 25 °21'10" and 25 °24'34.4"N latitude, and between 81 °06'52" and 80 °57'51.3" W longitude (Fig. 1). Site SRM is located at the mouth of the Shark River Estuary, and site SRS-6, SRS-5, and SRS-4 are located at approximately 4 km, 8 km, and 20 km upstream from the mouth, respectively. Tides at the Shark River Estuary are semi-diurnal with 1.1m mean tidal amplitude, and site SRM, SRS-6, and SRS-5 receive strong influence from tidal activities (Castañeda-Moya, 2010). The general setting of each study site is described below. More information about the location and vegetation composition of each site is described in Table 1.

Site SRM is located on the edge of Ponce de Leon Bay, at the mouths of Whitewater Bay and Shark River Estuary. It is flooded by tides 90% of the year with an average tidal range of 0.5 m (Castañeda-Moya et al., 2010). This site is situated in a fringing mangrove forest, where white mangroves (*Laguncularia racemosa*) and red mangroves (*Rhizophora mangle*) are co-dominant species (above ground biomass) (Chen and Twilley, 1999 a, b). Field observation suggests that the average mangrove canopy height at SRM is the highest (> 15m) among all 4 sites. Hurricane Wilma almost directly crossed site SRM in 2005. The storm surge flooded the site with 3 - 4 m of water and deposited 10 cm of marine sediment here (Castañeda-Moya et al., 2010).

Soil at site SRS-6 (Table 1, Fig. 1) has an atomic nitrogen to phosphorus ratio (N: P) of 28 (Chen and Twilley, 1999b). This site is flooded 233 days annually with a pore-water salinity of 27 ± 2.6 ppt. It is occupied by white mangroves with red mangroves and black mangroves (*Avicennia germinans*) as co-dominant species. Site SRS-6 has the highest plant diversity along the Shark River transect, and the average mangrove canopy height is approximately 10 meters (Castañeda-Moya, 2010). Strong winds and storm surge from Hurricane Wilma caused damage to approximately 1,250 ha of mangrove forest along the west coast of the ENP, resulting in 90% mortality of trees with diameters at breast height greater than 2.5 cm (Whelan et al., 2009; Smith et al., 2009). The storm surge flooded site SRS-6 with 2 - 3 m of water and deposited approximately 5 cm of marine sediment on the surface of the mangrove forest (Castañeda-Moya et al., 2010).

Soil at site SRS-5 (Table 1, Fig. 1) has an atomic nitrogen to phosphorus ratio (N: P) of 46 (Chen and Twilley, 1999b). This is flooded 197 days annually with a pore-water salinity of 20.8 ± 3.1 ppt. It is totally occupied by red mangroves with very few other mangrove species. The average mangrove canopy height at this site is approximately 8 meters (Castañeda-Moya, 2010).

Soil at site SRS-4 (Table 1, Fig. 1) has an atomic nitrogen to phosphorus ratio (N: P) of 105 (Chen and Twilley, 1999b), therefore it is very phosphorus limited. According to a multi-year (2005-2010) monitoring study of the Shark River Estuary (Castañeda-Moya, 2010), this site is mainly influenced by freshwater runoffs and flooded 165 days annually with a pore-water salinity of 4.6 ± 1.1 ppt. It is occupied by

red mangroves with white mangroves as co-dominant species. It is the only site along the SRS transect where *Conocarpus erectus* is found and black mangrove is absent. The average mangrove canopy height at this site is less than 5 meters.

Review of paleoecological records from the region

Previous study indicates that marl prairie is the oldest wetland type formed on the Everglades limestone platform at ~12–13 ka during the last deglaciation (Kropp 1976). Marl prairies are marl-forming and short-hydroperiod freshwater environment representing a transitional period between subaerial limestone terrains and peat-accumulating wetland (Gleason and Stone, 1994). Periphyton is a common component of marl prairies and responsible for calcitic marl deposits underlying wide areas of wetland peat in the Everglades (Willard et al., 2001). Marl prairies are found in the northern Everglades to the Shark River Slough, Whitewater Bay, Cape Sable, and Florida Bay (Gleason and Stone, 1994, Lodge, 2010).

Between 7,500 to 6,500 cal yr BP, sea-level (SL) record from south Florida shows that the SL was rising at a rate of more than 5 mm/yr (Wanless et al. 1994). The southwest Everglades lie atop the permeable Tamiami limestone platform where the water table is very sensitive to SL changes (Gleason and Stone, 1994). As a result of rapid SL rise, the oldest freshwater peats on the Florida Platform started to accumulate on marl prairies in the southwest Everglades at ~6,500 cal yr BP because of deeper water levels and longer hydroperiods (Scholl et al. 1969; Robbin, 1984). Microscopic studies of these peats indicate that they are composed primarily of *Cladium* and *Sagittaria* (Willard and Bernhardt, 2011).

Between 6,500 to 3,500 cal yr BP, the rate of SL rise slowed to 2.3 mm/year (Wanless et al. 1994), but the moderate to long hydroperiod wetlands were spreading on the south Florida platform during this period (Willard and Bernhardt, 2011). By 5,000 cal yr BP, up to 165 cm of freshwater peat had been accumulated on the Florida platform from the Florida Keys to Lake Okeechobee (Gleason and Stone 1994).

After 3,500 cal yr BP, the rate of SL rise slowed to 0.4 mm/year (Wanless et al. 1994). This allowed the stabilization of coastlines and the establishment of mangrove forests along the southwest Florida coast. The oldest definitive mangrove peats retrieved from southwest Florida are from the Ten Thousand Islands area and Whitewater Bay and were dated at 3,000 to 3,500 cal yr BP (Scholl et al., 1969; Parkinson 1989). By ~2,200 cal yr BP, mangrove peats are found up to 20 km inland from the coastlines in southwest Florida (Willard and Bernhardt, 2011). However, no pollen record is available to document the development of the earliest phase of mangrove estuaries.

Since AD 1930, the rate of SL rise has dramatically increased to 3.8 mm/yr, a rate that is 6 to 10 times that of the past 3,500 years (Wanless et al, 1994). Inland replacement of freshwater marshes by mangrove wetlands has been observed in the ENP as a result of salt water intrusion and salinity changes in groundwater (Ross et al., 2000).

Table 1. Radiocarbon dating results for core SRM, SRS-6, SRS-5, and SRS-4. Dates in parentheses are rejected due to extreme age reversal.

Core ID	Depth (cm)	Material	Conventional C^{14} age (yr BP)	2-σ Calibrated range (Cal yr BP)
SRM	56	Leaf	145 ±25	0 - 280
	139	Leaf	1180 ±30	990 - 1180
	179	Leaf	1940 ±30	1820 – 1970
	243	leaf	2860 ±30	2880 – 3070
	246	Wood	155 ±25	(Rejected)
	246	Wood	> Modern	(Rejected)
	260	Leaf	2240 ±30	(2150 – 2340)
	300	Bark	3540 ±35	3700 – 3910
	374	Organic silt	4160 ±30	4780 - 4830
	374	Roots	2940 ±30	(3000 – 3210)
	440	Leaf	1090 ±20	(Rejected)
	446	Organic silt	5800 ±30	6500 - 6670
	446	Roots	4060 ±30	(4760 – 4800)
	448	Plant debris	6620 ±260	(6940 – 7980)
SRS-6	114	Leaf	500 ±25	510 – 540
	200	Organic silt	2260 ±20	2160-2340
	232	Leaf	2970 ±90	2920-3360
	303	Organic silt	3570 ±25	3770-3970
	312	Leaf	1680 ±25	(1530-1630)
	378	Organic silt	4230 ±40	4630-4860
	381	Leaf	2580 ±40	(2500-2770)
SRS-5	80	Leaf	930 ±25	790-920
	155	Organic silt	2050 ±25	1930-2110
	171	Leaf	1270 ±25	(1150-1280)
	190	Organic silt	2560 ±20	2540-2750
	240	Leaf	1280 ±30	(1150-1290)
	248	Organic silt	4010 ±25	4420-4520
SRS-4	42	Leaf	> Modern	(Rejected)
	50	Leaf	145 ±20	0-280
	90	Organic silt	1180 ±30	990-1220
	100	Organic silt	1530 ±20	1360-1520
	125	Organic silt	2460 ±20	2400-2700
	151	Leaf	2330 ±50	(2160-2680)
	156	Shell hashes	3900 ±25	4250-4420

Materials and methods

A 525, 445, 250, and 185 cm sediment core was extracted from site SRM, SRS-6, SRS-5, and SRS-4, respectively by using a Russian peat borer in May 2010. The GPS coordinates of each coring location are described in Table 1. All cores contain the complete depositional history above the bedrock platform. The 50-cm core segments were measured and photographed in the field before being wrapped by multiple layers of plastic wrap to ensure minimal water loss. All the cores are currently stored in the Global Change and Coastal Paleoecology Laboratory at Louisiana State University.

Thirty-four samples were sent to the NOSAMS Laboratory at Woods Hole Oceanographic Institution (WHOI) and Beta Analytic Inc., in Miami, Florida for AMS ^{14}C measurements. Among those 34 ^{14}C samples, 14 are from core SRM, 7 are from core SRS-6, 6 are from core SRS-5, and 7 are from core SRS-4. All ^{14}C dates are calibrated using the Calib 7.0 program (Stuiver et al., 2010) and reported as calibrated years before present (cal yr BP) in this study. The chronology of core SRM is described in **Chapter 4**. Sedimentation rates for core SRS-6, SRS-5, and SRS-4 are determined by linear interpolation between radiocarbon samples. More information about the ^{14}C samples is described in Table 2.

In the laboratory, all the cores are scanned by a handheld Olympus Innov-X DELTA Premium X-ray fluorescence (XRF) analyzer at 2 cm interval with a sampling time of 90 s under standard soil mode to measure elemental concentrations (ppm) of 32 chemical elements (Fig. 5). Loss-on-ignition (LOI) analysis was performed on all the cores at continuous 1 cm intervals to establish core stratigraphy (Dean, 1974).

Samples were heated at 105 ℃ to calculate water % (wet weight), 550 ℃ for organics % (dry weight), and 1000 ℃ for carbonates % (dry weight) (Fig. 2).

For palynological analysis, sixty-seven samples were taken from core SRM at 5 to 10 cm resolution; 39 samples were taken from core SRS-6 at 10 to 15 cm resolution; 26 samples were taken from core SRS-5 at 10 cm resolution; and 20 samples were taken from core SRS-4 at 5 to 10 cm resolution. Each sample contains 0.9 mL of sediments. Samples were processed using standard procedures (Liu et al., 2011; Kiage and Liu, 2009). The hydrofluoric acid treatment was omitted because samples contained mostly peat and limited amount of silicates. One commercial *Lycopodium* (L_c) tablet (~ 18,583 grains) was added to each sample as an exotic marker to calculate the pollen concentration (grains/cm^3). Approximately 300 grains of pollen and spores were counted in most of the samples and were used as the pollen sum for calculating pollen percentages of all taxa. Foraminifera linings, dinoflagellates tests, and charcoal fragments (>10 μm in size) were also counted for each sample, but their percentages were calculated outside of the sum. The identification of pollen was based on published pollen keys by McAndrews et al. (1973) and Willard et al. (2004). The palynological results are reported in percentage (%) and concentration diagrams (Fig. 5, 6). More information about the treatment of pollen samples and calculation of pollen concentration can be found in **Chapter 3**.

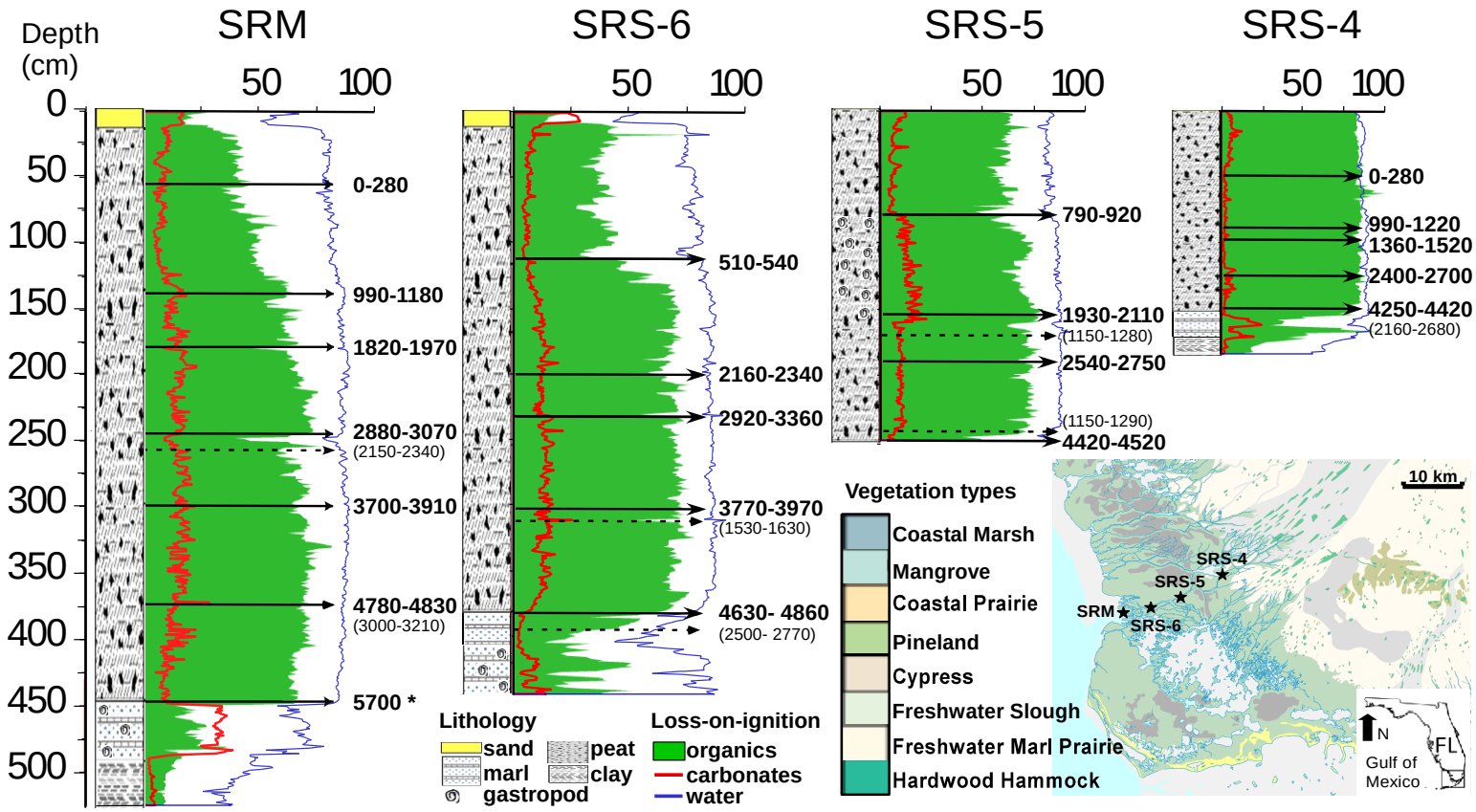

Figure 2. Lithology, loss-on-ignition diagram, and ^{14}C dates for core SRM, SRS-6, SRS-5 and SRS-4. Arrows with solid lines point to accepted dates at corresponding depth. Arrows with dash lines point to rejected dates at corresponding depth. A map showing vegetation types surrounding the study sites is added to the figure to facilitate the interpretation of data.

Results

Stratigraphy and chronology

Approximately 10 cm of carbonate-rich clastic sediments occurred at the top of core SRM and SRS-6 is attributed to Hurricane Wilma. A Photograph of these hurricane deposits is shown in Figure 3. Their sedimentary, chemical, and palynological characteristics are described in **Chapter 5**. The stratigraphic and ^{14}C dating results from all cores are shown in Fig 2.

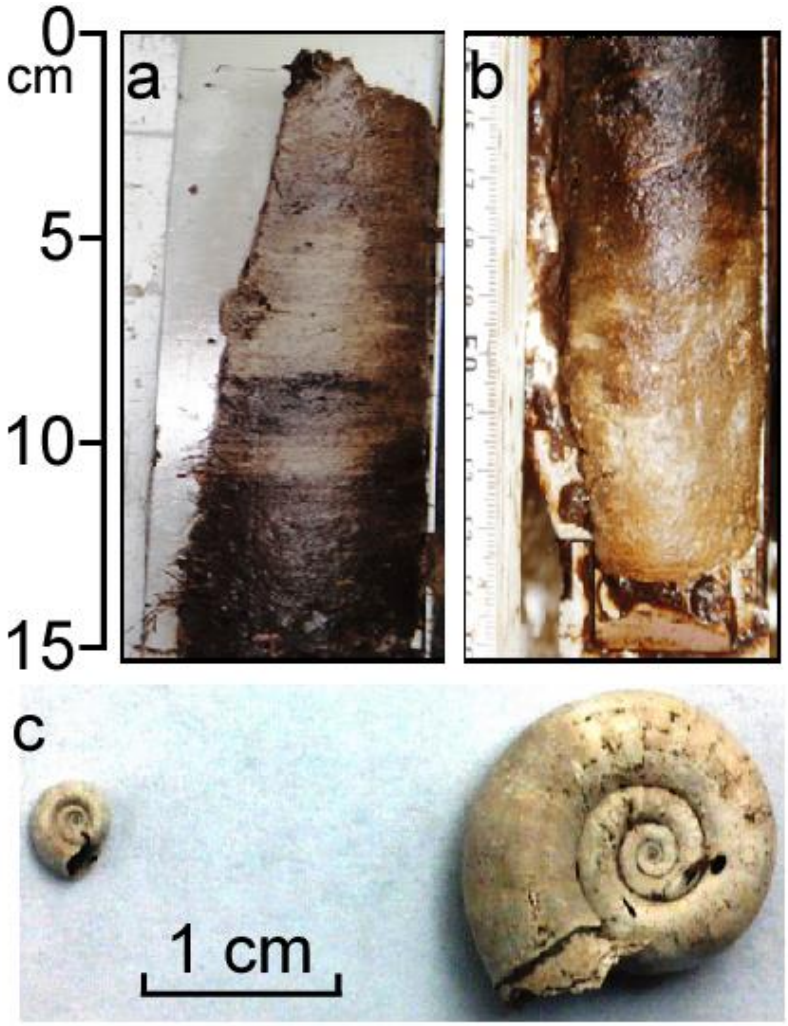

Figure 3. a) Photo of storm deposits from the top of core SRM. b) Photo of marl sediments from the bottom of core SRS-6. c) Photo of freshwater snails *Helisoma trivolvis* sp.

Core SRM is the longest core (525 cm) from the Shark River transect. From 525 to 485 cm is homogeneous clay (525-485 cm) with very low contents of water, organics and carbonate. From 485 to 445 cm are marl sediments. This section contains shell hashes of the freshwater snail *Helisoma trivolvis* sp., and is low in water and organics and high in carbonates content. Above the marl sediments are more than 4 m of continuous peat (445-10 cm) with very high contents of water and organic matter and relatively low concentration of carbonates. The peat sediments have an estimated basal age of ~5,700 cal yr BP. ^{14}C samples from 56, 139, 179, 243, 300, and 374 cm give a date of ~180, 1140, 1880, 2950, 3800, and 4800 cal yr BP. More information about the chronology of core SRM can be seen in **Chapter 4**.

Core SRS-6 is 450 cm long. From the bottom to 375 cm are marl sediments. Although visual inspection reveals no differences, marl sediments in core SRS-6 show different stratigraphy comparing with that in core SRM. The bottom half of this marl section (450 to 410 cm) contains shell hashes of the freshwater snail *Helisoma trivolvis* sp. (Fig. 3), but does not have high content of carbonates or low content of water. The top has low contents of carbonates and water. Organic content of the marl sediments is not consistent comparing with that in core SRM. Pictures of these marl sediments and freshwater snails can be seen in Figure 3. From 375 to 10 cm is peat with very high content of water. Peat from 125 to 10 cm has low content of organics comparing with that in the bottom half of the peat section. The peat sediments have a basal age of ~4750 cal yr BP. ^{14}C samples from 114, 200, 232, and 303 cm give a date of ~525, 2250, 3140, and 3870 cal yr BP.

Core SRS-5 consists of 250 cm of continuous peat. Water content is consistently high throughout the core. Peat from ~150 to 90 cm is coarse and relatively high in carbonates. Peat from 90 cm to the top has relatively low content of organics and carbonates. Core SRS-5 has a basal age of ~4470 cal yr BP. ^{14}C samples from 80, 155, and 190 cm give a date of ~850, 2020, and 2650 cal yr BP.

Core SRS-4 is 185 cm long and consists of clay (185 to 175 cm), marl (175 to 160 cm), and peat (160 to 0 cm). Although much shorter, stratigraphy of core SRS-4 is very similar to that of core SRM. The peat sediments have a basal age of ~4340 cal yr BP. ^{14}C samples from 50, 90, 100, and 125 cm give a date of ~140, 1100, 1440, and 2550 cal yr BP.

XRF and pollen analyses

The XRF, pollen percentage, and pollen concentration results of the four cores are given in Fig 4, 5, and 6. Cores SRM, SRS-6, and SRS-4 are divided into 4 corresponding pollen zones. Core SRS-5 is divided into 3 corresponding pollen zones with zone 1, the basal pollen zone, missing at this site. Key features of each pollen zone are outlined in Table 1.

Core SRM

In core SRM, the basal clay is pollen barren and most likely a bedrock substrate caused by acidic leaching. Therefore it is excluded from the discussion of the sedimentary history of the Shark River Estuary. Zone I (485 to 450 cm, >5,700 cal yr BP) is occupied by upland taxa, particularly *Salix*, *Pinus*, and *Quercus*. Poaceae is consistently present, and there is regular occurrence of other herbaceous taxa

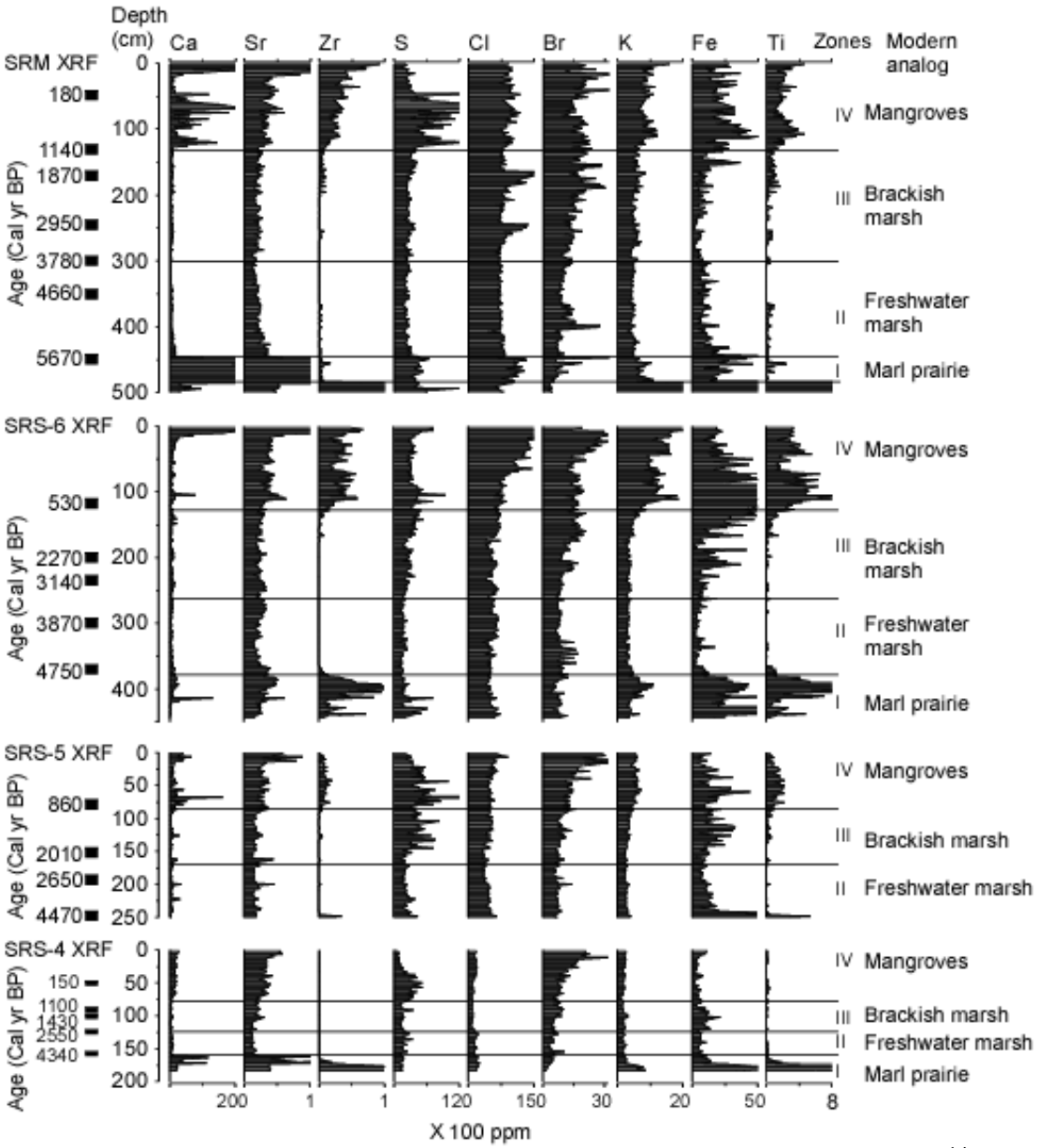

Figure 4. XRF diagrams from core SRM, SRS-6, SRS-5, and SRS-4. Accepted ^{14}C dates are added to the left side of each core at corresponding depth.

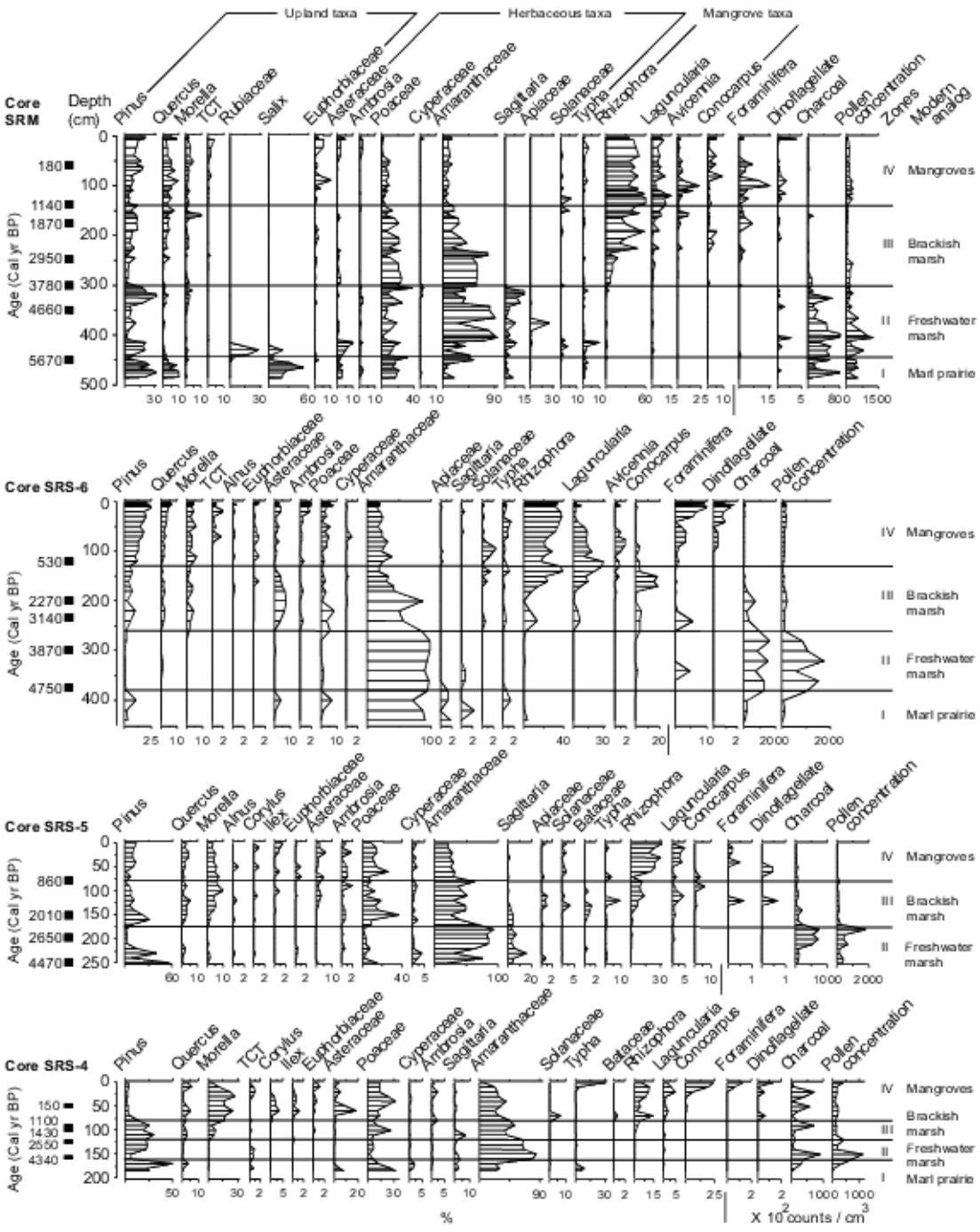

Figure 5. Pollen percentage diagrams for core SRM, SRS-6, SRS-5, and SRS-4. Accepted ^{14}C dates are added to the left side of each core at corresponding depth. The concentration curves for marine planktons, charcoal fragments and pollen sum are added on the right to facilitate comparison.

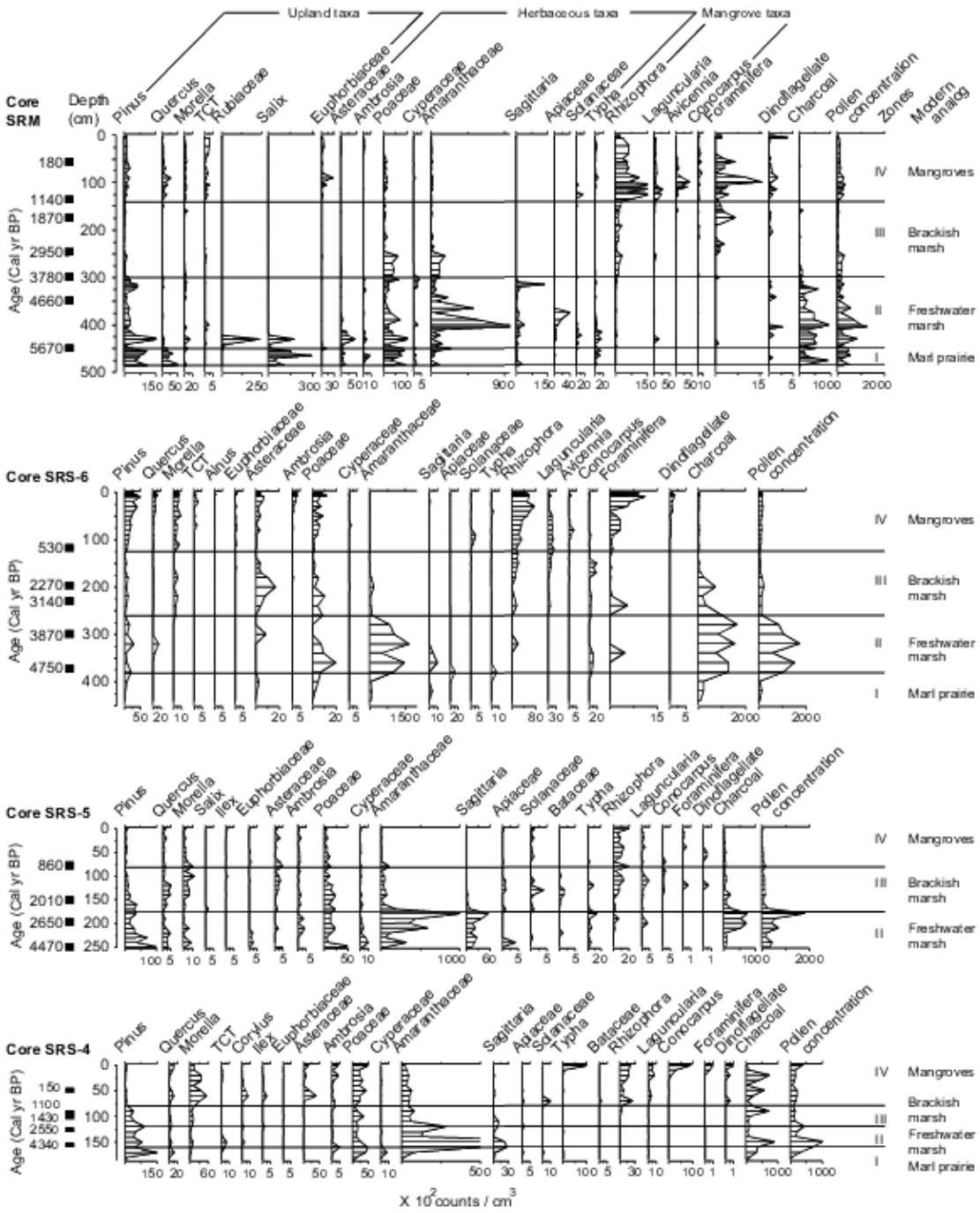

Figure 6. Concentration diagrams of pollen, marine planktons, and charcoal fragments for core SRM, SRS-6, SRS-5, and SRS-4. Accepted ^{14}C dates are added to the left side of each core at corresponding depth.

(Amaranthaceae, *Sagittaria,* and *Typha*). XRF results reveal that sediments in zone I have very high contents of Ca and Sr.

Zone II (450 to 300, 5,700 to 3,800 cal yr BP) is characterized by abundant charcoal and a marked shift to herbaceous taxa. The bottom of this zone contains mostly upland taxa (*Salix*, *Pinus*, and Rubiaceae), and some herbaceous taxa (Asteraceae, Poaceae, and *Typha*) also commonly occur. From 410 to 350 cm, Amaranthaceae becomes the most dominant pollen taxa. At the top of zone II, *Pinus* and *Sagittaria* are the most abundant taxa. XRF analysis shows low concentration of all detected chemical elements in zone II.

Zone III (300 to 140 cm, 3800 to 1140 cal yr BP) is characterized by the increase of mangrove taxa. Poaceae and Amaranthaceae are still very plentiful at the bottom of the zone, but all mangrove species start to appear and increase in abundance. From 250 cm, *Rhizophora* becomes the most common species, while most upland and herbaceous taxa become less abundant. Dinoflagellates and foraminifera linings appear in higher concentrations more consistently. XRF results show higher contents of Br and Ti comparing with zone II

Zone IV (140 to 10 cm 1140 cal yr BP to present) is characterized by the total dominance of *Rhizophora*. *Rhizophora* accounts for >50% of the pollen sum and is very high in concentration, while upland and herbaceous taxa are generally less abundant. Other mangrove genera (*Laguncularia*, *Avicennia,* and *Conocarpus*) and dinoflagellates and foraminifera linings are also present in higher abundance. XRF results show a significant increase in the concentrations of Ca, Sr, Zr, S, Fe, and Ti.

Core SRS-6

In zone I (450 to 380 cm, >4800 cal yr BP), although the pollen percentage diagram indicates Amaranthaceae as the most dominant species, the pollen

concentration diagram reveals that all pollen taxa including Amaranthaceae are very scarce in this zone. XRF results show high concentrations of Zr, Fe, and Ti.

Zone II (380 to 260 cm, 4,800 to 3,430 cal yr BP) is characterized by abundant charcoal and Amaranthaceae. *Pinus* consistently occur, and Poaceae and *Sagittaria* are abundant at the bottom half of the zone. XRF analysis shows low concentrations of all detected chemical elements in zone II.

Zone III (260 to 140 cm, 3430 to 1060 cal yr BP) is characterized by the appearance of mangrove species. Pollen concentration diagram shows that Amaranthaceae disappears from the pollen assemblage from 180 cm, but all mangrove species except for *Avicennia* are consistently present. Other common taxa include *Pinus*, *Morella*, Asteraceae, and Poaceae. XRF results show increase in in the concentrations of Br and Fe.

Zone IV (140 cm to the surface) contains mostly mangrove pollen. Pollen of *Rhizophora* maintains high representation throughout this zone. Pollen of *Laguncularia* and *Avicennia* is abundant at the bottom half of the zone but decreases towards the top of zone IV. Some upland (*Pinus*, *Quercus*, TCT, and *Morella*) and herbaceous taxa (Asteraceae, *Ambrosia*, and Poaceae) continue to be present. Dinoflagellates and foraminifera linings are present in higher abundance. XRF results show an increase in the concentrations of all detected chemical elements.

Core SRS-5

In core SRS-5, marl is absent at the bottom of the core, therefore it has only 3 corresponding pollen zones. Pollen assemblages of core SRS-5 are very similar to those of core SRS-6. Zone II (bottom to 175 cm, 4500 to 2380 cal yr BP) is characterized by abundant charcoal and Amaranthaceae. *Sagittaria*, *Pinus*, Poaceae, and Cyperaceae are consistently present. Zone III (175 to 80 cm, 2380 to 860 cal yr

BP) is characterized by the appearance of mangrove species except for *Avicennia*, which is absent from the core. *Pinus* and Poaceae continue to be present; *Quercus*, *Morella*, Asteraceae, and *Ambrosia* become more abundant; and *Sagittaria* becomes rare. The pollen assemblage of zone IV (80 cm to the surface) is very similar to that of zone III, except that *Rhizophora* becomes the dominant species. XRF results show low contents of all detected chemical elements at zone II and III, and their concentrations increase in zone IV.

Core SRS-4

In core SRS-4, the bottom 10 cm consists of pollen barren clay. *Pinus*, Poaceae, Cyperaceae, and Amaranthaceae are the most abundant species in the pollen assemblage of zone I (175 to 160 cm, >4400 cal yr BP). Zone II and III extend from 160 to 120 cm and 120 to 80 cm respectively, and are dated to 4400 to 2330 cal yr BP and 2330 to 860 cal yr BP. Their pollen assemblages are very similar to that of zone II and zone III in core SRS-5. Zone IV extends from 80 cm to the surface, and contains mostly *Morella*, Poaceae, Amaranthaceae, and *Rhizophora*. *Laguncularia* increases toward the top of the zone, and *Conocarpus* becomes the most dominant species of the top 20 cm of the core. Unlike the other cores, the concentration of charcoal is very high in zones III and IV in core SRS-4. XRF analysis shows very high concentrations of Ca and Sr in zone I; low concentration of all detected elements in zone II and III; and increases of Ca, Sr, S, and Br in zone IV. Unlike the other cores, Zr is absent from the top half of core SRS-4.

Discussion

Evolution of the Shark River Estuary

Where the Shark River Estuary is situated today appears to dry out frequently prior to the mid-Holocene. Basal clay layers in core SRM and SRS-4 are devoid of

pollen. This suggests a subaerial condition below the “wetness” threshold for pollen preservation. The absence of pollen also precludes knowledge of the vegetation types present. Our study sites were most likely situated on an arid or frequently dried out terrestrial environment that was not inundated long enough to promote marl or peat accumulation during the early to mid-Holocene.

Each stage of the landscape-scale vegetation development at the Shark River Estuary is displayed in Figure 7. By 6000-5700 cal yr BP, marl sediments rich in shell hashes of freshwater snails started to accumulate at site SRM, the current mouth of the Shark River Estuary (Fig. 7a, Table 1). Such transition suggests that with low nutrient water presents for extended periods of time in the summer under high light conditions, allowing the flourish of algae and formation marl prairies at site SRM (Gleason and Stone, 1994; Willard, et al., 2001). By 4,800 cal yr BP, marl prairies were present at site SRS-4, at least 20 km from the mouth (Fig. 7b, Table 1). Because the Shark River Estuary lies atop the permeable Tamiami limestone where the water table is very sensitive to changes in hydrological conditions (Gleason and Stone, 1994), the spreading of marl prairies toward more inland area suggests a higher elevation of the phreatic aquifer due to SL rise. Abundant *Pinus*, *Salix* and Amaranthaceae in the pollen assemblage suggest that it was a mixture of short-hydroperiod and longer-hydroperiod prairies (Fig. 5 and 6), perhaps also with pine savannas in the immediate vicinity. Such areas (e.g., Lostman's Pines and Raccoon Point regions of Big Cypress National Preserve) are present in the interior of the Everglades region of South Florida today (Doren et al. 1993; Schmitz et al., 2002; Hanan et al., 2010). These habitats today have hydroperiods lasting less than 12 months and are thus dry seasonally, tending to burn more than once a decade, and even every 1-2 years if located adjacent to pine savannas (Platt 1999; Schmitz et al., 2002;

Slocum et al., 2003). Such high fire frequency could be inferred from the abundance of charcoal particles in the samples of pollen zone I. Most importantly, our study indicates not only that marl prairies have been present in southwestern Florida since the mid-Holocene, but also suggests that early wetland landscapes in the Shark River Estuary are likely to have resembled the fire-maintained landscapes occurring today in Big Cypress National Preserve and ENP (Schmitz et al., 2002, Slocum et al., 2003).

Peat accumulating landscapes (pollen zone II) started to appear at site SRM at ~5,600 cal year BP and spread to the entire Shark River Estuary by 4,400 cal yr BP (Table 1). The pollen assemblage of this stage of the wetland development is characterized by a marked decrease of upland taxa and increase of Amaranthaceae and charcoal fragments (Fig. 5 and 6). These palynological data are consistent with long-hydroperiod prairies similar to the ones existing in present-day northern to central Everglades (Willard et al., 2001, 2006). These habitats today have 12 month hydroperiods. The increase of Amaranthaceae and charcoal particle in these freshwater wetland habitats has been attributed to natural lightning-ignited fires (Slocum et al. 2003, 2010) and hurricanes (Armentano et al. 1995), when open space is generated and colonized by species like *Amaranthus australis* (Schmitz et al., 2002). Such transition from marl prairies to peat accumulating freshwater wetlands at the Shark River Estuary suggests an extended hydroperiod due elevated watertable caused by SL.

With the SL continuing to rise after the mid-Holocene, marine transgression gradually reduced the site-to-sea distance in south Florida (Wanless et al., 1994; Gleason and Stone, 1994). From 3,800 to 2,000 cal yr BP, freshwater environment at the Shark River Estuary was progressively replaced by brackish marsh (Fig. 7 c and d). This transition is clearly recorded by the palynological data (Fig. 5 and 6). Linings of

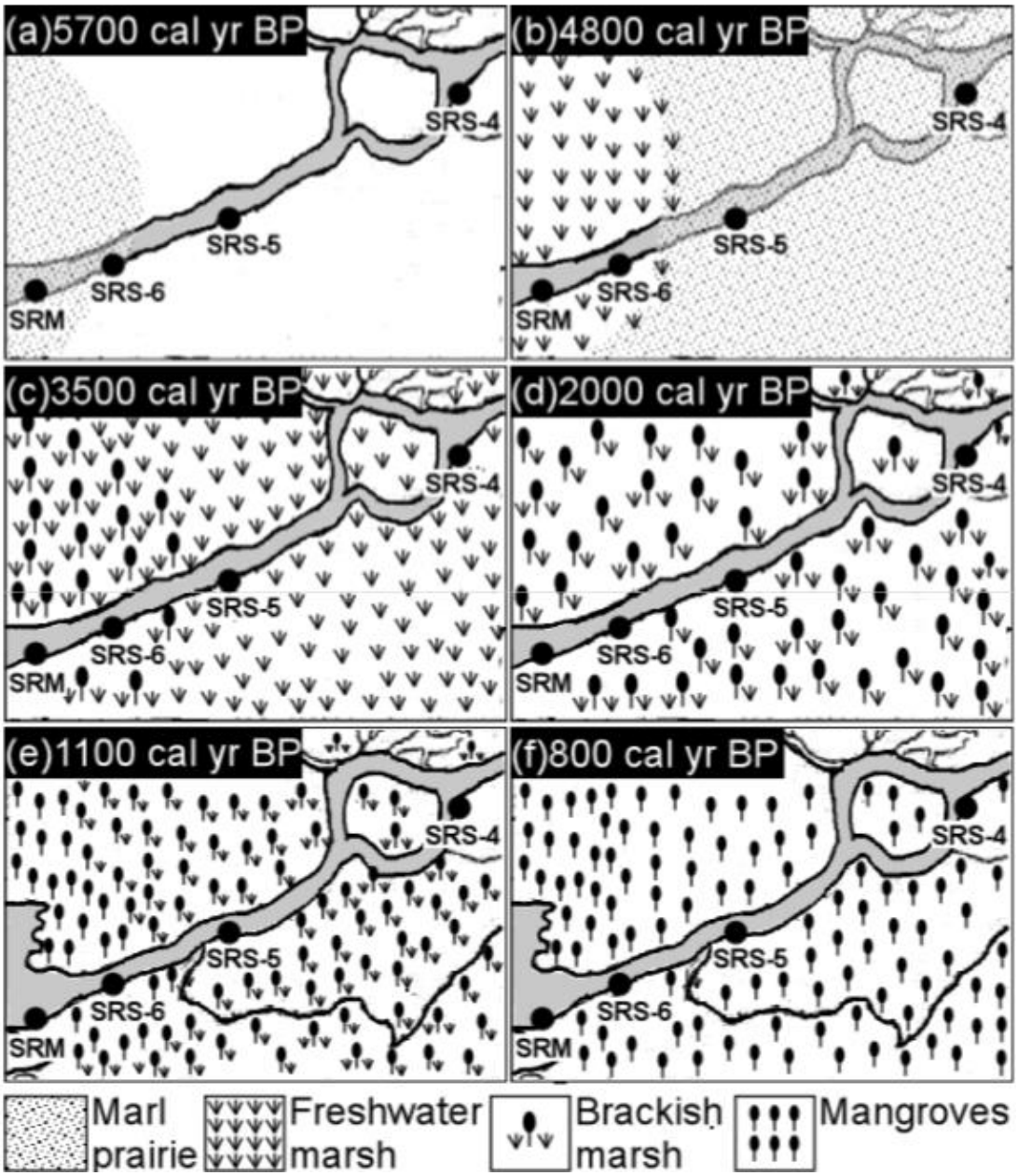

Figure 7. Model of the evolution of the Shark River Estuary. The time interval for each figure is selected to show each stage of the development of the Shark River Estuary.

foraminifera start to appear with greater regularity during this period (pollen zone III), while mangrove taxa gradually replace herbaceous taxa. Additionally, the abundance of microscopic charcoal fragments diminishes, indicating a changing environment (less fresh water and fewer fires) with greater marine influence (Willard et al., 2001; Willard and Cronin, 2007). Today, similar brackish marshes occur between mangrove forests and freshwater marshes in the Everglades (Willard et al., 2001). Using this as a modern analog, it could be inferred that by 3,800 cal yr BP, the Shark River Estuary was occupied by grasses and *Amaranthus*, with some scrub *Rhizophora* and occasional *Avicennia* and *Laguncularia*. Comparing with long-hydroperiod prairies, the frequency of fire was much reduced due to lower fuel loads (less graminoids biomass) and a 12 month hydroperiod (Ross et al., 2000).

The period from ~1,100 to 800 cal yr BP is characterized by the establishment of mangrove forest (Fig. 7 e and f). By 1,100 cal yr BP, Zr, the main constituent for Florida beach sand (Miller, 1945), started to consistently appear at site SRM (Fig. 4). Because tides (and episodic storms) are the only mechanism that consistently brings marine sediments, this chemical signature suggests that site SRM started to receive sand through tidal exchange at that time. Concurrently, the XRF diagrams show a higher content of all measured elements (Fig. 4). Most importantly, the concentration of all mangrove species and marine microfossils (foraminifera and dinoflagellate) increased significantly by 1,100 cal yr BP (Fig. 6). These results suggest that a mixed mangrove forest similar to today's was established at the mouth of the Shark River Estuary due to increased allochthonous sediment input. Such a mangrove ecosystem spread to site SRS-6 at ~1000 cal yr BP, and more inland sites (SRS-5 and SRS-4) at ~ 800 cal yr BP (Fig. 7 e and f). Nevertheless, *Conocarpus*, a mangrove associate growing at more freshwater environment has occupied our farthest upstream site

SRS-4 since 100 cal yr BP (Fig. 5, 6). Concentrations of most elements remain low (Fig. 4), but charcoal fragments are abundant throughout core SRS-4. These evidences suggest that the marine influence can hardly reach site SRS-4, which is located 20 km from the coast and experiences very little tidal influence today (Castañeda-Moya et al., 2010). Hence, transition to the modern coastal mangrove ecosystem was completed by about 800 cal yr BP in the Shark River Estuary.

Regional implications

Our study can be correlated with similar records from the region. Studies from Laguna de la Leche in Cuba (Peros et al., 2006) and Lake Wales Ridge region in south-central Florida (Watts, 1969; Watts and Stuiver, 1980; Grimm et al., 1993; Watts and Hansen, 1994) show a change toward "wetter" ecosystem after 5,000 cal yr BP. Although the initiation of peat-forming long-hydroperiod prairies in the Shark River Estuary was synchronous with these records, vegetation changes at these other locations may have been driven by different factors. The enhanced moisture at Lake Wales Ridge was likely caused by an increase in precipitation and decrease in solar insolation (Watts and Hansen, 1994), because the central Florida area is not very sensitive to the change of sea-level due to its slightly higher elevation (Donders, et al., 2005). In contrast, the Shark River Estuary and Laguna de la Leche are much more sensitive to SL change because they are much closer to the sea. We argue that the mid-Holocene SL rise is the one dominant cause of vegetation change at the Shark River Estuary, although the coastal plain climate may alter the tree-herb composition of the earliest peat-forming wetlands. Our pollen records indicate that the development of freshwater marshes was not synchronous throughout the Shark River Estuary. Instead, it started early at the coastal site (SRM), and then progressed upstream (SRS-4) as the Florida aquifer was elevated due to SL rise, thereby causing

wetter soil conditions toward the sea (Fig. 7). More importantly, the ages of the freshwater-brackish-mangrove transitions as well as the basal peat dates are time-transgressive toward further inland sites (Table 1). Based on these evidences, we believe that the shoreline in southwestern Florida has been undergoing a transgressive process driven by the SL rise from the mid-Holocene.

This marine transgression at the Shark River Estuary is consistent with other records from coastal areas in south Florida. Studies from Tampa Bay (van Soelen et al., 2010) and Charlotte Harbor (van Soelen et al., 2012) also document a transition from freshwater to marine environment after 3,500 cal yr BP. In addition, a study from Fakahatchee Strand State Preserve Park, southwest Florida, records an intensification of El Niño-Southern Oscillation (ENSO) after 3,500 cal yr BP (Donders et al., 2005). Intensification of ENSO is likely to have increased winter rainfall in the southeastern United States and reduced fire frequency and fire extent across long-hydroperiod prairie landscapes (Beckage et al. 2003). Such increases may facilitate the transition from long-hydroperiod prairies to brackish marshes as well.

Conclusion

Pollen records from the Shark River Estuary provide valuable paleoenvironmental information with which to understand the Holocene environmental history of south Florida. They also shed light on the processes driving millennial-scale ecological and hydrological change on subtropical coastlines. The Shark River Estuary has undergone three major transformations since the mid-Holocene: (1) Marl prairies were progressively replaced by long-hydroperiod prairies after ~5,700 cal yr BP. (2) Long-hydroperiod prairies were replaced by brackish marshes from 3,800 to 2,000 cal yr BP. (3) A significant expansion of mangroves occurred over the last 1000 years. The wetland transformation at the Shark

River Estuary can be correlated with paleolimnological records from southwest Florida and Cuba that indicate a rising water table after the mid-Holocene. The environmental changes at the Shark River Estuary are driven mostly by SL rise, although the fire-flood interaction of the long-hydroperiod prairies suggests that the coastal plain climate may have played a minor role. Our paleoenvironmental results highlight the complexity of subtropical estuarine environments and have important implications for understanding the biogeography and prehistory of the Everglades.

References

Beckage, B., Platt, W.J., Slocum, M.G., and Panko, B., 2003. Influence of the El Niño-Southern Oscillation on the fire regimes of the Florida Everglades. Ecology 84, 3124-3130.

Bernhardt, C.E., Willard, D.A., 2009. Response of the Everglades ridge and slough landscape to climate variability and 20th-century water management. Ecological Applications 19, 1723–1738.

Bridges, E.L., 2006. Landscape Ecology of Florida Dry Prairie in the Kissimmee River Region. In: F.N., Reed (Eds), Land of Fire and Water: The Florida Dry Prairie Ecosystem. Proceedings of the Florida Dry Prairie Conference.

Castañeda-Moya, E.,2010. Doctoral Dissertation: Landscape patterns of community structure, biomass and net primary productivity of mangrove forests in the Florida coastal Everglades as a function of resources, regulators, hydroperiod, and hurricane disturbance. Department of Oceanography and Coastal Sciences, Louisiana State University.

Castañeda-Moya, E., Twilley, R.R., Rivera-Monroy, V,H., Zhang, K.Q., Davis III, S.E., and Ross, M.S., 2010. Sediment and Nutrient Deposition Associated with Hurricane Wilma in Mangroves of the Florida Coastal Everglades. Estuaries and Coasts 33, 45-58.

Chen, R., and Twilley, R.R., 1999a. A simulation model of organic matter and nutrient accumulation in mangrove wetland soils. Biogeochemistry 44, 93-118.

Chen, R., and Twilley, R.R., 1999b. Patterns of mangrove forest structure and soil nutrient dynamics along the Shark River Estuary, Florida. Estuaries 22, 955-970.

Davison, W., 1988. Interactions of iron, carbon and sulphur in marine and lacustrine sediments. Geological Society, London, Special Publications 40, 131-137.

Dean, W.E.Jr., 1974. Determination of carbonate and organic matter in calcareous sediments and sedimentary rocks by loss on ignition: Comparison with other methods. Journal of Sedimentary Petrology 44, 242–248.

Donders, T.H., Wagner, F., Dilcher, D.L., Visscher, H., 2005. Mid- to late-Holocene El Niño-Southern Oscillation dynamics reflected in the subtropical terrestrial realm. PNAS 102, 10,904–10,908.

Doren, R.F., Platt,W.J., and Whiteaker, L.D., 1993. Density and size structure of slash pine stands in the everglades region of south Florida. Forest Ecology and Management 59, 295-311.

Ellison, J.C., 2008. Long-term retrospection on mangrove development using sediment cores and pollen analysis: A review. Aquatic Botany 89, 93–104.

Gleason, P.J. and Stone, P.A., 1994. Age, origin and landscape evolution of the Everglades peatland, In: S.M. Davis and J.C. Ogden (Eds.), Everglades, the Ecosystem and its Restoration. St. Lucie Press, Delray Beach, FL, pp. 149-198.

Grimm, E.C., Jacobson Jr., G.L., Watts, W.A., Hansen, B.C.S., Maasch, K.A., 1993. A 50,000-year record of climate oscillations from Florida and its temporal correlation with the Heinrich events. Science 261, 198–200.

Hanan, E.J., Ross, M.S., Ruiz, P.L., et al., 2010. Multi-Scaled Grassland-Woody Plant Dynamics in the Heterogeneous Marl Prairies of the Southern Everglades. Ecosystems 13, 1256-1274.

Hodell, D.A., Curtis, J.H., Jones, G.A., Higuera-Gundy, A., Brenner, M., Binford, M.W., Dorsey, K.T., 1991. Reconstruction of Caribbean climate change over the past 10,500 years. Nature 353, 790–793.

Kiage, L.M., and Liu, K.B., 2009. Palynological evidence of climate change and land degradation in the Lake Baringo area, Kenya, East Africa, since AD 1650. Palaeogeography, Palaeoclimatology, Palaeoecology 279, 60-72.

Kropp, W., 1976. Geochronology of Corkscrew Swamp Sanctuary. In: Cypress Wetlands for Water Management, Recycling and Conservation. University of Florida, Gainesville, pp 772–785

Liu, K.B., Li, C., Bianchette, T.A., McCloskey, T.A., Yao, Q., and Weeks, E., 2011. Storm deposition in a coastal backbarrier lake in Louisiana caused by Hurricanes Gustav and Ike. Journal of Coastal Research, Special Issue 64, 1866-1870.

Lodge, T.E., 2010, The Everglades Handbook: Understanding the Ecosystem, second edition, Boca Raton, Florida: CRC Press.

McAndrews, J.H., Berti, A.A., and Norris, G., 1973. Key to the Quaternary pollen and spores of the Great Lakes region. Royal Ontario Museum.

Miller, R., 1945. The heavy minerals of Florida beach and dune sands. American Mineralogist 30, 65–75.

NOAA, 2013, National Oceanic and Atmospheric Administration, Hurricane Center, Historical Hurricane Tracks website: http://maps.csc.noaa.gov/hurricanes/# (Accessed 24 December 2014)

Parkinson, R.W., 1989. Decelerating Holocene Sea-Level Rise and Its Influence on Southwest Florida Coastal Evolution: A Transgressive/Regressive Stratigraphy. Journal of Sedimentary Petrology 59, 960-972.

Peros, M.C., Reinhardt, E.G., Davis, A.M., 2007. A 6000-year record of ecological and hydrological changes from Laguna de la Leche, north coastal Cuba. Quaternary Research 67, 69–82.

Platt, W.J. 1999. Southeastern pine savannas., In Anderson, R.C., Fralish, J.S., and Baskin, J., (Eds), The savanna, barren, and rock outcrop communities of North America. Cambridge University Press, Cambridge, England, pp. 23-51

Platt, W.J., Huffman, J.M., Slocum, M.G., Beckage, B., 2006. Fire Regimes and Trees in Florida Dry Prairie Landscapes. In: F.N., Reed (Eds), Land of Fire and Water: The Florida Dry Prairie Ecosystem, Proceedings of the Florida Dry Prairie Conference.

Ramírez-Herrera, M.T., Lagos, M., Hutchinson, I., Kostoglodov, V., Machain, M.L., Caballero, M., Goguitchaichvili, A., Aguilar, B., Chaguéé-Goff, C., Goff, J., Ruiz-Fernández, A.C., Ortiz, M., Nava, H., Bautista, F., Lopez, G.I., and Quintana, P., 2012. Extreme wave deposits on the Pacific coast of Mexico: tsunami or storms? A multi-proxy approach. Geomorphology 140, 360-371.

Robbin, D.M., 1984, A new Holocene sea level curve for the upper Florida Keys and Florida reef tract, in Gleason, P.J. (Eds.), Environments of South Florida, Present and Past II (2nd ed.): Miami Geological Society, p. 437–458.

Ross, M.S., Meeder, J.F., Sah, J.P., Ruiz, P.L., and Telesnicki, G.J., 2000. The southeast saline Everglades revisited: 50 years of coastal vegetation change. Journal of Vegetation Science 11, 101–112.

Schmitz, M., Platt, W.J., and DeCoster, J., 2002. Substrate heterogeneity and numbers of plant species in Everglades savannas (Florida, USA). Plant Ecology 160, 137-148.

Scholl, D.W., Craighead, F.C., Stuiver, M., 1969. Florida submergence curve revised: its relation to coastal sedimentation rates. Science 163, 562–564.

Slocum, M.G., Platt, W.J., and Cooley, H.C., 2003. Effects of differences in prescribed fire regimes on patchiness and intensity of fires in subtropical savannas of Everglades National Park, Florida. Restoration Ecology 11, 91-102.

Simard, M., Zhang, K.Q., Rivera-Monroy, V.H., Ross, M.S., Ruiz, P.L., Castañeda-Moya, E., Twilley, R.R., and Rodriguez, E., 2006. Mapping height and biomass of mangrove forests in Everglades National Park with SRTM elevation data. Photogrammetric Engineering and Remote Sensing 72, 299-311.

Smith, T.J., Anderson, G.H., Balentine, K., Tiling, G., Ward, G.A., Whelan, K.R.T., 2009. Cumulative impacts of hurricanes on Florida mangrove ecosystems: Sediment deposition, storm surges and vegetation. Wetlands 29, 24-34.

Stuiver, M., Reimer, P.J., and Reimer, R.W., 2010. CALIB radiocarbon calibration program (http://calib.qub.ad.uk/calib) (Accessed 24 December 2014)

van Soelen, E.E., Lammertsma, E.I., and Cremer, H., 2010. Late Holocene sea-level rise in Tampa Bay: Integrated reconstruction using biomarkers, pollen, organic-walled dinoflagellate cysts, and diatoms. Estuarine, Coastal and Shelf Science 86, 216–224.

van Soelen, E.E., Brooks, G.R., Larson, R.A., Damsté, J.S.S., and Reichart, G.J., 2012. Mid- to late-Holocene coastal environmental changes in southwest Florida, USA. The Holocene, 1-10.

Wanless, H.R., Parkinson, R.W., Tedesco, L.P., 1994. Sea Level Control on Stability of Everglades Wetlands, In: Davis, S.M., and Ogden, J.C., (Eds). Everglades: the ecosystem and its restoration, St. Lucie Press, p. 199-222.

Watts, W.A., 1969. A pollen diagram from Mud Lake, Marion County, northcentral Florida. Geological Society of America Bulletin 80, 631–642.

Watts, W.A., Hansen, B.C.S., 1994. Pre-Holocene and Holocene pollen records of vegetation history from the Florida peninsula and their climatic implications. Palaeogeography, Palaeoclimatology, Palaeoecology 109, 163–176.

Watts, W.A., Stuiver, M., 1980. Late Wisconsin climate of northern Florida and the origin of species-rich deciduous forest. Science 210, 25–327.

Whelan, K.R.T., Smith, T.J.I., Anderson, G.H., and Ouellette, M.L., 2009. Hurricane Wilma's impact on overall soil elevation and zones within the soil profile in a mangrove forest. Wetlands 29, 16–23.

Willard, D.A., Weimera, L.M., and Riegel, W.L., 2001, Pollen assemblages as paleoenvironmental proxies in the Florida Everglades. Review of Palaeobotany and Palynology 113, 213-235.

Willard, D.A., Cooper, S.R., Gamez, D., and Jensen, J., 2004, Atlas of pollen and spores of the Florida Everglades. Palynology 28, 175-227.

Willard, D.A., and Bernhardt, C.E., 2011. Impacts of past climate and sea level change on Everglades wetlands: placing a century of anthropogenic change into a late-Holocene context. Climatic Change 107, 59-80.

Willard, D.A., and Cronin, T.M., 2007. Paleoecology and ecosystem restoration: case studies from Chesapeake Bay and the Florida Everglades. Front Ecology Environment 5, 491–498.

CHAPTER 7. SUMMARY AND CONCLUSION

Restatement of purpose

This research examines the paleoenvironments of four study sites along the Shark River Estuary, through the extraction and analysis of a total of ~15 m of sediment cores. Using a multi-proxy approach, the main objective of this study was to: (1) review the Holocene pollen and associated paleoecological records of mangrove ecosystems in the western North Atlantic (WNA); (2) establish the spatial and statistical relationships between surface pollen assemblages and local vegetation in the Everglades; (3) use the sedimentary signature of Hurricane Wilma as a modern analog to reveal other paleohurricane events in the sedimentary record; (4) document evolution of the Shark River Estuary from the mid-Holocene; (5), identify the timing of the freshwater-brackish-marine transitions in the Shark River Estuary during the Holocene; and (6) assess the role of climate change and sea-level rise in driving the millennial-scale estuarine vegetation dynamics in the Everglades.

Chapter 2.

Chapter 2 reviews the pollen and associated paleoecological records of mangrove-dominant environments from 24 study sties in the WNA from the mid-Holocene. Through the examination of pollen, marine microfossils, microscopic charcoal, mangrove peat stratigraphy, and chemical and isotopic records from WNA, the results suggest that winter sea-surface temperature (SST) is an important control over the distribution and late Holocene dispersal pattern of *Rhizophora*, as evidenced by the progressive migration of *Rhizophora* from the south side of the Caribbean Basin toward the Gulf Coast, which spanned thousands of years. This gradual expansion was likely driven by an increase in the boreal winter insolation of ~25 W/m^2 in the tropics, which increased the winter SST of the WNA by up to 2 ℃

(Chollett et al., 2012). With warmer winter SST and stable sea-level rise (SLR) after 3500 cal yr BP, *Rhizophora* was able to establish at higher latitudes and eventually colonized the coastlines of Yucatan, South Florida, and Bermuda.

Additionally, this review of the pollen and paleoecological records from the WNA reveals a consistent, though spatially and temporally variable, decline of *Rhizophora* from 3000 to 1000 cal yr BP. It might be caused by a period of elevated hurricane activities, drop in the regional sea-level, or dry climate.

Chapter 3.

Chapter 3 examines 18 modern pollen samples from a 20 km transect along the SRS and 7 samples from 3 major wetland sub-environments along the main park road in the ENP. By comparing vegetation groups classified by Grimm's (1987) CONISS and PCA and surface pollen analyses with the local vegetation of sampling locations, the 25 surface pollen assemblages from the ENP are classified into five vegetation groups, which are marl prairie, pineland, inland mangroves, mangrove forests, and hurricane damaged mangrove fringe. These groups broadly correspond with various local vegetation types around the sampling sites. This study indicates that palynological data from sediment cores from the Everglades can be used to reconstruct past wetland responses to a variety of environmental and climatic changes and to predict future responses.

Chapter 4.

Chapter 4 presents the palynological record from core SRM, which was retrieved from the mouth of Shark River Estuary in Everglades National Park. This record contains 5,700 years of vegetation history. Palynological and XRF data from core SRM indicate that wetlands have been present at the mouth of the Shark River Estuary since the mid-Holocene. Initial wetland habitat, a short-hydroperiod

graminoid-dominant marl prairie, existed more than 5,700 cal yr BP. It was similar in species composition, ecological fire regimes, and landscape organization to habitats currently present in the central Everglades. During the period from ~5,700 to 5,250 cal yr BP, plant communities consisting of short- and long-hydroperiod prairies with imbedded sloughs and surrounded by uplands prevailed. By ~5,250 cal yr BP, these habitats were replaced by long-hydroperiod prairies that were herb-dominant, which lasted about 1,000 yr. Between 4,200 to 3800 cal yr BP, as a response to increasing but perhaps more seasonal precipitation, sloughs imbedded in frequently-burned long-hydroperiod prairies/marshes were formed. These data suggest that freshwater wetlands in the southwestern Everglades date back to at least the mid-Holocene and are dynamic ecosystems, changing almost continuously on millennial timescales. The multi-proxy data record a clear transition from a freshwater to a coastal/estuarine environment from ~3,800 to 1,150 cal yr BP. During this period, relatively stable sea levels allowed the colonization of mangroves, causing a shift to mangrove-dominant forest at the study site.

At ~1,150 cal yr BP, a mixed mangrove forest resembling the present day vegetation composition was established at the study site, suggesting that the modern mangrove-dominant coastline was formed at the Shark River Estuary at that time. Accelerated sea level rise should both generate new habitats suitable for mangroves, and also remove current shoreline habitats. Thus, accelerated sea level rise should result in the generation of transient mangrove forests that will not reach the ages that they used to when shorelines are transgressing more slowly or are stable. Such dynamics should result in a dynamic non-equilibrium front of developing mangrove forest that moves inland, but is lost on the ocean-ward side at rates dependent on sea level rise and hurricane activities.

Chapter 5.

Chapter 5 evaluates the distinctive carbonate-rich clastic layer left by Hurricane Wilma (2005) at the top of core SRM. Multi-proxy analyses reveal the unique sedimentary signature of Hurricane Wilma. By using Hurricane Wilma as a modern analog and statistical analyses of the multi-proxy record, six major hurricane events are inferred at ~3000, 1700, 950, 580, 350, and 120 cal yr BP. The numerical analysis also confirms that the modern mangrove coastline was formed at the mouth of the Shark River Estuary by ~1150 cal yr BP, as the shoreline became stabilized

This study produces the first multi-proxy record of paleo-hurricane activities for South Florida, which is vital for the study of global climate change and forecasting future impacts of tropical cyclones. The study also applies an objective approach, numerical analysis, to paleotempestology studies. Further paleoecological studies are needed to produce a high-resolution pollen record for the better understanding of the long-term process of post-storm forest succession and habitat recovery in the Everglades landscape.

Chapter 6.

Chapter 6 presents palynological, x-ray fluorescence, and loss-on-ignition data from all 4 cores retrieved from a 20 km transect along the Shark River Estuary. The results indicate that the initial development of freshwater marshes was not synchronous throughout the Shark River Estuary. Instead, it started early at the coastal sites (SRM), and then progressed upstream (SRS-4) as the Florida aquifer was elevated due to SLR. More importantly, the ages of the freshwater-brackish-mangrove transitions as well as the basal peat dates are time-transgressive towards further inland sites. These data suggest that the shoreline in southwestern Florida was going through a transgressive process driven by the SLR from the mid-Holocene. Based on these

evidences, we argue that the mid-Holocene SLR was the predominant cause of vegetation change at the Shark River Estuary, although the coastal plain climate may have altered the tree-herb composition of the earliest peat-forming wetlands.

Future research

As indicated in Chapter 4, no palynological records older than 5000 cal yr BP were available from the Everglades. This dissertation presents an estimated 5700 year palynological record from the Shark River Estuary, the largest freshwater outlet in the Everglades. Due to its unique hydrological and ecological settings, much regional paleoenvironmental work must be performed to verify the findings and further test the hypotheses presented in this dissertation. Results from this study suggest that the modern mangrove-dominant shoreline at the mouth of the Shark River Estuary is more than 2,000 years younger than previously estimated (Parkinson, 1989; Gleason and Stone, 1994; Wanless et al., 1994; Lodge, 2010). Sedimentological data should be retrieved from other mangrove estuaries along the coastlines of south Florida to validate the regional significance of this conclusion. Future research could also generate new sedimentary records from Taylor Slough in Everglades National Park in south Florida. Taylor Slough has different morphological and physical settings, opposed to the mixed mangrove forests discussed in this study. By doing a comparative study, the sensitivity of these areas to relative sea-level rise can be determined.

Additionally, there is still no consistent view regarding the long-term response of mangrove communities to hurricanes. Hurricanes can strongly influence the structure and composition of mangrove forests. These large-scale disturbances bring sediments, nutrients, as well as stressors (strong wind, hypersaline conditions, and floodwater inundation) to mangrove-dominant coasts (Chen and Twilley, 1999a, b;

Mancera-Pineda et al., 2009; Piou et al., 2006; Urquhart, 2009; Whelan et al., 2009; Castañeda-Moya et al., 2010; Gonzalez et al., 2010). Some studies suggest that *Rhizophora mangle* suffers higher initial mortality compared with *Avicennia germinans* and *Laguncularia racemosa* due to its lack of resprouting capability (Baldwin et al., 1995, 2001; Thaxton et al., 2007). The direct landfall of major hurricanes has been documented to kill canopy trees in a *Rhizophora mangle*-dominant forest and give opportunities for shade-intolerant species including other mangrove species and herbaceous plants at low salinity sites to colonize and form a mixed forest (Smith et al., 1994, 2009; Baldwin et al., 1995, 2001; Vegas-Villarrúbia and Rull, 2002; Hogarth, 2007; Piou et al., 2006; Thaxton et al., 2007). However, the complete recovery of severely damaged mangrove forests requires time spans of decades to centuries, which are beyond the duration of most ecological studies, and thus the regeneration process and successional patterns are not well understood. It appears that the duration and forest recovery trajectory may vary from one storm to another depending on the severity and nature of the impact, among other factors, such as original species composition and physiognomic structure at the impacted site. Further paleoecological studies are needed to better understand these long-term changes in mangrove forests at different temporal and spatial scales in the Everglades landscape.

References

Baldwin, A.H., W.J. Platt, K.L. Gathen, J.M. Lessman, and T.J. Rauch, 1995. Hurricane damage and regeneration in fringe mangrove forests of southeast Florida, USA. Journal of Coastal Research 21, 169-183.

Baldwin, A.H., Egnotovich, M.S., Ford, M.A., and Platt, W.J., 2001. Regeneration in fringe mangrove forests damaged by Hurricane Andrew. Plant Ecology 57, 151-164.

Castañeda-Moya, E., Twilley, R.R., Rivera-Monroy, V,H., Zhang, K.Q., Davis III, S.E., and Ross, M.S., 2010. Sediment and Nutrient Deposition Associated with Hurricane Wilma in Mangroves of the Florida Coastal Everglades. Estuaries and Coasts 33, 45-58.

Chen, R., and Twilley, R.R., 1999a. A simulation model of organic matter and nutrient accumulation in mangrove wetland soils. Biogeochemistry 44, 93-118.

Chen, R., and Twilley, R.R., 1999b. Patterns of mangrove forest structure and soil nutrient dynamics along the Shark River Estuary, Florida. Estuaries 22, 955-970.

Chollett I, Müller-Karger FE, and Heron SF, et al., 2012. Seasonal and spatial heterogeneity of recent sea surface temperature trends in the Caribbean Sea and southeast Gulf of Mexico. Marine Pollution Bulletin 64, 956-965.

Gleason, P.J. and P.A. Stone, 1994. Age, origin and landscape evolution of the Everglades peatland, In: S.M. Davis and J.C. Ogden (Eds.), Everglades, the Ecosystem and its Restoration. St. Lucie Press, Delray Beach, FL, pp. 149-198.

Grimm, E.C., 1987. CINISS: A FORTRAN 77 program for stratigraphically constrained cluster analysis by method of incremental sum of square. Computer and Geoscience 13, 13–35.

Gonzalez, C., Urrego, L.E., Martinez, J.I., Polania, J., and Yokoyama, Y., 2010. Mangrove dynamics in the southwestern Caribbean since the 'Little Ice Age': A history of human and natural disturbances. Holocene 20, 849–861.

Hogarth, P.J., 2007. The biology of mangroves and seagrasses, second edition, Oxford University Press

Hodell, D.A., Curtis, J.H., and Jones, G.A., et al., 1991. Reconstruction of Caribbean climate change over the past 10,500 years. Nature 352, 790–793.

Kjellmark, E., 1996. Late Holocene Climate Change and Human Disturbance on Andros Island, Bahamas. Journal of Paleolimnology 15, 133-145.

Lodge, T.E., 2010, The Everglades Handbook: Understanding the Ecosystem, second edition, Boca Raton, Florida: CRC Press.

Mancera-Pineda, J.E., Twilley, R.R., and Rivera-Monroy, V.H., 2009. Carbon (^{13}C) and nitrogen (^{15}N) isotopic discrimination in mangroves in Florida Coastal Everglades as a function of environmental stress. Contributions in Marine Science 38, 109-129.

Parkinson, R.W., 1989. Decelerating Holocene Sea-Level Rise and Its Influence on Southwest Florida Coastal Evolution: A Transgressive/Regressive Stratigraphy. Journal of Sedimentary Petrology 59, 960-972.

Piou, C., Feller, I., Berger, U., and Chi, F., 2006. Zonation patterns of Belizean offshore mangrove forests 41 years after a catastrophic hurricane. Biotropica 38, 365-374.

Smith, T.J., Robblee, M.B., Wanless, H.R., and Doyle, T.W., 1994. Mangroves, Hurricanes, and Lightning Strikes. BioScience 44, 256-263.

Smith, T.J., Anderson, G.H., Balentine, K., Tiling, G., Ward, G.A., Whelan, K.R.T., 2009. Cumulative impacts of hurricanes on Florida mangrove ecosystems: Sediment deposition, storm surges and vegetation. Wetlands 29, 24-34.

Thaxton, J.M., S.J. DeWalt, and W.J. Platt, 2007. Spatial patterns of regeneration after Hurricane Andrew in two south Florida fringe mangrove forests. Florida Scientist 70, 148-156.

Urquhart, G.R., 2009. Paleoecological record of hurricane disturbance and forest regeneration in Nicaragua. Quaternary International 195, 88-97.

Vegas-Vilarrúbia, T., and Rull, V., 2002. Natural and human disturbance history of the Playa Medina mangrove community (eastern Venezuela). Caribbean Journal of Science 38, 66-76.

Wanless, H.R., Parkinson, R.W., Tedesco, L.P., 1994. Sea Level Control on Stability of Everglades Wetlands, In: Davis, S.M., and Ogden, J.C., (Eds). Everglades: the ecosystem and its restoration, St. Lucie Press, pp. 199-222.

Whelan, K.R.T., T.J.I. Smith, G.H. Anderson, and M.L. Ouellette. 2009. Hurricane Wilma's impact on overall soil elevation and zones within the soil profile in a mangrove forest. Wetlands 29, 16–23.

VITA

Qiang Yao was born in Kunming, Yunnan, China in 1982. He received a Bachelor of Science in Biology in March 2008 from Mahidol University International College, Bangkok, Thailand. In August 2008, he enrolled in the Louisiana State University in Baton Rouge, Louisiana and began his doctoral program in Oceanography and Coastal Studies under the direction of Dr. Kam-biu Liu. Qiang plans to receive his doctorate in May, 2015. Throughout his tenure at LSU, Qiang has worked as a research assistant and a teaching assistant. He has performed fieldwork in Texas, Louisiana, and Florida. He has co-authored papers in the Journal of Coastal Research and Quaternary Research. After graduation, Qiang is looking forward to start a career as a coastal scientist.